Theses and Dissertations | 1. Thesis and Dissertation Collection, all items

2023-03

CONJUNCTION SCREENING AND COLLISION AVOIDANCE MANEUVER STRATEGIES FOR LOW THRUST SPACECRAFT

de Oliveira, Giuliano F.

Monterey, CA; Naval Postgraduate School

https://hdl.handle.net/10945/71993

NAVAL
POSTGRADUATE
SCHOOL

MONTEREY, CALIFORNIA

THESIS

CONJUNCTION SCREENING AND COLLISION AVOIDANCE MANEUVER STRATEGIES FOR LOW THRUST SPACECRAFT

by

Giuliano Freitas Batista de Oliveira

March 2023

Thesis Advisor:	Jennifer Hudson
Co-Advisor:	Marcello Romano

Approved for public release. Distribution is unlimited.

THIS PAGE INTENTIONALLY LEFT BLANK

REPORT DOCUMENTATION PAGE		*Form Approved OMB No. 0704-0188*

1. AGENCY USE ONLY *(Leave blank)*	2. REPORT DATE March 2023	3. REPORT TYPE AND DATES COVERED Master's thesis	
4. TITLE AND SUBTITLE CONJUNCTION SCREENING AND COLLISION AVOIDANCE MANEUVER STRATEGIES FOR LOW THRUST SPACECRAFT		**5. FUNDING NUMBERS**	
6. AUTHOR(S) Giuliano Freitas Batista de Oliveira			
7. PERFORMING ORGANIZATION NAME(S) AND ADDRESS(ES) Naval Postgraduate School Monterey, CA 93943-5000		**8. PERFORMING ORGANIZATION REPORT NUMBER**	
9. SPONSORING / MONITORING AGENCY NAME(S) AND ADDRESS(ES) N/A		**10. SPONSORING / MONITORING AGENCY REPORT NUMBER**	
11. SUPPLEMENTARY NOTES The views expressed in this thesis are those of the author and do not reflect the official policy or position of the Department of Defense or the U.S. Government.			
12a. DISTRIBUTION / AVAILABILITY STATEMENT Approved for public release. Distribution is unlimited.		**12b. DISTRIBUTION CODE** A	

13. ABSTRACT (maximum 200 words)

The number of objects in space has raised concern about the risk of operational satellites and debris colliding. The U.S. Space Surveillance Network currently tracks more than 27,000 objects; of these 7,500 are active payloads and 19,500 are debris. Satellite operators follow conjunction analysis procedures to ensure safe operations in this congested environment, and it is not rare for operators to have only the systems tool kit (STK) as a conjunction analysis tool. In this case, a common approach is to perform conjunction screening using the two-line elements (TLE) catalog. Even though it is the easiest and fastest way to perform this process in STK, NASA does not recommend this practice due to TLE's low accuracy. Instead, NASA recommends using the special perturbation (SP) catalog developed for this purpose. Yet, the use of the SP catalog in STK is less straightforward than it is for TLE. This work proposes a program that allows the use of the full SP catalog for the screening process in STK. In the conjunction analysis process, an action is required when risk of collision exceeds an acceptable limit. For low-thrust satellites, it is challenging to select and perform a conjunction avoidance maneuver (CAM) that significantly reduces the collision risk. Tangential CAM and drag maneuvers are tested for the ICEYE satellites, a small electric-propulsion SAR satellite. Results show these two approaches are feasible for the ICEYE case, but some technical concerns are identified.

14. SUBJECT TERMS collision avoidance maneuver, CAM, space situational awareness, spacecraft collision probability, low-thrust, continuous-thrust, conjunction analysis, systems tool kit, STK, two-line elements, TLE catalog, special perturbation, SP catalog, screening process, risk assessment		**15. NUMBER OF PAGES** 153	
		16. PRICE CODE	
17. SECURITY CLASSIFICATION OF REPORT Unclassified	**18. SECURITY CLASSIFICATION OF THIS PAGE** Unclassified	**19. SECURITY CLASSIFICATION OF ABSTRACT** Unclassified	**20. LIMITATION OF ABSTRACT** UU

Standard Form 298 (Rev. 2-89)
Prescribed by ANSI Std. 239-18

THIS PAGE INTENTIONALLY LEFT BLANK

Approved for public release. Distribution is unlimited.

CONJUNCTION SCREENING AND COLLISION AVOIDANCE MANEUVER STRATEGIES FOR LOW THRUST SPACECRAFT

Giuliano Freitas Batista de Oliveira
Major, Brazilian Air Force
BEE, Federal University of Rio Grande do Norte (UFRN), 2003

Submitted in partial fulfillment of the
requirements for the degree of

MASTER OF SCIENCE IN SPACE SYSTEMS OPERATIONS

from the

NAVAL POSTGRADUATE SCHOOL
March 2023

Approved by: Jennifer Hudson
Advisor

Marcello Romano
Co-Advisor

James H. Newman
Chair, Space Systems Academic Group

iii

THIS PAGE INTENTIONALLY LEFT BLANK

ABSTRACT

The number of objects in space has raised concern about the risk of operational satellites and debris colliding. The U.S. Space Surveillance Network currently tracks more than 27,000 objects; of these 7,500 are active payloads and 19,500 are debris. Satellite operators follow conjunction analysis procedures to ensure safe operations in this congested environment, and it is not rare for operators to have only the systems tool kit (STK) as a conjunction analysis tool. In this case, a common approach is to perform conjunction screening using the two-line elements (TLE) catalog. Even though it is the easiest and fastest way to perform this process in STK, NASA does not recommend this practice due to TLE's low accuracy. Instead, NASA recommends using the special perturbation (SP) catalog developed for this purpose. Yet, the use of the SP catalog in STK is less straightforward than it is for TLE. This work proposes a program that allows the use of the full SP catalog for the screening process in STK. In the conjunction analysis process, an action is required when risk of collision exceeds an acceptable limit. For low-thrust satellites, it is challenging to select and perform a conjunction avoidance maneuver (CAM) that significantly reduces the collision risk. Tangential CAM and drag maneuvers are tested for the ICEYE satellites, a small electric-propulsion SAR satellite. Results show these two approaches are feasible for the ICEYE case, but some technical concerns are identified.

THIS PAGE INTENTIONALLY LEFT BLANK

TABLE OF CONTENTS

LIST OF FIGURES

x

xi

THIS PAGE INTENTIONALLY LEFT BLANK

LIST OF TABLES

LIST OF ACRONYMS AND ABBREVIATIONS

AGI	Analytical Graphics, Inc
ASAT	anti-satellite test
CA	conjunction analysis
CAM	collision avoidance maneuver
CDM	conjunction data message
FEEP	field emission electric propulsion
GEO	geostationary orbit
GSOC	German Space Operations Center
HAC	high-accuracy catalog
HIE	high-interest events
IADC	Inter-Agency Space Debris Coordination Committee
Isp	specific impulse
LEO	low Earth orbit
MATLAB	Matrix Laboratory
NASA	National Aeronautics and Space Administration
ODTK	Orbit Determination Tool Kit
O/O	owner/operator
RSO	resident space object
SAR	synthetic aperture radar
SP	special perturbation catalog
SSN	Space Surveillance Network
STK	systems tool kit
TPBVP	two-point boundary value problem
TLE	two-line elements
USSPACECOM	United States Space Command

THIS PAGE INTENTIONALLY LEFT BLANK

ACKNOWLEDGMENTS

To God for the gift of life and for guiding me through difficult times.

To my parents, sisters, brother-in-law, and nephews for all their encouragement, love, and prayers.

To my beautiful wife and daughters, for all their love, support, and understanding of my absences as I pursued this graduation. Without you, none of this would be possible.

I would like to express my gratitude to my advisor, Dr. Jennifer Hudson, for her availability, advice, and support, which was fundamental to the preparation of this thesis.

To the Naval Postgraduate School for providing me with the best professors and an ideal environment in which to study.

Finally, I would like to thank the Brazilian Air Force for this opportunity for professional growth.

THIS PAGE INTENTIONALLY LEFT BLANK

I. INTRODUCTION

A. BACKGROUND

In recent years the so-called NewSpace industry has changed the way space services are provided, moving from complex, large, and expensive satellites to small, simple, and cheap satellites. NewSpace makes possible the development of satellite mega-constellations, systems with hundreds or thousands of satellites; an example is the Starlink mega-constellation which plans to have 42,000 satellites in orbit in its final configuration [1]. A second door opened by NewSpace is the opportunity for developing countries to access space by taking advantage of the simplicity and low cost of launching and operating small satellites.

Although the growth in the number of payloads in space represents more available services and products, it also increases the concern about operational satellites and debris colliding. The U.S. Space Surveillance Network (SSN) tracks more than 27,000 objects, of which 7,500 active payloads and 19,500 pieces of debris are now orbiting the Earth [2]. Figures 1 and 2 show the evolution of space objects in the Earth's orbit and the number of payloads launched per year since the beginning of space exploration; as we can see, between 2017 and 2019, on average 400 payloads were launched per year, double the maximum found previously, which was 240 payloads occurring in 2013 [2]. These numbers jumped again between 2020 and 2022, with 2254 new payloads launched in 2022, and the trend has continued to increase; in the first one and a half months of 2023 alone, more than 400 new payloads went into orbit. With the decrease in satellites' size and weight, the number of payloads per launch has risen also; an average of 1.5 payloads per launch before 2017 grew to 4 between 2017 and 2019 and reached an average of 12.5 payloads per launch in the following three years (see Figure 3) [2].

1
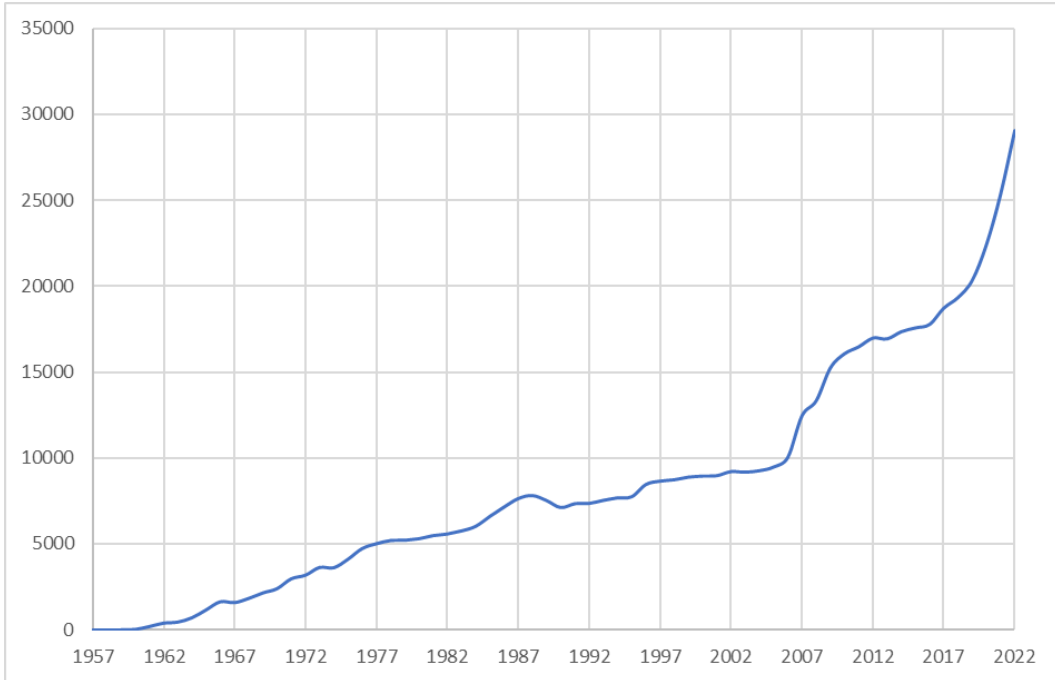
Figure 1.   Number of objects in space. Adapted from [2].
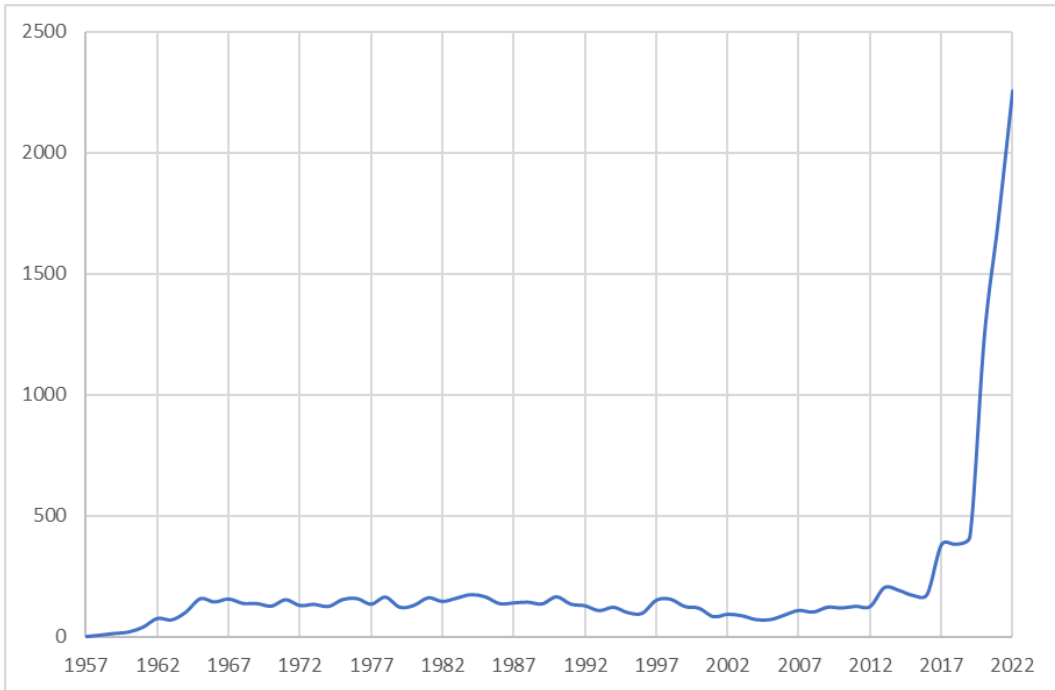
Figure 2.   Payloads launched per year. Adapted from [2].
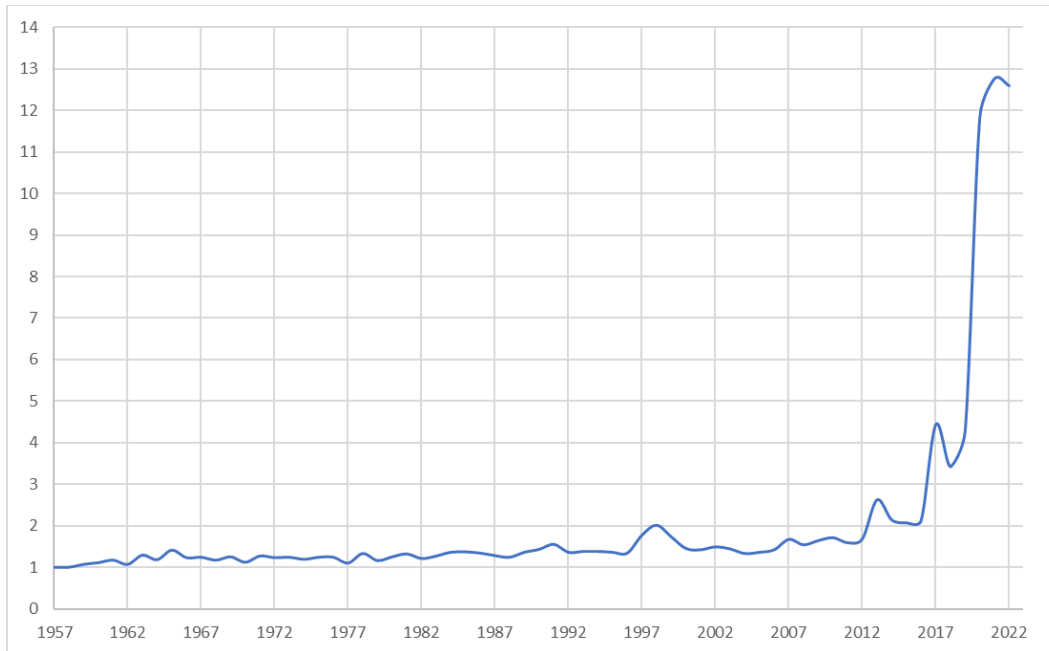
Figure 3.   Payload-to-launch ratio. Adapted from [2].

Although the rise in payload launches is an issue in terms of potential collisions, the most critical factor contributing to the risk of space collisions is debris, which has also increased in the past few years. The Inter-Agency Space Debris Coordination Committee (IADC) defines space debris as "all human-made objects, including fragments and elements thereof, in Earth's orbit or re-entering the atmosphere that are non-functional" [3]. Orbits below 2,000 kilometers in altitude have the highest concentration of debris. Three events contribute to this undesirable situation: a collision in 2009 between the retired Russian satellite Cosmo-2251 and the active Iridium-33 and the anti-satellite (ASAT) tests carried out by China in 2007 [4] and Russia in 2021 [5]. These two ASAT tests alone generated at least 3,587 pieces of debris large enough to be tracked by U.S. SSN, which is more than half of the total active payloads in space.

The growth in the number of objects in space, whether debris or operational satellites, has caused global concern about the increasing possibility of collisions between objects. While growth in payload launches mean more services available, the increase in debris orbiting the Earth has only harmful consequences. Different techniques, rules, and technologies are emerging to address the debris problem in the Earth's orbit. One idea is

3

to remove debris actively; many techniques and technologies have been proposed for this approach [6]. Another approach is the creation and improvement of post-mission disposal rules. Following this reasoning, in September 2022 the U.S. Federal Communications Commission adopted a new rule that decreases from 25 to five years the time an operator must deorbit a low Earth orbit (LEO) satellite after its lifetime, as reported by Spacenews website [6]. In parallel with the development of actions to reduce the amount of debris in Earth's orbit, operators must continue applying their conjunction analysis procedures to ensure safe operations in this increasingly congested environment.

The conjunction screening and collision risk assessment are part of the conjunction analysis process that determines whether a collision risk is significant enough to perform a collision avoidance action. Conjunction analysis typically has four steps: 1. Screening the objects data catalog; 2. Computing the risk assessment of identified collisions; 3. Improving orbit estimations of the objects involved in conjunction.; and 4. Performing a collision avoidance action [7]. It is not rare for operators to have only the Systems Tool Kit (STK) as a conjunction analysis tool. In this scenario a common approach is to perform the screening process using the two-line elements (TLE) catalog, which is publicly available from the Space-Track website. Even though it is the easiest and fastest way to perform this process in STK, NASA does not recommend the use of TLE for conjunction analysis due to its low accuracy. Instead, it recommends using the special perturbation (SP) catalog that was developed for this purpose [8]. The use of the SP catalog in STK is not as straightforward and simple as the TLE, and consequently, it makes the process more time consuming due to the amount of ephemeris data present in this catalog.

Usually, collision avoidance action involves executing a collision avoidance maneuver (CAM), an atypical maneuver that takes a satellite out of its nominal orbit to reduce the risk of collision to acceptable values. CAMs impact a mission in different ways. For example, fuel consumption required for the maneuver reduces the useful life of the satellite. Such a maneuver can also cause temporary interruption of services due to the need to change the satellite's attitude or even an operational restriction that limits the use of the payload while the thrusters are firing. Another possible collision avoidance action involves

4

using satellite aerodynamics, such as changing the attitude to increase the drag area, which results in a decrease in the semi-major axis.

Generally speaking, there are two main categories of satellite maneuvers: impulsive and low/continuous. While impulsive maneuvers fire high-thrust thrusters for a short time and change the magnitude and direction of the velocity vector instantaneously, low/ continuous maneuvers use low-thrust thrusters with high specific impulse (Isp) and fire them for a considerable time interval [9]. Satellites powered by impulsive propulsion systems have been used on a large scale for decades, having already well-defined and tested collision avoidance maneuver strategies. On the other hand, the use of low-thrust satellites has increased significantly only in the last few years, when the more advanced studies of CAM strategies for this type of propulsion system also began. An example of a small satellite equipped with a low-thrust propulsion system is the ICEYE satellite, which is a small electric-propulsion synthetic aperture radar (SAR) satellite. ICEYE is currently the largest operational SAR constellation, with 20 satellites in a LEO sun-synchronous orbit.

Typically, two groups of CAM strategies exist for low-thrust satellites. The first group applies a constant thrust in an optimal direction to reach the minimum collision probability, maximum miss distance, or minimum fuel consumption. The second group uses tangential maneuvers with the possibility of changing the starting point of the maneuver and/or the thrust arc length, which has the same objectives as the optimal maneuvers.

This thesis proposes a MATLAB-STK program that allows the use of the full SP catalog for the screening process in STK and tests the performance and feasibility of the tangential maneuver (prograde/retrograde) and the drag maneuver for the case of the ICEYE satellite.

B. OBJECTIVES

The primary research objectives are to study the possibility of using the complete SP catalog in the STK software to perform the conjunction screening process and to review state-of-the-art methods of continuous thrust/low thrust collision avoidance strategies.

The subsidiary research questions are:

- Is it possible to implement an automatic screening process using the full SP catalog in STK?

- Can prograde and retrograde tangential conjunction avoidance maneuvers perform effectively for the ICEYE satellite, given the constraints on thrust magnitude and attitude control?

- Is an aerodynamic maneuvering strategy feasible for the ICEYE satellite, given its structural dimensions?

C. METHODOLOGY

The study methodology involves computer simulation using MATLAB and STK to perform the screening process of the object of interest against the full SP catalog and to implement tangential (prograde/retrograde) and drag collision avoidance maneuvers.

All simulations are performed considering the satellite in its operational orbit; orbit insertion and disposal maneuvers are beyond the scope of this study.

II. CONJUNCTION ANALYSIS

There are two main reasons to conduct satellite conjunction analysis; first, satellite owners want to prevent their mission from premature failure due to preventable collisions, and second to mitigate the risk of increasing, even more, the amount of debris in Earth's orbit. Of course, the first reason is more of an individual owner issue, while the second one is broader and applies to all space players since the increase in debris can challenge access to space in the future. This chapter describes a typical conjunction analysis procedure.

A conjunction analysis procedure aims to determine whether the risk is high enough to require a collision avoidance maneuver or other mitigating action. The collision probability method that uses a threshold to assess the risk of collision and decide whether or not to maneuver the spacecraft is the most used approach; typical collision probability threshold values are 1e-04 and 1e-05, with the former being the most used by operators [8]. Collision analysis procedures typically have four steps: 1. Screening the objects data catalog; 2. Computing the risk assessment; 3. Improving orbit estimations of objects involved in conjunction; and 4. Performing a collision avoidance action [7]. These four steps, which are applied with some modifications by the German Space Operations Center (GSOC) [10] and the National Aeronautics and Space Administration (NASA) [8], are described in the following subsections.

A. SCREENING THE OBJECTS DATA CATALOG

The object of interest must be compared with all resident space objects (RSO) in the catalog to identify potential conjunctions. Some objects are known to never be in conjunction due to orbit parameters; for example, if the spacecraft of interest is in geostationary orbit (GEO) orbit, any object in a circular LEO orbit will never cross the geostationary belt. Therefore, filtering the catalog to exclude known objects that cannot collide with the object of interest reduces computational effort. Three common filters designed by Hoots et al. [11] are:

1.   Apogee/Perigee filter or Altitude filter: The filter admits only object pairs with overlapping altitudes [12]. If a difference between q, the larger of the

two perigees, and Q, the smaller of two apogees, is greater than D, the defined distance threshold, then the secondary does not need to be considered [11].

$$q - Q > D$$

Figure 4 shows one example of an accepted candidate and one filtered candidate excluded from the catalog.
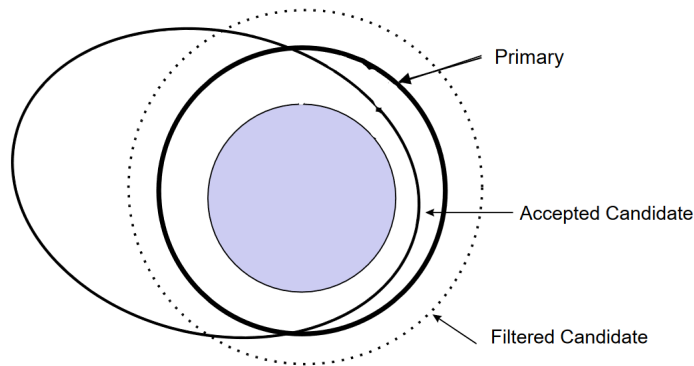
Figure 4.   Apogee/Perigee filter. Source: [12].

2.   Geometric filter or Radial distance: The filter rejects pairings whose orbits at the intersection of their orbital planes have radius separations larger than the maximum extension of the collision reference ellipsoid. This filter does not consider the position of objects in the orbits; only geometry is considered. If the minimum distances are greater than the separation distance threshold D, satellites cannot have a close encounter of interest [11]. In Figure 5, the minimum distances a and b must be smaller than threshold D for pairing to be considered.

8
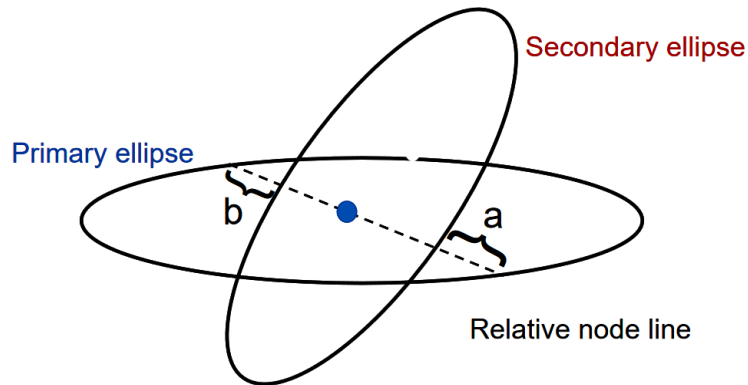
Figure 5.   Geometric filter. Source: [12].

3.   Orbit phase filter: The filter rejects object pairs that, even overlapping, are separated in time at the orbit intersection point. In other words, the satellites must pass simultaneously at the region where the minimum distances are smaller than the defined threshold [11]. Figure 6 shows the relative node crossing of primary and secondary objects.
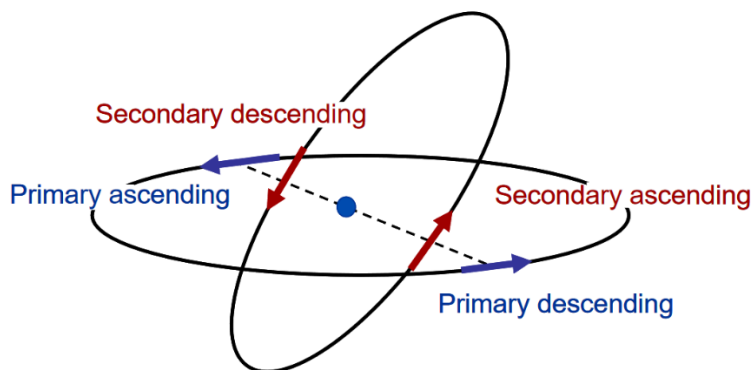
Figure 6.   Relative node crossing. Source: [12].

Alfano and Finkleman [12] tested these filters and concluded that the radial distance filter, called the orbit path filter in their work, has a poorer performance when compared with the other filters.

The 18th Space Control Squadron (18 SPCS) Conjunction Assessment Team uses the High Accuracy Catalog (HAC) and ephemerides provided by owner/operators (O/O) to perform three types of screenings:

1. HAC vs. HAC: SP catalog data for all RSOs screened against SP catalog data for all other RSOs.
2. O/O Ephemeris vs. HAC: Ephemeris provided by the satellite O/O screened against the SP catalog data for all RSOs.
3. O/O Ephemeris vs. O/O Ephemeris: Ephemeris provided by the satellite O/O screened against ephemeris provided by all other O/Os. [13]

The 18 SPCS screening process is performed at least once a day. "If the parameters of the conjunction fall within criteria that identify a close approach and the close approach involves an active satellite, the 18 SPCS will notify the O/O of the active satellite(s)" [13] by sending a conjunction data message (CDM).

A different CDM is generated for every single conjunction between two objects that exceeds the collision probability threshold. The CDM's basic content includes:

Object1/Object2 positions/velocities at TCA with respect to one of a small set of widely used reference frames (ITRF, GCRF—see reference [F11], EME2000);
Object1/Object2 covariances at TCA with respect to an object centered reference frame;
the relative position/velocity of Object2 with respect to an Object1 centered reference frame;
information relevant to how all the above data was determined. [14]

The CDM is an alert and can motivate a deeper analysis of the encounter by the satellite operator, culminating in the conception and execution of a maneuver if the risk exceeds the defined threshold. Figure 7 shows part of a CDM for an ICEYE satellite and debris from IRIDIUM 3; see Appendix A for the complete CDM file.

```
CCSDS_CDM_VERS                    =1.0
COMMENT                           =CDM_ID:377427675
CREATION_DATE                     =2022-11-04T06:48:32.000000
ORIGINATOR                        =CSpOC
MESSAGE_FOR                       =ICEYE-X17
MESSAGE_ID                        =000052762_conj_000034705_2022310125637_30806495279695
TCA                               =2022-11-06T12:56:37.426000
MISS_DISTANCE                     =701                       [m]
RELATIVE_SPEED                    =12690                     [m/s]
RELATIVE_POSITION_R               =340.9                     [m]
RELATIVE_POSITION_T               =-338.2                    [m]
RELATIVE_POSITION_N               =511                       [m]
RELATIVE_VELOCITY_R               =24.1                      [m/s]
RELATIVE_VELOCITY_T               =-10613.5                  [m/s]
RELATIVE_VELOCITY_N               =-6956.3                   [m/s]
COLLISION_PROBABILITY             =0.00000106482
COLLISION_PROBABILITY_METHOD      =FOSTER-1992
COMMENT Screening Option = Covariance
OBJECT                            =OBJECT1
OBJECT_DESIGNATOR                 =52762
CATALOG_NAME                      =SATCAT
OBJECT_NAME                       =ICEYE-X17
```

Figure 7.   Part of a CDM_ID: 377427675 for conjunction between the
satellite ICEYE-X17 and debris from IRIDIUM 33. Source [2].

In parallel with sending data for screening by the 18 SPCS and waiting for the CDMs, operators used to have their own screening procedure. If the operator does not have a customized software solution, one typical option is to use the STK's collision analysis tool, AdvCAT. As in the process just described, the operator must compare the object of interest against an entire space catalog. There are two main catalogs of space objects, the TLE and the special perturbations (SP) catalog, both available on the Space-Track website [2]. While the TLE is publicly available, the SP catalog is available for users with dedicated agreements with the U.S. Space Command (USSPACECOM).

When using STK, the easiest and fastest way to perform the screening process is to use the TLE catalog. One approach using TLE catalog for assessing potential conjunctions is presented in [15]; TLE is also used in STK documentation and training. However, TLE does not provide orbit accuracy for conjunction analysis (CA), and its use for CA is not recommended by NASA. "Some entities use Two-Line Elements (TLEs) to perform CA. This practice is not recommended because the TLE accuracy is not sufficient to perform the necessary CA calculations" [8]. For CA uses, an SP space catalog has been developed and maintained by the 18th Space Control Squadron, the U.S. Space Force unit, on behalf

11

of USSPACECOM. Unlike the TLE, the SP catalog is composed of a set of ephemerides that can be interpolated to obtain the position and velocity of an object at any point within the ephemeris range, typically three days. The short period is one limitation since CA usually propagates the orbital data for seven days. Another weakness of the SP catalog is that, like TLE, it does not have a covariance matrix related to the orbital data.

STK does not import the SP catalog directly as it does with the TLE one, so some work must be done before using the entire SP catalog in STK. This research found at least two different ways to do that: insert all objects one by one into STK or create a collection of objects called SatelliteCollection in STK. In this work, the first option was rejected due to the huge number of objects in the catalog. Following is the step-by-step procedure for the second approach:

1. Download the SP catalog from the Space-Track website: unlike the TLE catalog, the SP catalog is not public; an agreement is required to access it.

2. Generate a .csv file containing information of all objects in the SP catalog.

3. Include a SatelliteCollection object in STK and configure it using the .csv and .eci files. [16]

A MATLAB program was developed in this study to avoid using the TLE catalog for conjunction analysis. The program automatically imports the SP catalog to STK and performs the screening process of the object of interest against the full SP catalog using the AdvCAT tool. Appendix B presents the script which can be used once the SP catalog has been downloaded and unzipped. The output of this script is a CSV file with a list of high-interest events (HIE) based on the threshold defined by the user. Table 1 presents the output of a screening process of an ICEYE satellite against the full SP catalog using the MATLAB script. The results section of this work presents the results of the screening process using the TLE and SP catalogs, respectively.

Table 1.   Screening process report

Conjunction Report for object\48917 against the full SP Catalog						
Conjunctions with probability higher than the defined threshold = 1.00e-04						
Object 2	Max Collision Probability	TCA	Min Range	Min Range - Radial	Min Range - CrossTrack	Min Range - InTrack
Conjunctions with probability higher than the defined threshold = 1.00e-06						
Object 2	Max Collision Probability	TCA	Min Range	Min Range - Radial	Min Range - CrossTrack	Min Range - InTrack
44950.e	8.84E-06	13 Nov 2022 03:44:04.392756038	7.26E-01	6.59E-01	2.16E-01	-2.17E-01
51052.e	1.31E-06	14 Nov 2022 10:46:11.960565684	1.99E+00	1.80E+00	4.60E-01	7.36E-01
35271.e	1.05E-05	14 Nov 2022 10:47:13.194244707	6.51E-01	2.64E-02	4.91E-01	4.27E-01

It is important to note that 18 SPCS makes some assumptions to compute the collision probability reported in the CDM if, for example, they do not know the two objects' respective size, shape, and attitude. All assumptions made bring more conservatism to the collision probability calculation to avoid missing any HIE [13]. Regarding the MATLAB script, the maximum collision probability is calculated using the Salvatore Alfano method [17] implemented in STK. The maximum collision probability approach is chosen because the SP catalog does not provide the covariance matrices for the objects.

The Alfano method computes the maximum collision probability based on the objects' orbit position uncertainty, miss distance, and conjunction geometry. Figure 8 gives one example of his result charts. In this chart, two objects with a summed spherical radius of 5 meters and a miss distance of 1,000 meters, numbers shown on the upper right, reach the maximum collision probability of 10^{-5}. Any conjunction between these two objects with a miss distance greater than 1,000 meters falls into a dilution region where the calculation is invalid. From this chart, it can be concluded that an operator who uses a collision probability threshold of 10^{-4} does not need to compute the collision probability nor perform any collision avoidance action because, with 1,000 meters of miss distance, the maximum probability is 10^{-5} never reaching threshold. For the last example, the miss-distance limit for which the threshold of 10^{-4} is never reached can be found by interpolation.

13
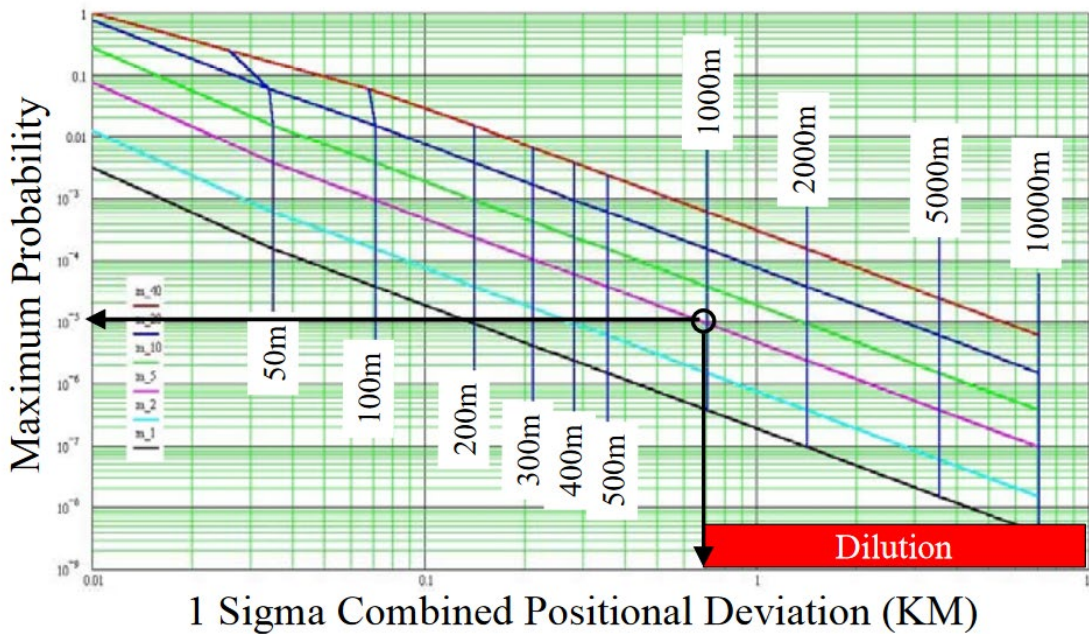
Figure 8.   Sample Alfano chart of maximum collision probability. Source:
[17].

B.   IMPROVING ORBIT DATA OF OBJECTS INVOLVED IN CONJUNCTION

The accuracy of the close-approach prediction depends on the quality of orbit determination for primary and secondary objects. If the position and velocity of both objects are known deterministically, that is, precisely, the conjunction analysis would directly answer whether the objects will collide or not within a particular time interval [18]. However, the relative position between the two objects is not precisely known, and the answer to whether the objects will collide in a specific time interval is not a simple true or false; in fact, it requires a probabilistic approach, and accuracy depends on the quality of the orbit data.

To calculate the risk of collision of two objects more accurately, whenever possible, the operator should refine the orbit data after receiving a CDM or identifying a high-risk event. Regarding the controlled object, the operator can refine the orbit data using the latest orbit determination data or even perform a new orbit determination by increasing the number of measurements, for example. On the other hand, for the second object that the

14

operator does not normally track, the operator can plan optical or radar tracking campaigns to obtain a more accurate orbit, including the covariance matrix [10]. In addition, the orbit data of both objects involved in the conjunction must be examined to determine whether they are fit to be used as described in [8]:

> Finally, the data used to calculate the parameters that feed the risk assessment decision, namely the state estimates and accompanying uncertainty volumes (covariances) for the primary and secondary objects, must be examined to determine whether they manifest problematic elements that would prevent the calculated parameters from serving as a basis for CA mitigation actions. In such cases, it is possible that executing a mitigation action based on those data could make the CA situation worse rather than better.

This last step can avoid, for example, the use of the object state reported in the CDM that was propagated more than the orbit determination time span to reach the time of closest approach (TCA).

C. COMPUTE THE RISK ASSESSMENT

There are different methods and tolerance for calculating and assessing the likelihood of a satellite collision. The two most frequently used methods are miss distance and collision probability at TCA. In the first approach, conjunction is considered high-risk when the distance between the two objects at TCA is less than a defined threshold. This method is conservative and results in many non-necessary collision avoidance actions. NASA recommends that operators employ the collision probability for conjunction assessment method [8]. Even being the most applied technique in the industry, the collision probability method requires attention regarding the premises adopted by the analytical methods and the treatment of the input data. Another consideration is the problem of probability dilution.

This section briefly explains the probability dilution problem, the encounter regions, the covariance matrices, and different methodologies for computing collision probability.

15

1. Probability Dilution

Probability dilution is a primary concern about collision probability. Alfano [17] says we are in a dilution region when given a fixed-mean miss distance at TCA as the variance in the position estimate increases, and the collision probability decreases. In the same way, Balch [19] states this phenomenon "leads to the absurd implication that as data quality decreases, the safety of the satellites being modeled increases. This is a real-word Ostrich Paradox—a situation in which lack of knowledge creates the illusion of safety." Hejduk [20] proposes a graphic way to see if a collision likely falls in a dilution region; Figure 9 shows a plot of collision probability on the y-axis versus the ratio of covariance size to miss distance. Considering the miss distance mean fixed and coming from right to left, we can see that in the dilution region the largest covariance size results in the lowest collision probability; if we keep decreasing the covariance size, we reach a peak, known as the maximum collision probability, and after that, we fall within the robust region in which collision probability calculation has robust results.
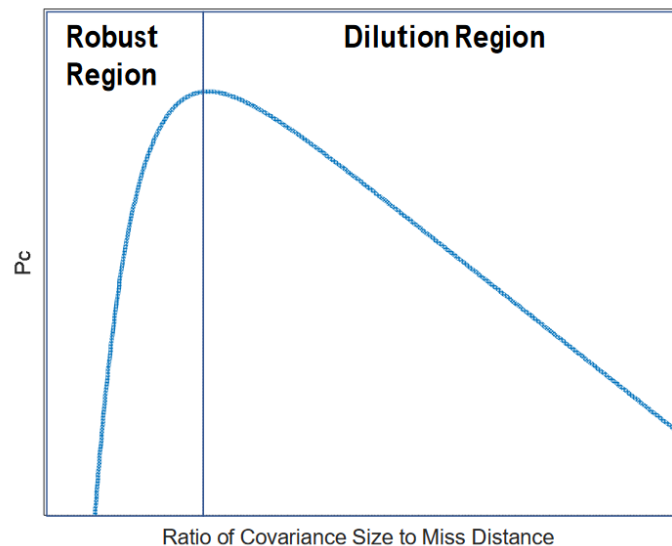
Figure 9.   Pc vs. the ratio of covariance size to miss distance. Source: [20].

Work has been done attempting to solve this issue in [19], [21], [22], but on a practical note, NASA [8] states that "Given that about 85% of the conjunctions that a

16

satellite actually faces cannot be addressed at all because nothing is known about them, it does not make sense that, for the small number of conjunctions for which only poor data are available, large and disruptive mitigations are required." Consequently, NASA concludes that it "is acceptable to treat low-Pc dilution region cases as a small extension of the untracked/uncataloged object conjunctions and not pursue a mitigation action" [8].

2.   Covariance Ellipsoids

The outcome of the orbit determination process is the state vector and the covariance ellipsoids representing the position and velocity uncertainty. As described by Chan [23], to compute the collision probability, we can consider the relative position of one object in relation to the other to obtain the probability density function (pdf) describing the uncertainty of its relative position and then integrate over the region of space swept by the volume of interest as one object moves relative to another. Figure 10 illustrates the covariance ellipsoids of primary and secondary objects with a non-perfect alignment of the velocity vector with their major principal axis.

Assuming the random variables associated with each pdf, which describe the uncertainties of the position of the two objects, are independent or uncorrelated, the relative position covariance C of the two objects can be obtained by the sum of the individual covariances, all expressed in the same coordinate system [23]:

$$C = C_P + C_S$$

where the subscript P and S refer to the primary and secondary objects, respectively.

17
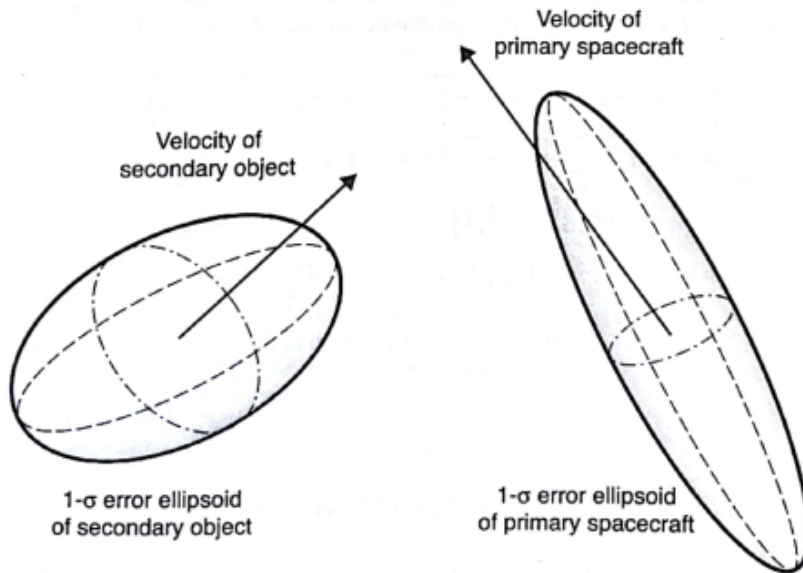
Figure 10.   Covariance ellipsoids of primary and secondary objects. Source: [23].

Figure 11 illustrates a projection plane perpendicular to the vector **n**, obtained by the cross-product of the velocity vectors of primary V_P and secondary V_S. The coordinate system (X, Y, Z) is defined with Y in the direction of the relative velocity V_{PS} of the primary object with respect to the secondary, Z parallel to the vector **n**, and X defined to form the right-hand triad with Y and Z. The other two coordinate systems (X′, Y′, Z′) and (X′′, Y′′, Z′′) are associated with the primary and secondary objects, respectively. The unit vectors Z′ and Z′′ are parallel to **n**, and X′ and X′′ complete the right-hand triad in their respective coordinate systems.

18
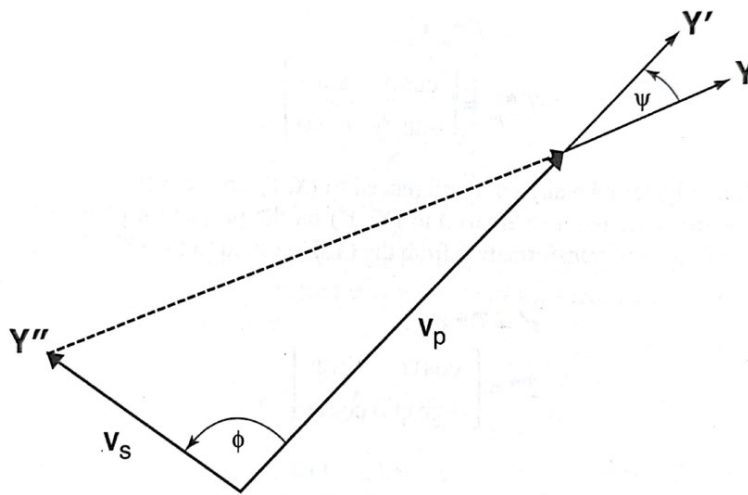
Figure 11.   Projection plane perpendicular to $n \equiv V_p \times V_s$. Source: [23].

The angles ϕ and Ψ are computed from:

$$\cos \varnothing = \widehat{V}_P \cdot \widehat{V}_S \; ; 0 \leq \varnothing \leq \pi$$

$$\cos \psi = \widehat{V}_{PS} \cdot \widehat{V}_P \; ; 0 \leq \varnothing \leq \pi$$

Assuming the major axes of the covariance ellipsoid for the objects are aligned with their respective velocity vectors, the intermediate axes are essentially (but not exactly) aligned in their crosstrack direction, and their minor axes are essentially (but not exactly) aligned in the radial direction, the combined covariance C′ in the (X′, Y′, Z′) coordinate system is given by [23]:

19

$$
C' = \begin{bmatrix} C'_{11} & C'_{12} & 0 \\ C'_{21} & C'_{22} & 0 \\ 0 & 0 & C'_{33} \end{bmatrix}
$$

where

$$C'_{11} = a_p^2 + a_s^2 \cdot \cos^2\phi + b_s^2 \cdot \sin^2\phi$$

$$C'_{12} = C'_{21} = \frac{1}{2} \cdot \left(a_s^2 - b_s^2 \right) \cdot \sin(2 \cdot \emptyset)$$

$$C'_{22} = b_p^2 + a_s^2 \cdot \sin^2\emptyset + b_s^2 \cdot \cos^2\emptyset$$

$$C'_{33} = c_p^2 + c_s^2$$

and where a_p^2, b_p^2, c_p^2 are respectively the crosstrack, intrack, and radial variances of the primary object in the (X′, Y′, Z′) system and a_s^2, b_s^2, c_s^2 are respectively the crosstrack, intrack, and radial variances of the secondary object in the (X″, Y″, Z″) system.

$$
C_p{}' = \begin{bmatrix} a_p^2 & 0 & 0 \\ 0 & b_p^2 & 0 \\ 0 & 0 & c_p^2 \end{bmatrix} ; \quad C_s{}'' = \begin{bmatrix} a_s^2 & 0 & 0 \\ 0 & b_s^2 & 0 \\ 0 & 0 & c_s^2 \end{bmatrix}.
$$

The combined covariance C in the (X, Y, Z) coordinate system is obtained by:

$$C = \begin{bmatrix} C_{11} & C_{12} & 0 \\ C_{21} & C_{22} & 0 \\ 0 & 0 & C_{33} \end{bmatrix}$$

where

$$C_{11} = C'_{11} \cdot \cos^2\psi + C'_{22} \cdot \sin^2\psi - C'_{12} \cdot \sin(2 \cdot \psi)$$

$$C_{12} = C_{21} = \frac{1}{2} \cdot \left(C'_{11} - C'_{22} \right) \cdot \sin(2 \cdot \psi) + C'_{12} \cdot \cos(2 \cdot \psi)$$

$$C_{22} = C'_{11} \cdot \sin^2\psi + C'_{22} \cdot \cos^2\psi + C'_{12} \cdot \sin(2 \cdot \psi)$$

$$C_{33} = C'_{33}$$

3.   Encounter Region

The nonlinear relative motion between two objects in space can be approximated as rectilinear in certain cases. When this approximation is possible, we assume that the objects move along a straight line and the collision probability calculation can be reduced from a three-dimensional integral to a two-dimensional integral. This subsection focuses on the encounter region and transit time where this assumption is valid.

The Gaussian pdf of the relative position of the primary object with respect to the secondary in terms of the combined covariance C, and the collision probability is given by:

$$f_3(x,y,z) = \frac{1}{\sqrt{(2\pi)^3 |C|}} \cdot e^{-\frac{1}{2} \cdot r^T \cdot C^{-1} \cdot r}$$

$$P = \iiint f_3(x,y,z)\, dx\, dy\, dz$$

Chan [23] defined that for 15-digit accuracy, a path length of 85 Km in the y-direction is required in LEOs; this path is reduced to 30 Km for two-digit accuracy. For GEOs, path lengths of 255 Km and 90 Km are required for 15-digit and two-digit accuracy, respectively. The outcome of this process is the reduction of the pdf to a two-dimensional integral. Pdf and probability of collision are reduced to:

21

$$f_2(x,z) = \frac{1}{2 \cdot \pi \cdot \sigma_x \cdot \sigma_z \cdot \sqrt{1 - \rho_{xz}^2}} \cdot e^{-\left[\left(\frac{x}{\sigma_x}\right)^2 - 2 \cdot \rho_{xz} \cdot \left(\frac{x}{\sigma_x}\right) \cdot \left(\frac{z}{\sigma_z}\right) + \left(\frac{z}{\sigma_z}\right)^2\right] \Big/ 2 \cdot \left(1 - \rho_{xz}^2\right)}$$

$$P = \iint f_2(x,z)\, dx\, dz$$

Figure 12, illustrates the non-linear relative motion between two spacecraft and the required path length for the rectilinear approximation to be valid.
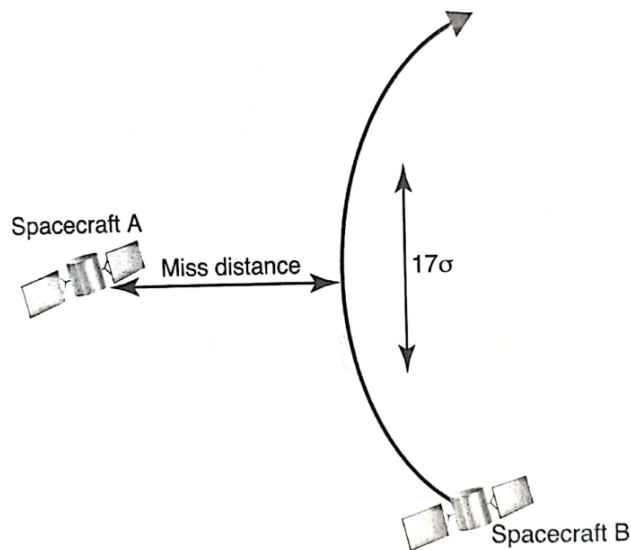
Figure 12.   Requisite path length for integration. The length must be 17σ (85 Km for LEO and 225 Km for GEO). Source: [23].

4.   Rectilinear Approximation Test and Collision Probability Computation Using STK

The AdvCAT tool offers the following methods for calculating collision probability: Collision Probability (Analytical), Collision Probability (Numeric), Collision Probability (Patera 2005), Collision Probability (Maha), adjoining parallelepipeds (bundles), and adjoining tubes (cylinders). The first four methods, which are based on the works of Ken Chan, Sal Alfano, Russell Patera, and P. C. Mahalanobis, respectively, assume rectilinear relative motion. When one of the four mentioned methods is chosen, the calculation will be done without any alert to the operator, even if the conjunction does not

22

offer the necessary characteristics for the approximation of rectilinear motion to be valid. Therefore, it is important that the operator be aware of this and perform a linear relative motion test to define the appropriate method for use in the calculation of the collision probability. The operator may conclude that it is always better to choose one of the last two methods listed, as they do not apply approximate linear movement, thus avoiding problems. Although this conclusion is proper, the operator must consider that these methods require very intensive calculations and return very close values when linearity is valid. Thus, they can be avoided without loss of accuracy in the calculation in many cases.

STK offers a tool to test linearity of the relative motion [24]. The test consists of determining the minimum relative velocity to ensure the pre-specified probability difference will not be exceeded. Therefore, the rectilinear motion approximation is valid if the relative velocity at TCA exceeds the minimum.

Appendix C contains a proposed MATLAB-STK integration program that, given two STK ephemeris files (.e file) with covariance, performs the linearity test and the collision probability calculation accordingly. Table 2 shows the result of the linear motion test and probability calculation for a conjunction between the ICEYE X1 satellite and Cosmo debris. In this scenario, the conjunction did not meet the criteria for the linear motion assumption, so the method used to calculate the probability of collision was the adjoining tubes (cylinders), which does not apply the linearity assumption.

Table 2.   Collision probability report

Conjunction assessment between ICEYE_X1 and COSMOS_1484_DEBRIS objects			
TCA (UTCG)	Collision Probability	Comp. Method	Min Range (Km)
30 Oct 2022 15:54:21.521741912	1.20E-05	Nonlinear-Cylinders	4.46E-01

End of Report

It is important to note that when the rectilinear motion approximation is valid, the four mentioned methods are sufficiently accurate that the operator is free to choose any one of them [24].

23

D.   COLLISION AVOIDANCE ACTION

Once the risk of collision is greater than the threshold defined by the operator, a collision avoidance action must be applied to reduce the risk at TCA under an acceptable level without generating new post-high-risk conjunction (see an example of a conjunction analysis procedure in Figure 13). There are different techniques to reduce the probability of collision between two objects in space. The propulsive maneuver is most applied for satellites equipped with thrusters. Based on the type of propulsion system, spacecraft maneuvers can be classified into two groups: impulsive and continuous thrust maneuvers.

On impulsive maneuvers, short firings of onboard thrusters change the magnitude and direction of the velocity vector instantaneously while keeping the position vector. This definition is an idealization for the case where the position vector changes only slightly during the maneuver; it is valid for high-thrust rockets, for example [9]. Each impulsive maneuver changes the velocity by a magnitude of ΔV; this change is related to the consumed mass during the thrust firing Δm and the propellant's specific impulse (Isp). In mathematical terms,

$$\Delta v = Isp \cdot g_0 \cdot \ln\left(\frac{\Delta m}{m}\right)$$

where m is the mass of the spacecraft before the burn, and g_0 is the sea level standard acceleration of gravity. Specific impulse is defined as the thrust force produced per unit weight of fuel consumed per second expressed by the equation [25]:

$$Isp = \frac{Thrust\ Force}{Sea - level\ weight\ rate\ of\ fuel\ consumption}.$$

While impulsive maneuvers occur in approximately zero time, in the continuous/ non-impulsive maneuvers, the thrusters are fired for a considerable time and must be included in the equation of motion [9]:

$$\ddot{r} = -\mu \cdot \frac{r}{r^3} + \frac{T}{m}$$

where $\mathbf{r}$ = position vector, $\ddot{\mathbf{r}}$ = acceleration vector, $\mathbf{T}$ = thrust vector, m = spacecraft mass, and μ = gravitational constant. When thrusters are firing, spacecraft mass decreases at a rate of

24

$$\frac{dm}{dt} = \frac{T}{Isp \cdot g_0}.$$

Although maneuvers are the primary option for spacecraft equipped with propulsion systems, other collision avoidance action possibilities exist, such as the use of aerodynamic techniques. One option is to change the satellite attitude to increase the drag area in the direction of movement or to change the solar pressure force [18]. As a last option, the satellite operator who does not have a propulsion system can, when in conjunction with a maneuverable satellite, share its more accurate ephemeris data so that the second object operator can perform a safer avoidance maneuver [8].
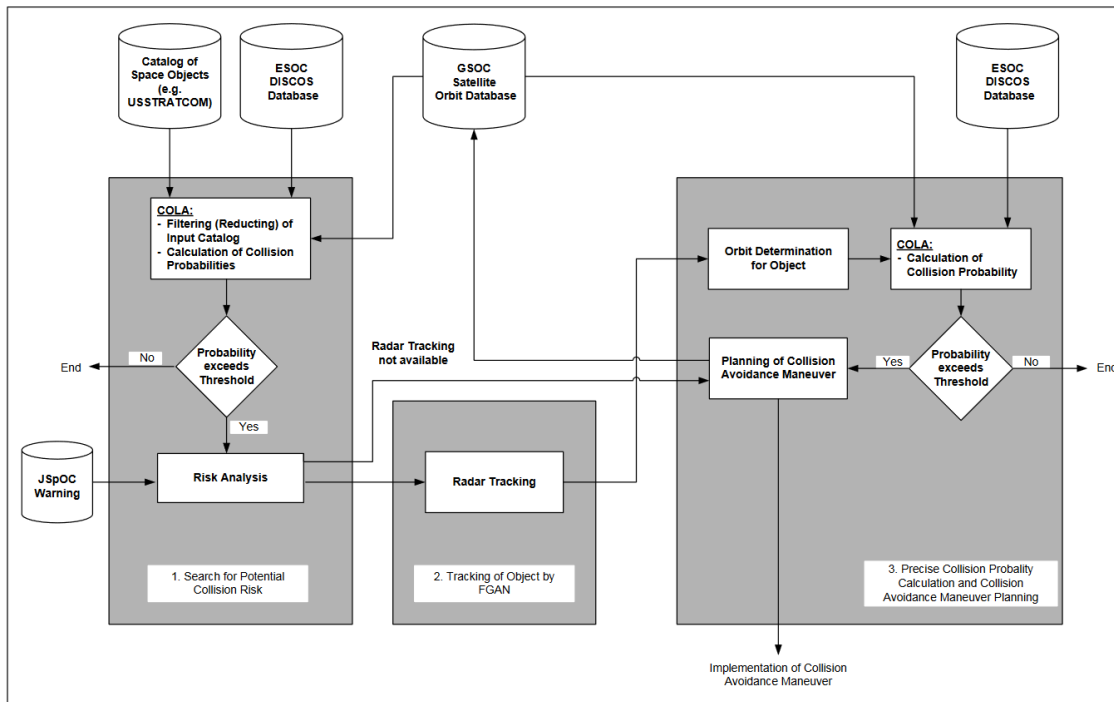
Figure 13.   Overview of the German Space Operation Center collision avoidance procedure. Source: [10].

THIS PAGE INTENTIONALLY LEFT BLANK

III. ICEYE CONSTELLATION

A. OVERVIEW

ICEYE is a Finnish company renowned for being the first to develop, launch, and operate a small SAR satellite called X1, which was launched in January 2018 [26]. The current ICEYE constellation has 20 satellites and continues to grow, as shown in Figure 14. Table 3 shows the current ICEYE satellite baseline parameters, and Figure 15 shows an artist's illustration of the ICEYE satellite generation 2.
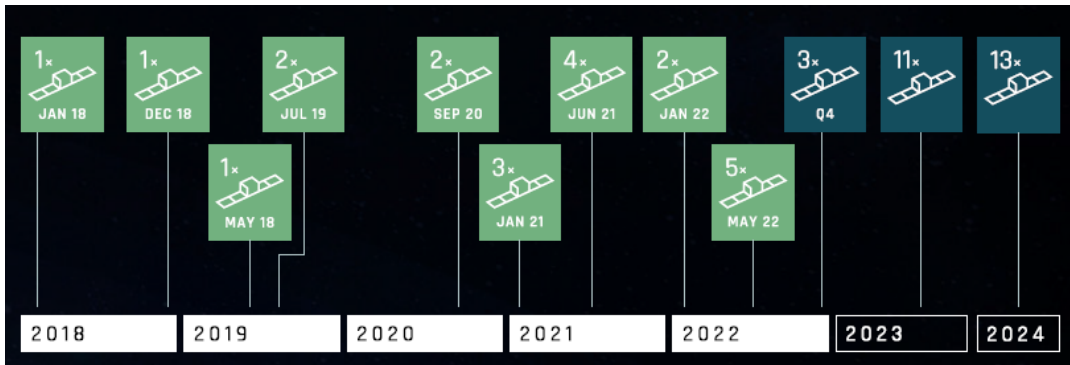
Figure 14.   ICEYE constellation development. Source: [27].
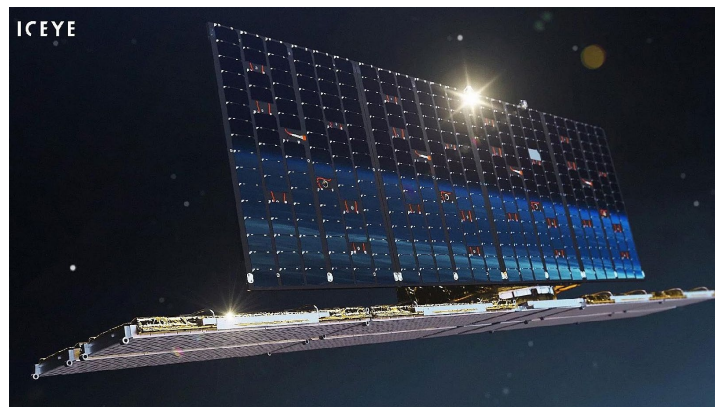
Figure 15.   ICEYE Generation 2 Satellite. Source: [28].

27

Table 3.   System parameters of the ICEYE baseline constellation. Source: [29].

SYSTEM PARAMETER	SPECIFICATION VALUE
carrier frequency	9.65 GHz
look side	both LEFT and RIGHT
antenna size	3.2 m x 0.4 m
PRF	2-10 kHz
range bw	40-300 MHz
peak power	4 kW
polarization	VV
incidence angle (Strip)	10-30 deg
incidence angle (Spot)	20-35 deg
incidence angle (Scan)	21-29 deg
mass	85 kg

ICEYE, currently the largest operational SAR constellation in orbit, enables monitoring of an area of interest every 24 hours, which was not possible before [27]. The ICEYE SAR payload has three imaging modes: strip, spot, and scan, as shown in Figure 16 and described in the following paragraphs:

- Strip mode: In this mode, the ground swath is illuminated with a continuous sequence of pulses while the antenna beam is fixed in its orientation. The beam is pointed off to the side of the satellite at an angle broadside to the satellite's flight path. This results in a long image strip parallel to the flight direction. ICEYE standard Strip products have a ground resolution of 3m in range and azimuth and cover an area of 30km (range) by 50km (azimuth). The strip length can be tailored up to a length of 500 km, in increments of 50 km.

- Spot mode: In Spot mode the radar beam is steered to illuminate a fixed point. This increases the illumination time and therefore increases the length of the synthetic aperture and improves azimuth resolution. ICEYE Generation2 satellites have a maximum 300 MHz pulse bandwidth in Spot Mode to achieve a 0.5 m slant range resolution (here is an explanation of where this comes from.). This will improve to 600 MHz for our

28

Generation3 version. ICEYE's standard Spot collection covers an area of 5 km x 5 km with a 1 m ground resolution for multi-looked amplitude images. These are formed from 4 independent looks to suppress speckle and increase image quality. Alternatively, customers can request an *extended area* spot image. This uses a slightly modified spot collection (sometimes called sliding spot) in which the beam is allowed to slide just a bit. This increases collection area and trades the number of looks to preserve resolution for amplitude images. The *Spot extended area* collection has a scene size of 15 km x 15 km at 1 m ground resolution with no multi-looking applied.

- Scan mode: This mode uses the phased array antenna to create multiple beams in the elevation direction. This beam steering illuminates a wide area via multiple adjacent strips, but it means that points on the ground are not illuminated for as long as in conventional Strip Mode. This reduces the resolution of a Scan product. In conventional scan mode, ground points are illuminated by different parts of the radar beam resulting in brighter and darker regions in the image. We compensate for this in our scan by also steering the radar beam sideways during each burst of radar pulses. This improves image quality. This technique is called Terrain Observation by Progressive Scans (TOPS or TOPSAR[1]). Our Scan product produces imagery that covers an area of 100 km x 100 km with a resolution better than 15 m. The length of a Scan product can be increased to 500 km. [30]
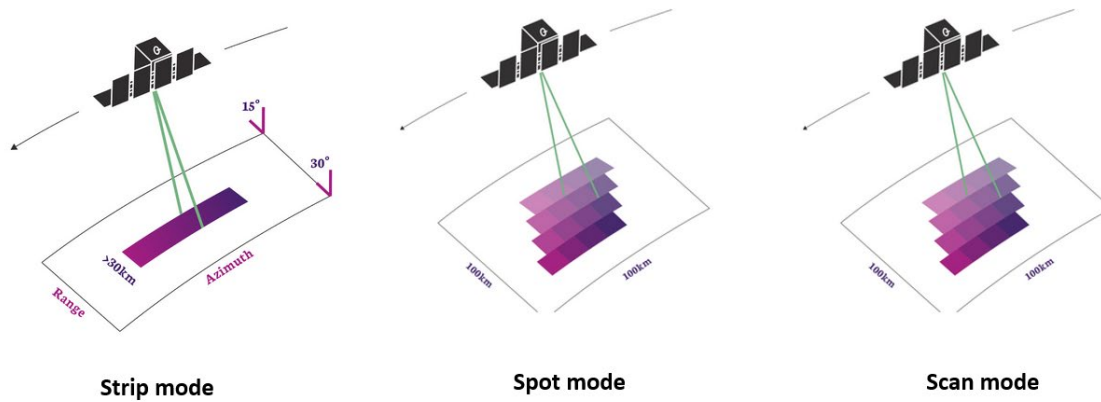
Figure 16.   ICEYE imaging modes. Source: [30].

B.   TECHNICAL CHARACTERISTICS AND OPERATIONAL CONSTRAINTS

This section focuses on the technical characteristics and operational constraints relevant to orbit maneuvering and collision probability calculations. Assumptions are made and highlighted for any essential data not available. ICEYE's configuration has changed since the X1 launch; for this work, the newest configuration is considered as much as possible.

1.   Technical Parameters

The physical configuration of the ICEYE satellite, with a total mass of 92 kg includes the main bus, the SAR antenna, and the solar panel [28]. The bus configuration has a size of 0.7 m (H) × 0.6 m (W) × 0.4 m (D) [31]. The antenna has a size of 3.2 m x 0.4 m [28], and this research assumed the solar array's total area is equal to the antenna area of 1.28 m^2.

ICEYE satellites are equipped with four IFM 350 nano thrusters [32] produced by ENPULSION spacecraft technology company using a high specific impulsive liquid metal electric Field Emission Electric Propulsion (FEEP) system developed by FOTEC [33]. Table 4 presents the main parameters of IFM 350 nano, and Figure 17 shows the thruster's flight configuration and the thruster in operation.

Table 4.   IFM 350 Nano Thruster. Source: [32].

PARAMETER	VALUE
Dynamic thrust range	10 µN to 0.5 mN
Nominal thrust	350 µN
Specific impulse	2,000 to 5000 s
Propellant mass	250 g
Total impulse	more than 5,000 Ns
Power at nominal thrust	35 W incl. neutralizer
Outside dimensions	94 x 90 x 78 mm
Mass (dry / wet)	640 / 870 g
Total system power	8 – 40 W
Hot standby power	3.5 W
Command interface	RS422/RS485
Temperature envelope (non-operational)	-50 to 120°
Temperature envelope (operational)	-20 to 50 °C
Supply voltage	12V, 28 V, other voltages upon request

(a) Flight configuration   (b) Operation
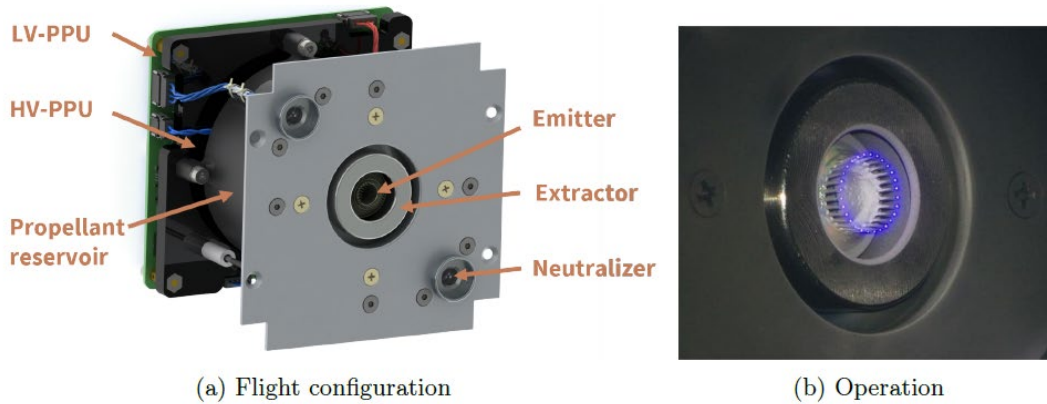
Figure 17.   IFM Nano Thruster. Source: [33].

This research assumed the ICEYE can perform prograde and retrograde maneuvers based on the movement possibilities stated in [28]: "The satellite orbital agility is provided via a set of ion thrusters positioned around the satellite. These provide a near limitless supply of maneuvering thrust, and also ensure that the constellation can be rapidly configured to increase the coverage rate of certain geographic regions in response to world events."

2. Operational Constraints

Power generation is a constraint for small SAR satellites due to the small solar panel area and because both the SAR system and data link require a substantial amount of power. One possible mitigation solution is to oversize the batteries to increase the imaging and downlink time [34]. The situation gets worse for satellites equipped with electric propulsion systems, which also require a significant amount of energy, thus limiting the operational modes of the payload. For this work we consider when propulsion systems are on payload and data links are off. Another limitation due to power constraints is the thrust arc duration; here, we consider 30 minutes of maneuver time as the maximum [32].

IV. COLLISION AVOIDANCE STRATEGIES

A. TANGENTIAL THRUST CONTROL STRATEGY

This section presents two approaches to designing a collision avoidance maneuver using tangential acceleration. The first one was presented by Hernando-Ayuso and Bombardelli [35] for conjunctions between two objects in circular orbits. A second strategy is a semi-analytical approach demonstrating the importance of planning low-thrust CAMs with sufficient lead time to TCA [36]. Since the tangential maneuver has a fixed thrust direction, the control parameters for the low-thrust propulsion system are limited to the magnitude and the starting and ending times of the collision avoidance maneuver [36].

1. Low-thrust CAM in a Circular Orbit

The work developed by Hernando-Ayuso and Bombardelli [35] shows tangential CAM performs similarly to an optimal direction CAM when applied with sufficient lead time to TCA. In this subsection, we focus only on the tangential approach of their study to see how the collision probability relates to the lead time to TCA and to the angle between the ζ axis and the x axis.

In their study, the authors made the following assumptions: both objects are in circular orbit; thrust acceleration is constant during the maneuver; and mass variation is negligible. Also, b-plane variables and the hypothesis of short-term encounter are employed. Figure 18 shows the B-plane geometry at the closest approach where v_1 and v_2 are the velocity vectors of objects S1 and S2, respectively, in an S2-centered reference frame (ξ, η, ζ) with ξ pointing toward the cross product of the velocity vector of S2 with the velocity vector of S1, η along the direction of the relative velocity of S1 with respect to S2, and ζ to complete a right-hand coordinate system. The expected position vector of S1 relative to S2 at TCA when projected in the S2-centered inertial frame is $r = (\xi, 0, \zeta)^T$. A two-dimensional position vector in the B-plane, called b-vector, constructed by the first and third elements of the r vector is defined as $b = (\xi, \zeta)^T$. The b-plane reference frame has the unit vectors:

33

$$u_\eta = \frac{v_1 - v_2}{|v_1 - v_2|}; \quad u_\xi = \frac{v_2 \times u_\eta}{|v_2 \times u_\eta|}; \quad u_\zeta = u_\xi - u_\eta.$$
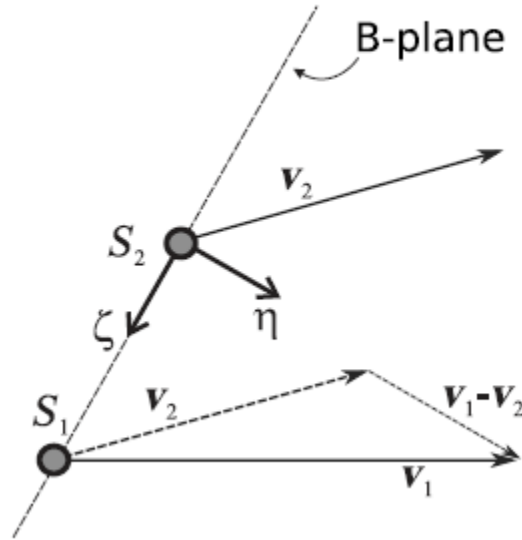
Figure 18.   B-plane geometry at the closest approach. Source: [35].

A CAM will produce a shift in S1 B-plane position vector of $\Delta r = (\Delta \xi, \Delta \eta, \Delta \zeta)^T$, which can be related to a maneuver-induced time-position shift $x = (\Delta t, \Delta r, \Delta z)^T$ through the linear relation:

$$\Delta r = RK\Delta x$$

where $\Delta t, \Delta r, \Delta z$ are, respectively, the accumulated time delay, radial shift, and out-of-plane shift of the maneuvered spacecraft at the conjunction true longitude compared with its "unmaneuvered" trajectory, and the R and K matrices read, for the circular case:

$$R = \begin{bmatrix} 0 & 0 & -1 \\ \sin\left(\frac{k}{2}\right) & -\cos\left(\frac{k}{2}\right) & 0 \\ -\cos\left(\frac{k}{2}\right) & -\sin\left(\frac{k}{2}\right) & 0 \end{bmatrix}; \quad K = \begin{bmatrix} -v_1 & 0 & 0 \\ 0 & 0 & \pm 1 \\ 0 & \pm 1 & 0 \end{bmatrix}$$

where v_1 is the velocity of object 1, k is the angle between the two orbital planes, and the minus (plus) sign must be employed when the ξ axis of the B plane points radially outward (inward). Using the first and third elements of r vector, an R' matrix reads, for the circular case:

$$R' = \begin{bmatrix} 0 & 0 & -1 \\ -\cos\left(\dfrac{k}{2}\right) & -\sin\left(\dfrac{k}{2}\right) & 0 \end{bmatrix}.$$

The thrust acceleration vector $u = \left(u_r, u_0, u_h \right)^T$, where components are respectively radial, transversal, and out-of-plane in a local-vertical-local-horizontal orbital frame. An infinitesimal time span δt produces a velocity variation of $\delta v = u\delta t$ which represents a displacement in B-plane of:

$$\delta b = R' \cdot K \cdot D \cdot u \cdot \delta t = M' \cdot u \cdot \delta t$$

$$\frac{\delta b}{\delta t} = M' \cdot u \qquad .$$

The differential equation above is the time evolution of the B-plane coordinates while the continuous thrust has been applied, and the **D** matrix for the circular case is:

$$D = \begin{bmatrix} D_{tr} & D_{t\theta} & 0 \\ D_{rr} & D_{r\theta} & 0 \\ 0 & 0 & D_{wh} \end{bmatrix}$$

with

$$D_{rr} = \frac{\sin(\Delta\theta)}{n_1}; \;\; D_{r\theta} = \frac{2 - 2\cdot\cos(\Delta\theta)}{n_1}; \; D_{tr} = \frac{2 - 2\cdot\cos(\Delta\theta)}{n_1{}^2 \cdot r_1}$$

$$D_{t\theta} = 4\cdot\frac{3\cdot\Delta\theta - \sin(\Delta\theta)}{n_1{}^2 \cdot r_1}; \; D_{wh} = \frac{\sin(\Delta\theta)}{n_1}$$

and where

$$\Delta\theta = \theta_c - \theta = \frac{t_c - t}{n_1}.$$

35

In the preceding equation, $\Delta\theta$ is the angular distance between the infinitesimal continuous-thrust maneuver θ and the point of TCA θ_c, and the mean motion is the function of orbital period $n_1 = 2 \cdot \pi / T_1$.

A tangential thrust acceleration of constant magnitude a_0 produces a radial variation and time delay of:

$$\Delta r_1 \cong 2 \cdot a_0 \cdot \frac{r_1^3}{\mu} [\Delta\theta_t + \sin(\Delta\theta_c) - \sin(\Delta\theta_t + \Delta\theta_c)]$$

$$\Delta t \cong a_0 \cdot \frac{r_1^{3.5}}{\mu^{1.5}} \left[3 \cdot \Delta\theta_t \left(\frac{\Delta\theta_t}{2} + \Delta\theta_c \right) - 8 \cdot \sin\left(\frac{\Delta\theta_t}{2} \right) \cdot \sin\left(\frac{\Delta\theta_t}{2} + \Delta\theta_c \right) \right]$$

where $\Delta\theta_t$ and $\Delta\theta_c$ are respectively the thrust arc and coast arc durations, and μ is the Earth's gravitational parameter.

Appling these two expressions in the $\Delta r = RK \Delta x$, presented above, the B-plane position at the end of thrust arc is:

$$\xi \cong \xi_0 \pm \Delta r_1$$

$$\zeta \cong \zeta_0 + a_0 \cdot \frac{r_1^3}{\mu} \cdot \cos\left(\frac{k}{2} \right) \cdot \left[3 \cdot \Delta\theta_t \left(\frac{\Delta\theta_t}{2} + \Delta\theta_c \right) - 8 \cdot \sin\left(\frac{\Delta\theta_t}{2} \right) \cdot \sin\left(\frac{\Delta\theta_t}{2} + \Delta\theta_c \right) \right]$$

where the plus (minus) sign must be employed when the ξ axis of the B plane points radially outward (inward).

The collision probability is calculated using García-Pelayo and Hernando-Ayuso's formula and can be used to choose the location of the tangential thrust arc. Also, the thrust arc duration can be adjusted to reach the desired collision probability.

$$P \cong \frac{S_A^2}{2\sigma_x\sigma_y} \left[1 + \frac{1}{8} \left(\frac{x^2/\sigma_x^2 - 1}{\sigma_x^2} + \frac{y^2/\sigma_y^2 - 1}{\sigma_y^2} \right) \right] \cdot \exp\left(-\frac{1}{2} \left(\frac{x^2}{\sigma_x^2} + \frac{y^2}{\sigma_y^2} \right) \right)$$

where S_A is the sum of the radii of objects 1 and 2, x and y are the B-plane position vector components along the corresponding eigenaxes, and σ_x and σ_y are semi-principal axes of the 1-sigma covariance ellipse. In terms of math, x and y are:

$$x = \xi \cdot \cos(\theta) + \zeta \cdot \sin(\theta)$$
$$y = \xi \cdot \sin(\theta) - \zeta \cdot \cos(\theta)$$

36

where θ is the angle between the ζ axis and the x axis.

Hernando-Ayuso and Bombardelli [35] used the following parameters to calculate the initial collision probability and then applied tangential collision avoidance maneuvers using the equations just presented to see how the lead time in terms of the number of revolutions before TCA changes maneuver performance in relation to collision probability. Variations in the orbital parameters were also made to evaluate their influence on the performance of the collision avoidance maneuver. The two objects are in circular orbit with inclination of 53 degrees. The maneuverable satellite with 300 kg and a nominal 10 mN thrust for a 60 deg thrust arc duration has an altitude of 550 km while the non-cooperative object has an altitude of 550.2 km. The combined position covariance has eigenvalues σ_x = 80 m and σ_y = 1500 m and is rotated with respect to the B-plane axis by an angle θ. The estimated pre-maneuver B-plane coordinates are assumed to be ξ_0 = 200 m and ζ_0 = 0 m, with the ξ axis of the B-plane pointing toward the Earth, and n_{rev} is the number of revolutions from the middle of the thrust arc until TCA. For a given thrust arc width $\Delta\theta_t$, the beginning and end of thrust arc and the coasting arc width $\Delta\theta_c$, are defined as:

$$\Delta\theta(t_0) = 2 \cdot \pi \cdot n_{rev} + \frac{\Delta\theta_t}{2}$$

$$\Delta\theta(tf) = 2 \cdot \pi \cdot n_{rev} - \frac{\Delta\theta_t}{2}$$

$$\Delta\theta_c = \Delta\theta(tf)$$

The equations for the circular case were implemented in MATLAB to reproduce the results; see Appendix D for the code.

Figure 19 shows the results for prograde CAMs with three different thrust arc durations, 60, 120, and 200 degrees. The results show an oscillatory behavior in terms of collision probability reduction with respect to the point where the CAM is performed with local minima and maxima located near complete and half values of the number of revolutions before TCA. These results can be used to define the point of performing the maneuver and the thrust arc duration. Since to reach the threshold, all maneuvers needed

37

to be performed with at least four revolutions before TCA, we can conclude the low-thrust collision avoidance maneuver lacks the last-minute option.
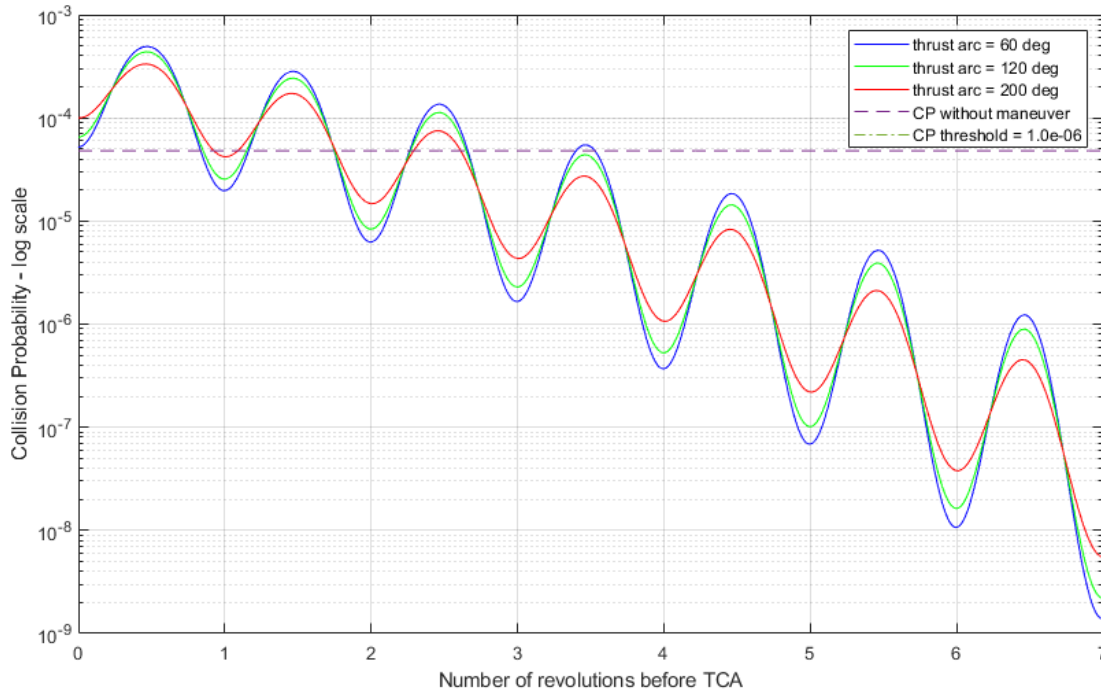
Figure 19.   Collision probability for CAM with thrust arc = 60, 120, and 200 deg.

Another point to be evaluated is the influence of θ angle on the collision probability. Collision avoidance maneuvers with a nominal thrust arc of 60 deg are performed for seven different θ angles. As we can see in Figure 20, for a prograde maneuver, small values of θ angle result in a need for longer lead time to decrease the collision probability under the threshold. On the other hand, if the spacecraft can perform retrograde maneuvers, the last-minute maneuver appears as one good option. As we can see in Figure 21, a retrograde maneuver in the scenario with θ angle = 1 (green line) performed 0.5 revolutions before TCA gives better results in terms of collision probability than does a prograde maneuver performing 5.5 revolutions in advance. From these two figures, we can conclude CAM performance is related to the θ angle. For angles smaller than 5 degrees, a last-minute retrograde maneuver performed better than a prograde maneuver, and for θ angle bigger

38

than 5 degrees, a prograde maneuver with enough lead time can result in a collision probability under the threshold.
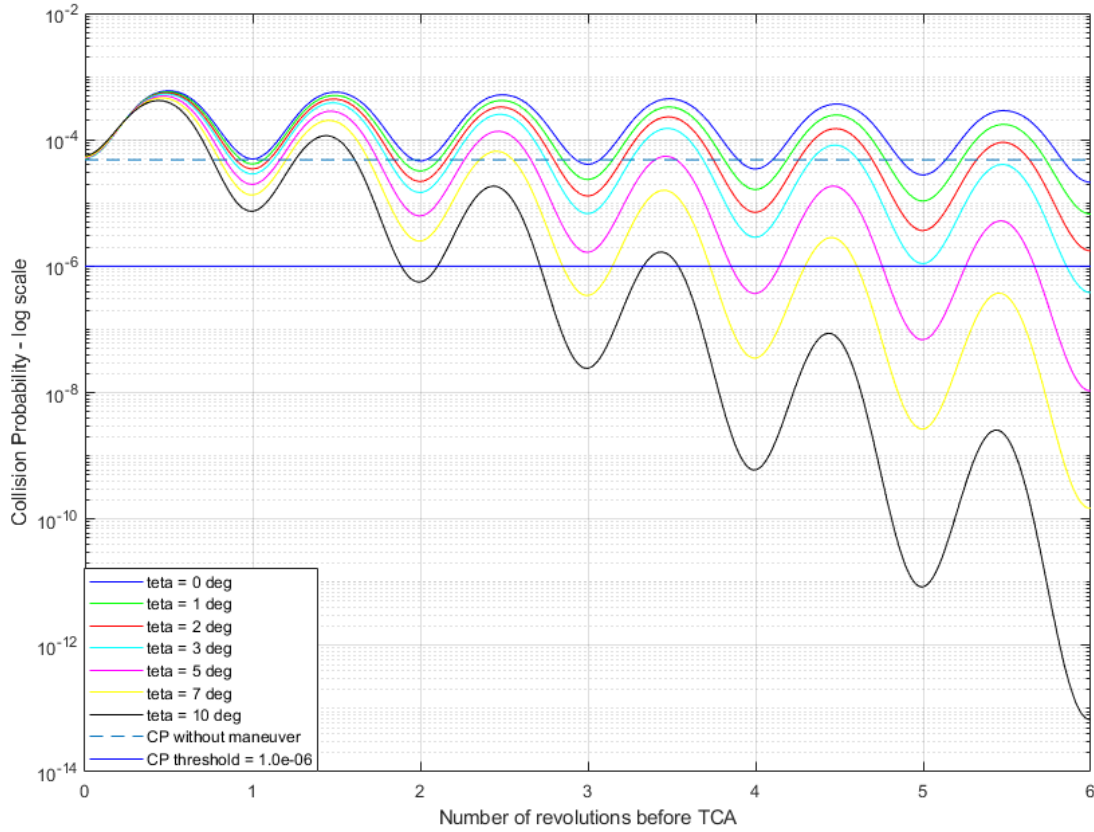
Figure 20. Collision probability for prograde CAM with thrust arc = 60 and different values of θ angle.
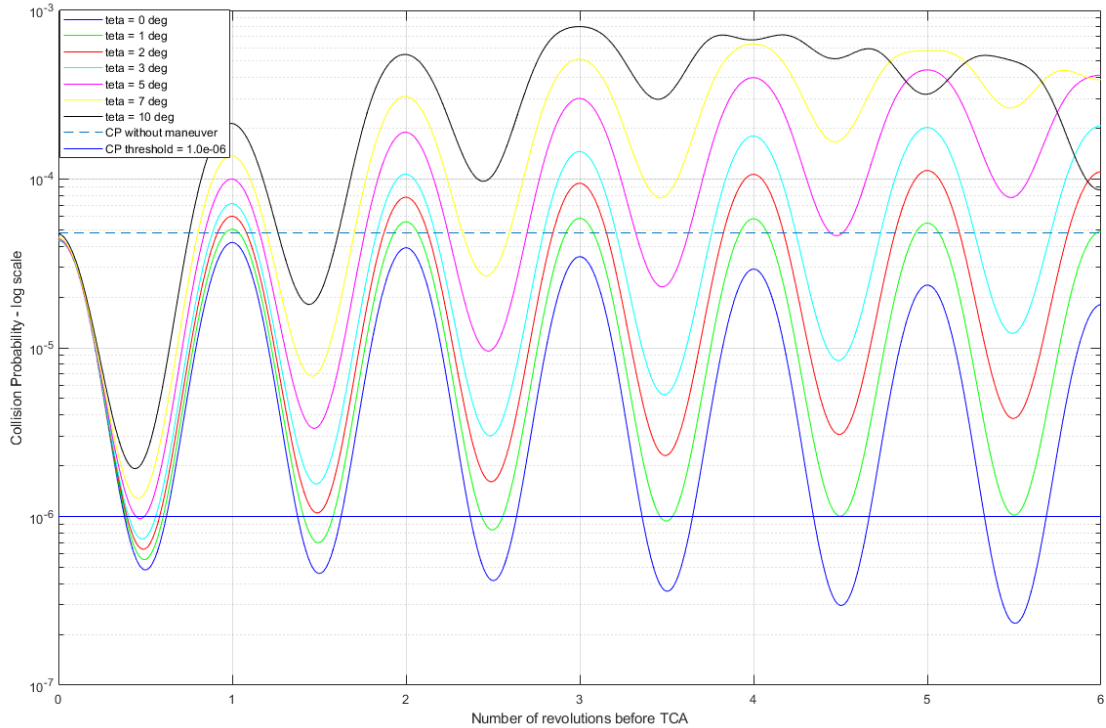
Figure 21.   Collision probability for retrograde CAM with thrust arc = 60 and different values of θ angle.

2.   A Semi-analytical Approach to Low-thrust Collision Avoidance Maneuver Design

This subsection describes the semi-analytical solution for a low-thrust CAM design obtained from [36]. As in the previous subsection, the authors use the b-plane to analyze the conjunction. They assume thrust acceleration is constant over one revolution, and mass variation is negligible for a typical CAM.

The vector $\boldsymbol{\alpha} = [a, e, i, \Omega, \omega, M]$ containing the Keplerian elements semi-major axis, eccentricity, inclination, right ascension of ascending node, argument of perigee, and mean anomaly is defined, and $\delta\boldsymbol{\alpha}$ represents the change in these elements at TCA. Gauss' planetary equations for a constant tangential acceleration a_t is represented in terms of eccentricity anomaly E.

Gauss' planetary equations:

$$\frac{da}{dt} = \frac{2\,a^2\,v}{\mu} \cdot a_t$$

$$\frac{de}{dt} = \frac{2\,(e + \cos(f))}{v} \cdot a_t$$

$$\frac{di}{dt} = o$$

$$\frac{d\Omega}{dt} = 0$$

$$\frac{d\omega}{dt} = \frac{2\,\sin(f)}{e\,v}\,a_t$$

$$\frac{dM}{dt} = n - \frac{2\,b}{e\,a\,v}\left(1 + \frac{e^2\,r}{p}\right)\sin(f)\,a_t$$

where f is the true anomaly.

Gauss' planetary equations in terms of E:

$$\frac{da}{dE} = a_t\,\frac{2\,a^3}{\mu}\sqrt{1 - e^2\cos^2(E)}$$

$$\frac{di}{dE} = o$$

$$\frac{d\Omega}{dE} = 0$$

$$\frac{d\omega}{dE} = a_t\,\frac{2\,a^2\sqrt{1 - e^2}}{\mu\,e}\sqrt{\frac{1 - e\cos(E)}{1 + \cos(E)}}\,\sin(E)$$

$$\frac{dM}{dE} = (1 - e\cos(E))\left(1 - a_t\,\frac{2\,a^2\left(1 - e^3\cos(E)\,\sin(E)\right)}{e\,\mu\sqrt{1 - e^2\cos^2(E)}}\right)$$

where dE/dt is approximated as:

$$\frac{dE}{dt} \approx \sqrt{\frac{\mu}{a^3}}\,\frac{1}{1 - e\cos(E)}.$$

Assuming E varies over one revolution and integrating the right side of the equations, the following primitives are reached:

$$H_a(E) = a_t \frac{2\,a^3\sqrt{1-e^2}}{\mu} E\left[E,\ -\frac{e^2}{1-e^2}\right]$$

$$H_e(E) = a_t \frac{2\,a^2\left(1-e^2\right)}{\mu\,e}\left[\frac{1}{2}\ln\left(\frac{\sqrt{1-e^2\cos^2(E)}\ +\ e\sin(E)}{\sqrt{1-e^2\cos^2(E)}\ -\ e\sin(E)}\right) - \frac{1}{\sqrt{1-e^2}}F\left[E,\ -\frac{e^2}{1-e^2}\right] + \sqrt{1-e^2}E\left[E,\ -\frac{e^2}{1-e^2}\right]\right]$$

$$H_i(E) = H_\Omega(E) = 0$$

$$H_\omega = a_t \frac{2\,a^2\sqrt{1-e^2}}{\mu\,e}\left[2\,a\sin\left(\frac{\sqrt{1-e}\cos(E)}{2}\right) - \sqrt{1-e^2\cos^2(E)}\right]$$

where F[·,·] and E[·,·] are the incomplete elliptic integrals of the first and second kind, respectively. These analytical equations approximate the variations of all elements in **α,** save for M. The mean variation of **α** elements for a continuous thrust CAM of one revolution takes the form of:

$$\Delta\alpha = H_\alpha(2\pi) - H_\alpha(0)$$

To compute M variation, it is necessary to numerically integrate over the whole CAM the equation dE/dt and over the fraction of the last, incomplete revolution the equation dM/dE, both of which were described previously. Due to the need for these two numerical integrations, the method is not considered entirely analytical.

The results in [36] were computed using the orbital elements for spacecraft and debris at TCA as presented in Table 5. This data was used in STK to compute the 6.5 meters miss distance at TCA. Figure 22 provides a 3D view at the time of closest approach. In their work, several different tangential maneuvers were performed with different maneuver durations (Δt_{CAM}) and lead times from the end of maneuver to TCA (ΔT_f); these are the only two maneuver variation options since the direction is fixed. Figure 23 shows the deflection in b-plane produced by a 10^{-6} m/s^2 acceleration with different Δt_{CAM} and Δt_f. The relation between the lead time and displacement can be seen when we analyze the result of a CAM with $\Delta t_{CAM} = 2$ orbital periods and varying Δt_f from 1 to 5 orbital periods; for that case, the displacement increases approximately 0.4 km. Therefore, the same acceleration applied for the same amount of time gives different results by varying the lead time.

Table 5.   Keplerian orbital elements at CA for spacecraft and debris. Source: [36].

	Spacecraft	Debris
a [km]	7093.637	7782.193
e [$-$]	0.0014624	0.0871621
i [deg]	98.2443	88.6896
Ω [deg]	303.5949	142.7269
ω [deg]	109.4990	248.1679
f_0 [deg]	179.4986	1.2233
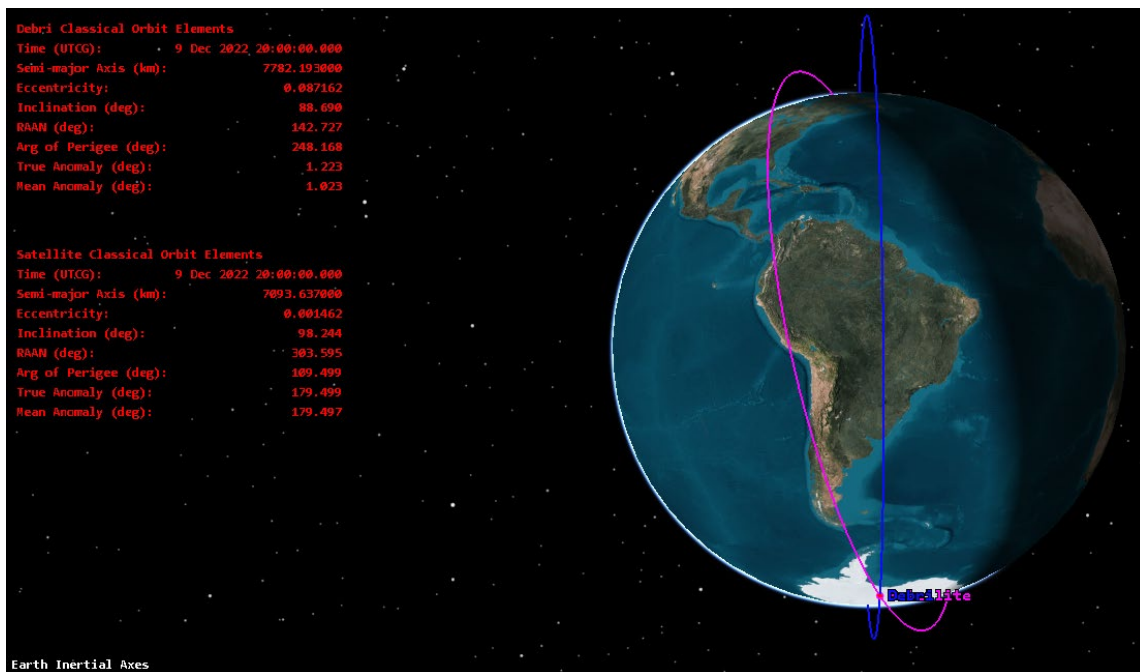
Figure 22.   3D view of encounter
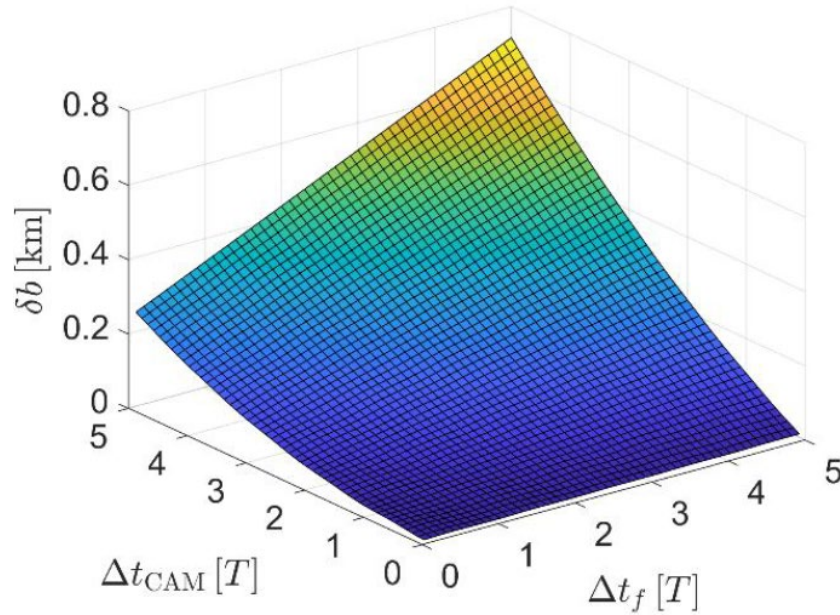
Figure 23.   Deflection in the b-plane for $at = 10{-}6 \; m/s2$ and different values
of CAM duration and lead time. Source: [36].

The main conclusion of Gonzalo, Colombo, and Di Lizia's work is that "the evolution of the CAM in the b-plane has confirmed the key role played by phasing, with displacements along the time axis dominating over displacements in the geometry axis. This highlights the importance of planning low-thrust CAMs with sufficient lead time, contrary to impulsive CAMs that can be typically performed in an efficient way up to half an orbital period before the predicted encounter" [36]. This conclusion is demonstrated in Figure 24 when we compare the displacement in ζ and ξ axis at TCA after CAM with different lead time; in that figure we can see a great displacement in ζ while a small displacement in ξ.
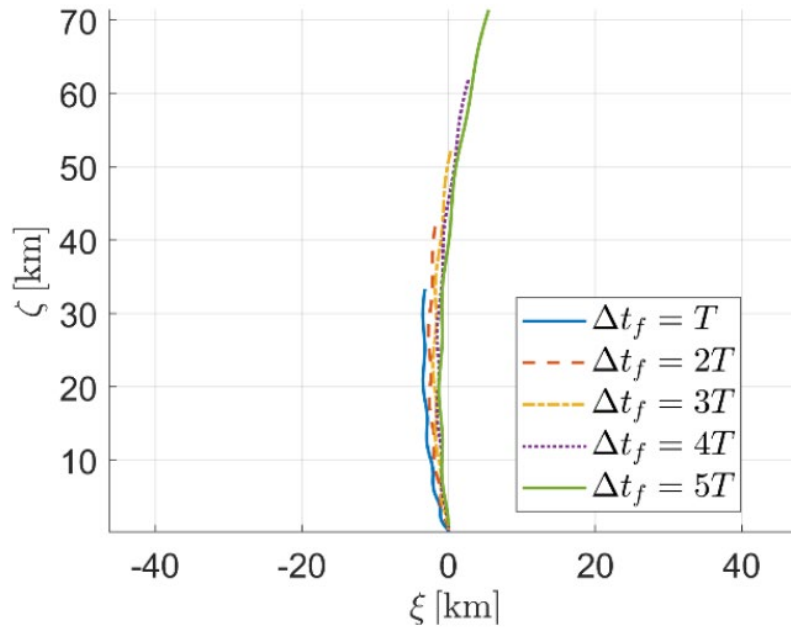
Figure 24.   B-plane representation of the evolution of the displacement with $\Delta tCAM \in [0, 5T]$, for $at = 10{-}4 \; m/s2$ and several Δtf. Source: [36].

B.   OPTIMAL DIRECTION LOW-THRUST COLLISION AVOIDANCE MANEUVER DESIGN

The optimally oriented CAM proposed by Hernando-Ayuso and Bombardelli [35] section VI is presented hereafter. In their work the optimal control theory was applied to minimize the probability of collision in the TCA by changing the direction of the acceleration vector. This solution is formulated on b-plane axes and assumes that the change in mass is neglected.

Considering the b-plane dynamic, the objective function is written as a Bolza problem:

$$ J = \frac{1}{2} \cdot (b^T \cdot Q \cdot b) \big|_{t = tf} + \int_{t0}^{tf} \lambda^T(t) \, M'(t) \, u \, dt $$

where **b** and **M´** have been characterized in the previous section, and λ is the costate

$$ \lambda = \left(\lambda_\xi, \; \lambda_\zeta \right)^T. $$

For the minimum probability, the Q matrix is replaced by

45

$$Q_{\mathrm{P}} = \begin{bmatrix} \dfrac{1}{\sigma^2_{\xi}} & -\dfrac{\rho_{\xi\zeta}}{\sigma_{\xi} \cdot \sigma_{\zeta}} \\[2em] -\dfrac{\rho_{\xi\zeta}}{\sigma_{\xi} \cdot \sigma_{\zeta}} & \dfrac{1}{\sigma^2_{\zeta}} \end{bmatrix},$$

and the Hamiltonian H is constructed as

$$H(\, u(t)\,, \lambda(t)\,, t\,) \; = \; \lambda^T(t) \cdot M'(t)\, u.$$

The acceleration vector **u** has magnitude limited by the maximum acceleration a_0. Applying Pontryagin's maximum principle, the optimum control **u** must maximize H. Hence, the acceleration magnitude must take its maximum value a_0, and the optimal acceleration vector must satisfy

$$u \; = \; \frac{\mathbf{a}_0 \cdot \mathbf{M'}^{\mathrm{T}} \cdot \lambda}{\left| \mathbf{M'}^{\mathrm{T}} \cdot \lambda \right|}.$$

A necessary condition for H to be maximum is

$$\frac{d\lambda}{dt} \; = \; -\frac{\partial H}{\partial b}.$$

Since the Hamiltonian does not depend on the B-vector coordinates, λ remains constant in time,

$$\lambda(\mathit{tf}) \; = \; \lambda(t) \; = \; Q \cdot b(\mathit{tf})\,, \quad \forall\, t \in \left(t_0,\, t_f \right).$$

The optimization has been reduced to a two-point boundary value problem (TPBVP) of dimension two:

$$\frac{db}{dt} \; = \; a_0 \cdot \frac{M' \cdot \mathbf{M'}^{\mathrm{T}} \cdot Q \cdot b(\mathit{tf})}{\left| \mathbf{M'}^{\mathrm{T}} \cdot Q \cdot b(\mathit{tf}) \right|}, \quad b(\mathit{to}) \; = \; \left(\xi_0,\, \zeta_0 \right)^T, \quad b(\mathit{tf}) \; = \; (\xi_{\mathrm{f}},\, \zeta_{\mathrm{f}})^T.$$

Hernando-Ayuso and Bombardelli [35] compared the performance of tangential maneuvers and the ideal control solution. The results demonstrated that the tangential solution behaves similarly to the ideal control solution when the collision probability reaches the global minimum, while it strongly differs from the optimal one when the phasing is unfavorable. Figure 25 presents the result of one of the test cases performed by those authors. In this figure, we can see that the minima of the ideal control maneuver,

46

represented by the orange line, always coincide with the minima obtained by a forward or retrograde tangential maneuver.
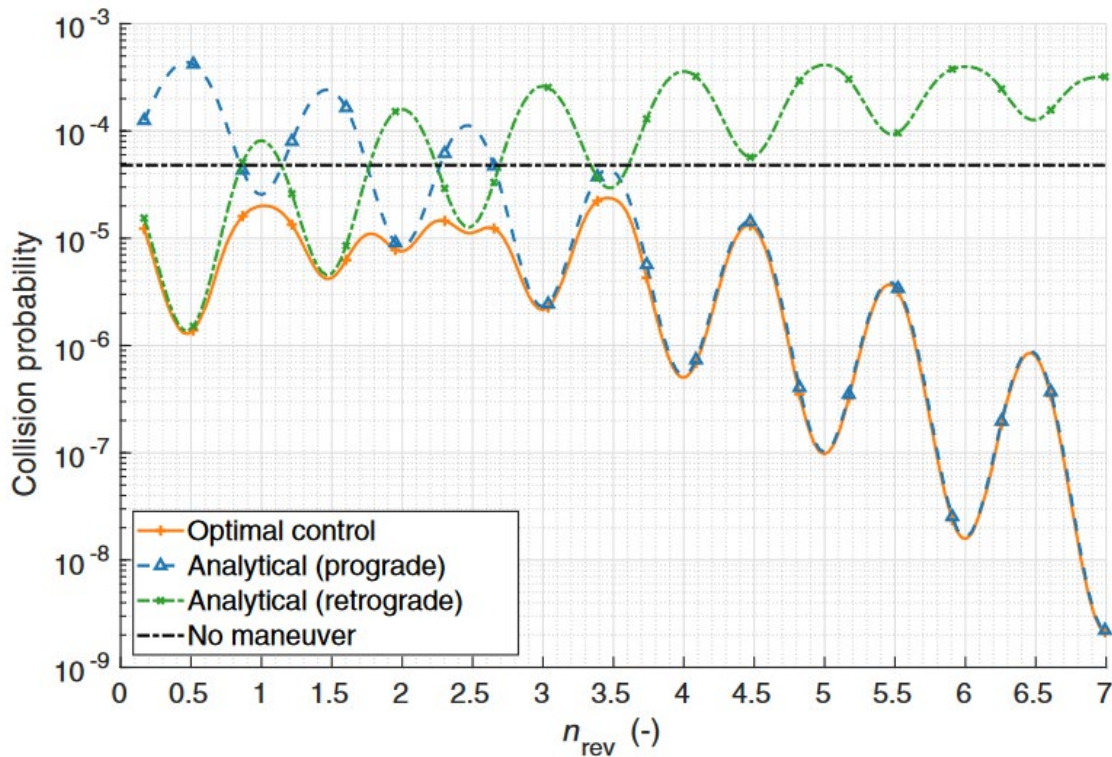
Figure 25.   Optimal and analytical (prograde/retrograde) collision probability. Source: [35].

C.   SPACECRAFT COLLISION AVOIDANCE USING AERODYNAMIC DRAG

Although the thruster maneuver is the preferable method of collision avoidance action for spacecraft equipped with a propulsion system, the use of aerodynamic drag is also possible. This method can save fuel for spacecraft equipped with propulsion systems and provide maneuverability for spacecraft for which the thrusters failed or which do not contain thrusters. As mentioned in previous sections of this work, the decrease in the amount of debris is in itself an action to decrease the amount of conjunctions. In this sense, the use of non-retractable drag devices, such as a 10 m^2 drag sail for a 3U CubeSat shown in Figure 26, can decrease the satellite's deorbit time by increasing the surface area, but it

47

also increases the chance of a collision with a second object due to the significant increase in the surface area. For an active reentry strategy or collision avoidance action, aerodynamic approaches using retractable devices or reorientation of the satellite can be applied without increasing the risk of collision. Two such possible approaches are presented in this work. The first one is a time-optimal solution described by Omar and Bevilacqua [32]; although their method can be applied by any satellite able to change the ballistic coefficient, it is demonstrated only for satellites equipped with a retractable drag device. On the other hand, Mishne and Edlerman [37] studied the feasibility of using drag and solar pressure for regular satellite maneuvers in space.
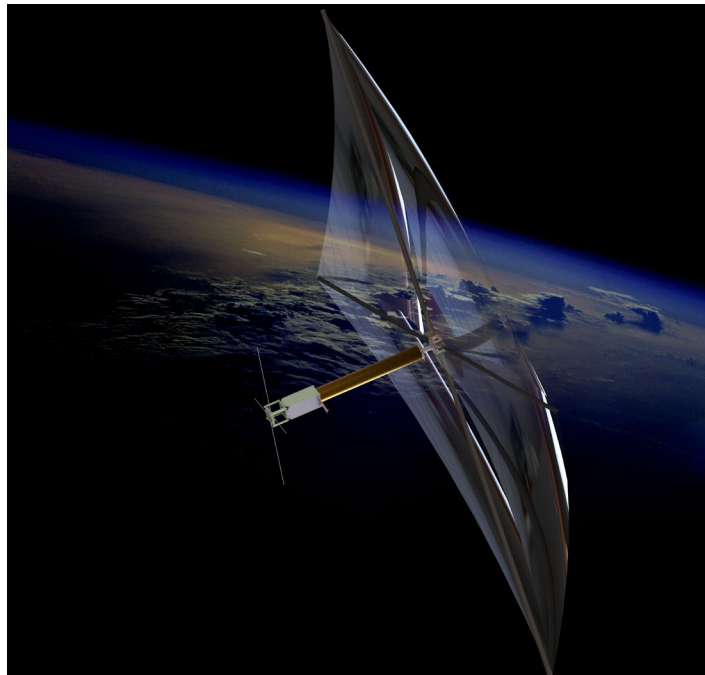
Figure 26.   10 m^2 drag deorbiting sail used in the InflateSail 3U CubeSat.
Source: [38].

1.   Spacecraft Collision Avoidance Using Aerodynamic Drag

A time-optimal collision avoidance solution using aerodynamic drag was developed by Omar and Bevilacqua [32]. The method discussed in their engineering note can be applied to any satellite that can modulate its ballistic coefficient either by using a retractable device or changing attitude. This method first uses an analytical solution to

48

compute how a change in ballistic coefficient affects the satellite's orbit and then calculates the minimum maneuver time to achieve the desired miss distance at TCA using a high-precision orbit propagator. The analytical solution assumes a circular orbit around a spherical Earth, a constant atmosphere density throughout the maneuver, and a small change in the semi-major axis.

The change in orbit is computed by the difference in the mean anomaly M:

$$\emptyset = M_r - M_n.$$

The subscripts "r" and "n" refer, respectively, to the initial unperturbed trajectory and new trajectory.

The time derivative of $\emptyset$ is expressed in terms of semi-major axis:

$$\frac{d\phi}{dt} = n_r - n_n$$

$$n = \sqrt{\frac{\mu_e}{a^3}}$$

$$\frac{d\phi}{dt} = \sqrt{\frac{\mu_e}{a_r^3}} - \sqrt{\frac{\mu_e}{a_n^3}}$$

$$\delta = a_n - a_r$$

$$\frac{d\phi}{dt} = \sqrt{\mu_e} \left(a_r^{-1.5} - \left(a_r + \delta \right)^{-1.5} \right)$$

where n is the mean motion and μ is the Earth's gravitational parameter. This equation is linearized in terms of δ using the binomial expansion theorem, and then a time derivative is taken to have the phi double dot expression.

$$\frac{d\emptyset}{dt} = \frac{3\,\delta\sqrt{\mu_e}}{2\,a_r^{2.5}}$$

$$\frac{d^2\emptyset}{dt^2} = \frac{3\,\sqrt{\mu_e}}{a_0^{2.5}} \frac{d\delta}{dt}$$

where a_0 is the initial semi-major axis.

The theorem of work energy is applied to get a relationship between $d\delta/dt$ and ballistic coefficient C_b.

$$E = \frac{-\mu_e}{2a}$$

$$\frac{dE}{dt} = \frac{\mu_2}{2a^2}\frac{da}{dt} = a_d v \approx -C_b \rho v^3 \approx -C_b \rho \left(\frac{\mu_e}{a}\right)^{1.5}$$

$$a_d = -\frac{C_d A}{2m}\rho v^2 = -C_b \rho v^2,$$

$$\frac{da}{dt} = -2 C_b \rho \sqrt{\mu_e a}$$

$$\frac{d\delta}{dt} = \frac{da_n}{dt} - \frac{da_r}{dt} = -2\rho \sqrt{\mu_e a_0}\left(C_{bn} - C_{br}\right)$$

where E is the orbital energy per unit of mass, a_d is the drag acceleration, and C_d is the drag coefficient.

Substituting the last equation into phi double dot expression, we have

$$\frac{d^2\emptyset}{dt^2} = -\frac{3\rho\mu_e}{a_0^2}\left(C_{bn} - C_{br}\right) = -\frac{3\rho\mu_e}{a_0^2}\Delta C_b.$$

The desired difference in mean motion can be calculated using the initial semi-major axis and the desired along-track component of miss distance Δx:

$$\Delta\emptyset_d = \frac{\Delta x}{a}.$$

If ΔC_b is maintained for a time Δt, then the total $\Delta\emptyset$ will be:

$$\Delta\emptyset = \frac{1}{2}\frac{d^2\emptyset}{dt^2}(\Delta t)^2 + \frac{d\emptyset_0}{dt}(\Delta t)$$

where $d\emptyset_0/dt$ is $d\emptyset/dt$ at the start of the analysis interval and equals zero at the beginning of the trajectory.

To reach the desired change in $\Delta\emptyset$, an off-nominal drag configuration must be kept for a certain period until t_s, and the nominal drag configuration must be reestablished between t_s and t_c, where t_s represents the lead time until the time of closest approach t_c. The total change in the mean motion $\Delta\emptyset_t$ at t_c is written as:

50

$$\Delta \emptyset_t = \frac{1}{2} \frac{d^2\emptyset}{dt^2} t_s^2 + \frac{d^2\emptyset}{dt^2} t_s \left(t_c - t_s \right)$$

$$- \left(\frac{1}{2} \frac{d^2\emptyset}{dt^2} \right) t_s^2 + \left(\frac{d^2\emptyset}{dt^2} t_c \right) t_s - \Delta \emptyset_t = 0.$$

Therefore, given a desired change in the mean motion $\Delta\emptyset_{td}$, the last equation can be solved using the quadratic formula to get the required t_s. From the two t_s values returned by the quadratic formula, the smallest positive value should be chosen. Recall that Cb should be set to Cb_{md} where Cb_{md} is the Cb that maximizes the magnitude of $\Delta C_b = C_b - C_{b\ nominal}$ for $t \le t_s$ and should be set to Cb nominal for $t > t_s$. If both ts values are imaginary, this means that it is not possible to achieve the desired change in the mean motion. In this case, Cb should be set to Cb_{md} until time t_c to achieve the greatest $\Delta\emptyset_t$ possible.

Due to the assumptions, this analytical solution is not accurate when applied in a realistic scenario. To address that, the authors refined the estimated Cb using a high-precision orbit propagator. To do that, they propagated two orbits until t_c, with one using the maneuver calculated using the analytical solution and a second without any change in drag area. The actual miss distance $\Delta\emptyset_{ta}$ is computed by the difference in mean anomaly between these two trajectories at t_c. Therefore, the aiming miss distance $\Delta\emptyset_{t\ aim}$ can be interactively adjusted based on the difference between the desired and actual miss distance:

$$\Delta\emptyset_{t\ aim} = \Delta\emptyset_{t\ aim} + 0.5 \left(\Delta\emptyset_{td} - \Delta\emptyset_{ta} \right).$$

The interactive process consists of using an average atmospheric density computed between the start of simulation until t_c to calculate $\ddot{\emptyset}$. Then, $\ddot{\emptyset}$ is used to calculate the new t_s required to achieve the updated $\Delta\emptyset_{t\ aim}$. The interactive process of updating atmosphere density ρ and aiming miss distance, computing t_s, and propagating a new trajectory continues until a t_s is obtained that yields $|\Delta\emptyset_{td} - \Delta\emptyset_{ta}|$ less than some specified tolerance. For example, this method determined that ts = 3.093 hours was necessary to achieve the 200 km along-track miss distance within a tolerance of 0.1 km. For this simulation a satellite equipped with a retractable drag device was used with $C_{b\ nominal} =$ 0.1375 m²/kg and $Cb_{md} = 0.002750$ m²/kg and debris with a ballistic coefficient of

51

0.008271 m^2/kg. The total time simulation is set to two days. We can see on the right side of Figure 27 that the desired along-track miss distance is reached at TCA. The two objects are at an altitude of 400 km at TCA with an epoch of 3 January 2014, and state vectors of satellite state vector = [6778, 0, 0, 0, 4.7366, 6.0347] and debris state vector = [6778, 0, 0, 0, 7.7486, 0].

Figure 28 shows the influence of two crucial parameters in achieving the maximum possible miss distance. In the left plot, we can see the effect of the satellite's altitude; the higher the altitude, the lower the ability to obtain a miss distance, which is expected since the atmospheric density decreases at higher altitudes. In the right plot, satellites at the same altitude but with different capacities to change the ballistic coefficient present different miss distances after the same maneuver period; in this case, the satellite with a greater ability to change the ballistic coefficient achieves better performance in terms of miss distance.
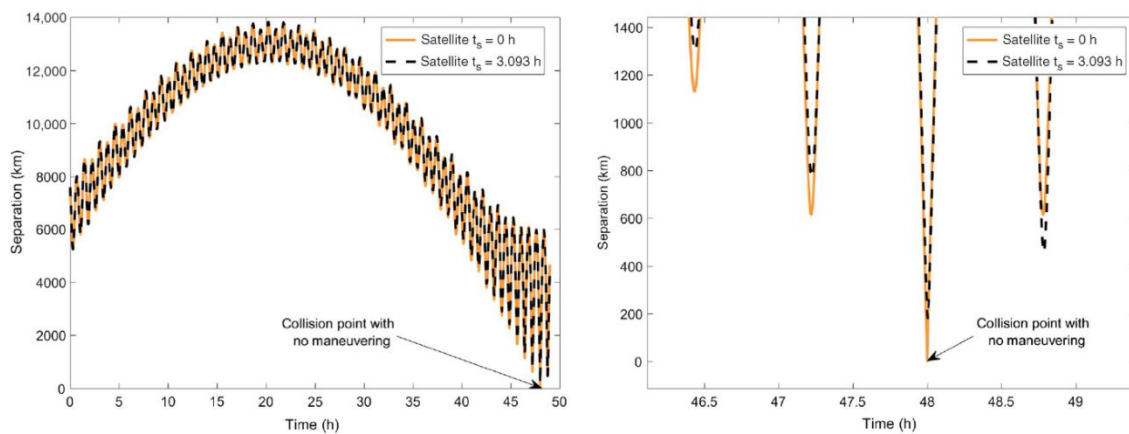
Figure 27.   Satellite–debris separation over time with (ts = 3.093 h) and without (ts = 0h) maneuvering. Source: [39].
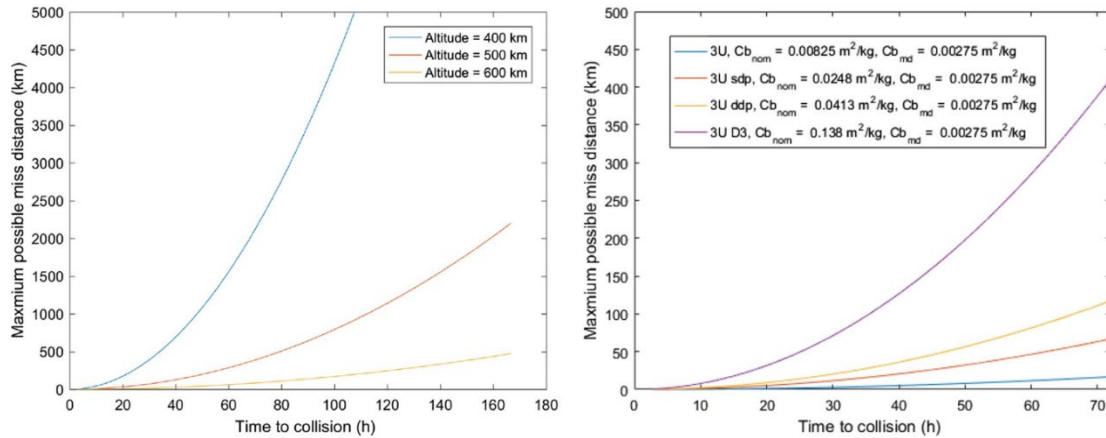
Figure 28.   Maximum achievable miss distance vs. time to collision for 3U
D3-equipped CubeSat at various altitudes (left) and for different satellites
in 500 km circular orbits (right). Source: [39].

The authors state "this approach results in the largest possible miss distance for a given amount of time a spacecraft can spend maneuvering" [39]. They also concluded that changing the attitude early, that is, a bigger t_s, decreases the needed off-nominal drag configuration time, which is desirable since when in this configuration, the payload typically cannot be used. It makes sense when compared to the previously described strategies that the change in attitude to increase the drag area works as a tangential retrograde maneuver.

2.   Collision-Avoidance Maneuver of Satellites Using Drag and Solar Radiation Pressure

Mishne and Edlerman's [37] study aims to analyze the feasibility of using drag and solar radiation pressure SRP forces for collision avoidance maneuvers. They consider orbits with an altitude between 600 and 800 km where both drag and SRP influence satellites. They assume the satellite has a solar panel, is not equipped with retractable devices that allow changing the drag force or solar pressure, the satellite can perform attitude maneuvers, and there is no propulsion system available. They also assume the satellite is in a circular orbit and has a significant difference between the maximum cross-section area and the minimum one, meaning the satellite does not have a spherical or box shape.

53

To perform the collision-avoidance maneuver, the satellite is oriented in an off-nominal attitude profile in such a way the combination of drag and SRP maximizes the effect at TCA. Figure 29 shows a summary of the control algorithm, which has the following main steps:

1.   Calculate the sun direction unit vector $\hat{s}$.

2.   Calculate a unit vector $\hat{z}$ perpendicular to the orbital plane by taking the cross product of position and velocity vectors.

$$\hat{z} = \frac{\mathbf{r} \times \mathbf{v}}{|\mathbf{r} \times \mathbf{v}|}$$

3.   Calculate the cosine of the beta angle.

$$\cos \beta = |\hat{z} \times \hat{s}|$$

4.   Calculate the instantaneous angular position θ.

$$\cos \theta = -\frac{\hat{s} \cdot \hat{r}}{\cos \beta}$$

$$\sin \theta = -\frac{\hat{s} \cdot \hat{v}}{\cos \theta}$$

5.   Use equations 28 to 40 in [37] to calculate the desired position vectors $\hat{z}_B$ and $\hat{d}$ in the inertial frame. The unit vector $\hat{d}$ is in the x_B, y_B plane as shown in Figure 30. The angle α is defined such that the vector d lies in the plane defined by vectors s and v.

$$\hat{d} = \hat{x}_B \cos \alpha + \hat{y}_B \sin \alpha$$

6.   Calculate $\hat{x}_B$ from

$$\hat{x}_B = \hat{d} \cos \alpha_{optimal} - \left(\hat{z}_B \times \hat{d} \right) \sin \alpha_{optimal}.$$
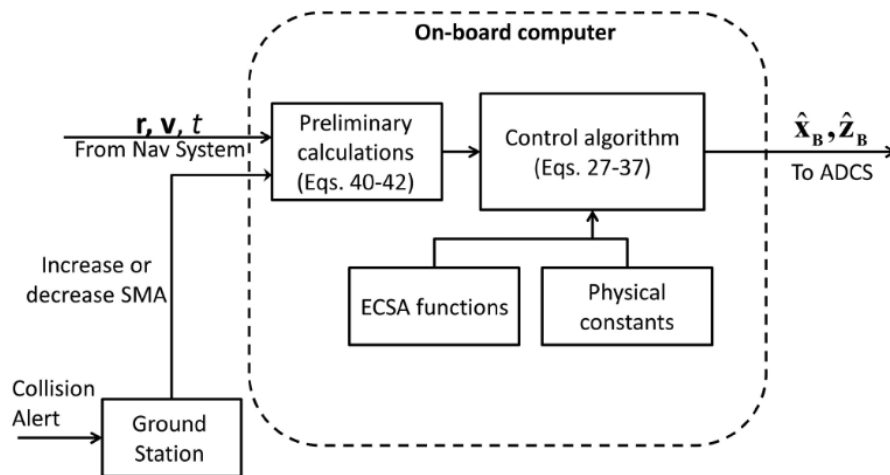
Figure 29. Summary of the control algorithm. Source: [37].
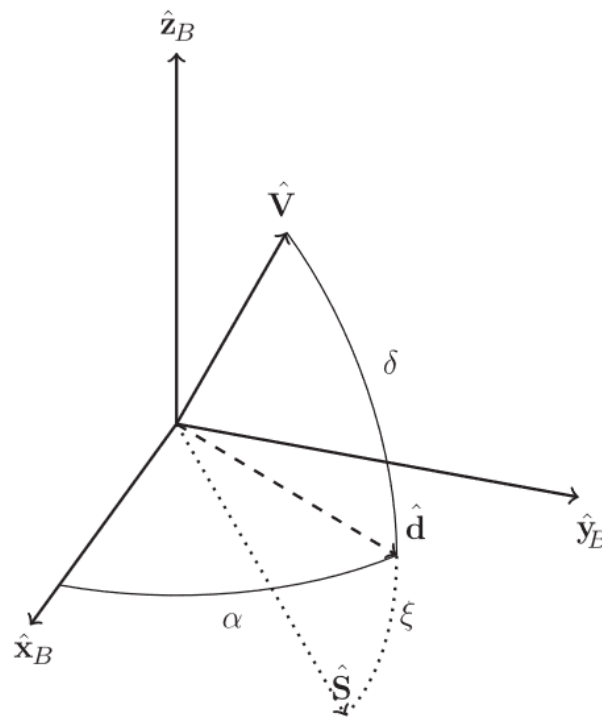
Figure 30. Spherical coordinate frame. Source: [37].

The authors demonstrated the feasibility of the proposed maneuver is dependent on the satellite's characteristics. Satellites with a high area-to-mass ratio and maximum-to-minimum area ratio perform better. Figure 31 shows how a satellite at 600 km altitude

55

performs in terms of along-track deviation after three days of maneuver. The R_s parameter is the maximum-to-minimum area ratio, and the collision probability is computed using Alfano's [17] maximum collision probability approach. Analyzing this result, we can see that a satellite with an area-to-mass ratio of 0.016 and $R_s = 6$ can acquire an along-track deviation of 5 km, which is equivalent to reducing the collision probability to less than 10^{-6}.
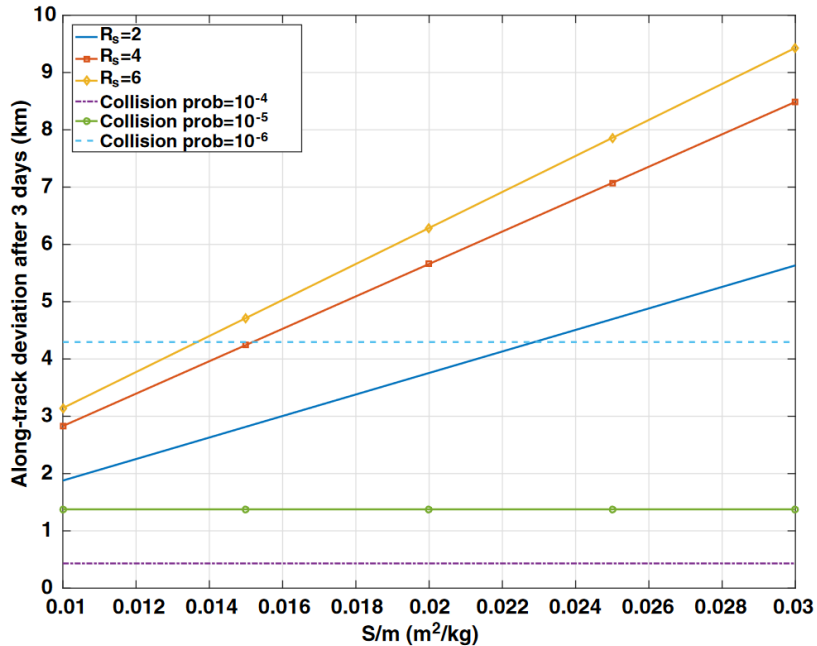
Figure 31.   Along-track deviation as a function of the satellite's properties.
Source: [37].

Other examples with a real satellite in LEO orbit between 600 and 800 km altitude show that the method is feasible and that the accumulated along-track deviation after three days of maneuver is sufficient to reduce the collision probability to under 10^{-4}, which is a typical threshold used by the space industry [8].

V.   SIMULATIONS AND RESULTS

The sequence and methodology applied to the simulations were as follows. First, we applied the SP catalog to the screening process by executing the proposed program to identify events with a probability greater than 10^{-5}, and tangential CAM and aerodynamic solutions were tested to see how they performed for these conjunctions.

A.   SCREENING PROCESS USING TLE AND SP CATALOGS

This work does not aim to compare the accuracy of both catalogs. We assumed SP is more accurate, so any difference in the screening process output is considered in favor of the SP catalog. Comparisons made here are in terms of the difference in the number of alerts and the collision probability value for the same alert. Table 6 to Table 13 show the results of the screening process for four different spacecraft. In pairs, the first image uses the SP catalog while the second uses the TLE catalog. When the process is executed using the SP catalog the object of interest is also propagated using its ephemeris in SP in the same way; when the TLE catalog is used, the object of interest is propagated using its data in TLE catalog.

For these analyses, two collision probability thresholds are defined, conjunctions with a probability greater than 10^{-5} are classified as in the red zone where a maneuver would be necessary and greater than 10^{-7} as in the yellow zone where the risk is not great enough to perform a maneuver but requires attention in its evolution. Analyses were performed using the catalogs dated 16 January 2023.

Table 6.   Screening process for ICEYE X-13 against full SP catalog

Conjunction Report for object\48916 against the full SP Catalog							

Conjunctions with probability higher than the defined threshold = 1.00e-05							
Object 2	Max Collision Probability	TCA	Min Range (Km)	Min Range - Radial (Km)	Min Range - CrossTrack (Km)	Min Range - InTrack (Km)	Approach Angle (deg)
47941.eci	1.59E-05	17 Jan 2023 15:22:20.853580592	4.23E-01	1.61E-02	-3.78E-01	-1.91E-01	126.5

Conjunctions with probability higher than the defined threshold = 1.00e-07							
Object 2	Max Collision Probability	TCA	Min Range (Km)	Min Range - Radial (Km)	Min Range - CrossTrack (Km)	Min Range - InTrack (Km)	Approach Angle (deg)
27119.eci	2.09E-06	19 Jan 2023 06:20:52.162034248	1.30E+00	-9.39E-02	7.75E-01	1.04E+00	73.4
47505.eci	9.51E-07	17 Jan 2023 21:48:42.322398839	1.93E+00	1.84E+00	3.39E-01	-4.60E-01	72.8
44496.eci	8.55E-07	19 Jan 2023 22:29:44.960808849	1.78E+00	6.33E-01	-1.56E+00	5.84E-01	138.9
27664.eci	7.11E-07	19 Jan 2023 09:48:29.243124050	2.27E+00	4.11E-01	-1.14E+00	1.91E+00	62.5
33505.eci	6.30E-07	17 Jan 2023 13:50:18.611641130	2.08E+00	2.05E+00	3.67E-01	-1.46E-01	135.8
44604.eci	6.10E-07	17 Jan 2023 06:36:15.457442432	2.35E+00	-5.62E-01	-2.22E-01	-2.27E+00	1.7
44498.eci	4.77E-07	19 Jan 2023 03:25:47.390694078	2.39E+00	1.38E-02	-2.22E+00	8.83E-01	136.6
47502.eci	3.41E-07	17 Jan 2023 17:03:01.981120141	3.22E+00	2.37E+00	1.29E+00	-1.75E+00	72.9
48963.eci	3.00E-07	19 Jan 2023 17:25:54.166715964	3.64E+00	2.65E+00	-2.20E-01	2.49E+00	1.2
52444.eci	2.81E-07	18 Jan 2023 16:51:08.651217725	3.61E+00	-3.40E-01	6.11E-01	-1.04E+00	60.8
07337.eci	2.74E-07	16 Jan 2023 23:35:35.040058791	3.39E+00	3.73E-01	2.61E+00	2.14E+00	102.5
44498.eci	2.62E-07	19 Jan 2023 05:00:56.240609559	3.22E+00	-4.96E-03	2.99E+00	-1.20E+00	136.4
49003.eci	2.58E-07	19 Jan 2023 00:47:15.443340195	3.76E+00	-1.10E+00	-1.83E+00	3.10E+00	61.1
55011.eci	1.45E-07	18 Jan 2023 11:18:01.931511520	4.97E+00	1.79E+00	2.62E+00	3.83E+00	68.9
51051.eci	1.37E-07	17 Jan 2023 21:00:52.124669451	5.16E+00	-1.07E+00	-2.63E+00	-4.30E+00	62.9
05358.eci	1.35E-07	18 Jan 2023 04:12:50.079487759	5.05E+00	-4.28E+00	-1.73E+00	-2.05E+00	80.5
49256.eci	1.01E-07	17 Jan 2023 09:05:50.883154886	6.26E+00	-6.20E+00	1.70E-01	-9.09E-01	22.2

Table 7.   Screening process for ICEYE X-13 against full TLE catalog

Conjunction Report for object\48916 against the full TLE Catalog							
Conjunctions with probability higher than the defined threshold = 1.00e-05							
Object 2	Max Collision Probability	TCA	Min Range (Km)	Min Range - Radial (Km)	Min Range - CrossTrack (Km)	Min Range - InTrack (Km)	Approach Angle (deg)
Conjunctions with probability higher than the defined threshold = 1.00e-07							
Object 2	Max Collision Probability	TCA	Min Range (Km)	Min Range - Radial (Km)	Min Range - CrossTrack (Km)	Min Range - InTrack (Km)	Approach Angle (deg)
tle 44498	1.25E-06	18 Jan 2023 22:40:24.478864388	1.47E+00	6.41E-01	1.23E+00	-4.84E-01	137.1
tle 27151	1.06E-06	19 Jan 2023 19:51:04.292015032	1.73E+00	7.82E-01	1.16E+00	-1.01E+00	98.1
tle 47505	6.50E-07	17 Jan 2023 21:48:42.331967246	2.31E+00	1.96E+00	7.24E-01	-9.83E-01	72.8
tle 33505	5.23E-07	17 Jan 2023 13:50:18.721430634	2.28E+00	2.09E+00	8.30E-01	-3.34E-01	135.8
tle 47502	4.78E-07	17 Jan 2023 17:03:01.942385076	2.70E+00	2.21E+00	9.18E-01	-1.24E+00	72.9
tle 54689	3.62E-07	20 Jan 2023 03:44:43.011055498	3.29E+00	3.28E+00	6.33E-03	-2.83E-01	7.9
tle 55010	3.01E-07	18 Jan 2023 00:11:28.242731839	3.42E+00	1.83E+00	1.63E+00	2.38E+00	68.9
tle 07337	2.68E-07	16 Jan 2023 23:35:35.059471256	3.41E+00	4.50E-01	2.61E+00	2.14E+00	102.5
tle 55012	2.41E-07	19 Jan 2023 21:25:16.838105339	3.82E+00	3.76E+00	4.04E-01	-5.98E-01	68.9
tle 55009	2.25E-07	17 Jan 2023 00:23:05.691604818	3.96E+00	2.06E+00	1.91E+00	2.79E+00	68.9
tle 41915	2.21E-07	17 Jan 2023 15:28:13.274734858	3.86E+00	-2.17E+00	-2.21E+00	2.30E+00	87.9
tle 05358	1.75E-07	18 Jan 2023 04:12:49.801795214	4.40E+00	-4.39E+00	1.41E-01	1.68E-01	80.5
tle 55012	1.62E-07	19 Jan 2023 23:48:07.716515070	4.66E+00	2.62E+00	-2.18E+00	-3.17E+00	68.9
tle 51051	1.53E-07	17 Jan 2023 21:00:52.070328281	4.84E+00	-1.03E+00	-2.47E+00	-4.03E+00	62.9
tle 55011	1.37E-07	18 Jan 2023 08:55:11.261626470	5.07E+00	5.07E+00	2.12E-02	-4.34E-02	68.9
tle 47201	1.37E-07	20 Jan 2023 06:09:07.664895823	5.08E+00	3.24E-01	-2.87E+00	-4.18E+00	68.9
tle 49003	1.36E-07	19 Jan 2023 00:47:16.102696820	5.15E+00	-1.09E+00	2.56E+00	-4.34E+00	61.1
tle 31820	1.36E-07	18 Jan 2023 13:41:26.501442688	5.04E+00	2.43E+00	-2.69E+00	3.50E+00	76
tle 47941	1.06E-07	17 Jan 2023 15:22:21.540236711	5.16E+00	1.55E-01	-4.61E+00	-2.32E+00	126.5
tle 27664	1.02E-07	19 Jan 2023 09:48:29.861644113	5.94E+00	1.34E-01	3.06E+00	-5.09E+00	62.5

Table 8.   Screening process for IRIDIUM 153 against full SP catalog

Conjunction Report for object\43078 against the full SP Catalog							
Conjunctions with probability higher than the defined threshold = 1.00e-05							
Object 2	Max Collision Probability	TCA	Min Range (Km)	Min Range - Radial (Km)	Min Range - CrossTrack (Km)	Min Range - InTrack (Km)	Approach Angle (deg)
12193.eci	6.79E-05	18 Jan 2023 16:34:24.451809471	1.90E-01	-2.25E-02	-1.89E-01	1.26E-02	172.4
31159.eci	1.64E-05	17 Jan 2023 11:30:33.260066410	4.21E-01	3.73E-02	-3.61E-01	2.15E-01	118.3
Conjunctions with probability higher than the defined threshold = 1.00e-07							
Object 2	Max Collision Probability	TCA	Min Range (Km)	Min Range - Radial (Km)	Min Range - CrossTrack (Km)	Min Range - InTrack (Km)	Approach Angle (deg)
55223.eci	1.16E-06	16 Jan 2023 19:37:18.914694097	1.75E+00	-1.74E+00	-8.44E-02	-1.26E-01	66.1
02142.eci	3.56E-07	18 Jan 2023 02:12:35.338066300	2.87E+00	-2.46E+00	-1.26E+00	7.68E-01	117.2
14122.eci	2.46E-07	18 Jan 2023 16:36:42.988643667	3.40E+00	-2.23E+00	-2.24E+00	-1.26E+00	123.5
05599.eci	2.33E-07	21 Jan 2023 07:52:18.161359143	3.53E+00	-2.12E+00	-2.44E+00	1.42E+00	119.6
37918.eci	2.19E-07	19 Jan 2023 07:08:49.238605002	3.36E+00	-1.53E+00	-2.97E+00	3.00E-01	168.7
35205.eci	2.11E-07	17 Jan 2023 00:39:10.553039023	4.14E+00	-4.08E+00	3.69E-01	6.52E-01	59.4
21500.eci	2.06E-07	19 Jan 2023 12:55:08.413576043	3.95E+00	3.40E+00	-1.45E+00	-1.38E+00	95.6
49483.eci	2.01E-07	16 Jan 2023 22:07:08.397277566	3.88E+00	-1.13E+00	-3.03E+00	2.13E+00	110
35422.eci	1.84E-07	18 Jan 2023 15:08:34.658389401	4.41E+00	-4.05E+00	-8.98E-01	1.49E+00	62.4
31024.eci	1.84E-07	18 Jan 2023 09:59:35.004115105	3.68E+00	1.50E+00	3.33E+00	-5.10E-01	162.5
25477.eci	1.80E-07	18 Jan 2023 07:54:05.952694476	4.56E+00	-1.79E+00	1.58E+00	3.88E+00	44.5
40569.eci	1.80E-07	19 Jan 2023 02:07:11.528110788	4.63E+00	-4.42E+00	3.16E-01	-1.34E+00	26.4
29869.eci	1.77E-07	18 Jan 2023 08:55:52.184359382	3.73E+00	-1.46E+00	3.42E+00	1.77E-01	174.2
37580.eci	1.76E-07	18 Jan 2023 06:50:40.323090513	4.66E+00	3.27E+00	-8.53E-01	-3.21E+00	31.4
02142.eci	1.48E-07	18 Jan 2023 04:43:07.823012448	4.45E+00	-4.32E+00	9.01E-01	5.50E-01	117.4
43324.eci	1.19E-07	20 Jan 2023 05:59:38.737704995	4.65E+00	3.78E+00	-2.62E+00	6.78E-01	151
25415.eci	1.15E-07	16 Jan 2023 20:11:23.822161997	5.51E+00	6.91E-01	-3.15E+00	4.47E+00	70.4
25160.eci	1.07E-07	20 Jan 2023 21:36:25.095319162	5.36E+00	1.49E-01	-4.27E+00	3.24E+00	105.8
25477.eci	1.06E-07	18 Jan 2023 07:03:54.159823063	5.94E+00	-4.19E-01	-2.24E+00	5.49E+00	44.5
22828.eci	1.00E-07	20 Jan 2023 06:33:28.249003154	6.18E+00	5.15E+00	9.88E-01	-3.27E+00	33.4

Table 9.   Screening process for IRIDIUM 153 against full TLE catalog

Conjunction Report for object\43078 against the full TLE Catalog							
Conjunctions with probability higher than the defined threshold = 1.00e-05							
Object 2	Max Collision Probability	TCA	Min Range (Km)	Min Range - Radial (Km)	Min Range - CrossTrack (Km)	Min Range - InTrack (Km)	Approach Angle (deg)
tle 12193	2.50E-05	18 Jan 2023 16:34:24.435860669	3.14E-01	-1.42E-01	-2.80E-01	1.89E-02	172.4
Conjunctions with probability higher than the defined threshold = 1.00e-07							
Object	Max Collision Probabili	TCA	Min Range (Kr	Min Range - Radial (Kn	Min Range - CrossTrack (Kn	Min Range - InTrack (Kn	Approach Angle (de
tle 31159	1.14E-06	17 Jan 2023 11:30:33.125644834	1.60E+00	-9.23E-02	-1.37E+00	8.12E-01	118.3
tle 02142	3.74E-07	18 Jan 2023 02:12:35.316087132	2.80E+00	-2.31E+00	-1.35E+00	8.22E-01	117.2
tle 49483	3.22E-07	16 Jan 2023 22:07:08.536432875	3.06E+00	-8.81E-01	-2.40E+00	1.68E+00	110
tle 55217	3.02E-07	19 Jan 2023 19:37:32.642798935	3.45E+00	-3.45E+00	-8.29E-02	-1.38E-01	62.1
tle 37918	2.90E-07	19 Jan 2023 07:08:49.642054636	2.92E+00	-1.56E+00	-2.45E+00	2.48E-01	168.7
tle 35422	2.27E-07	18 Jan 2023 05:05:46.810507408	3.97E+00	-2.94E+00	-1.38E+00	2.28E+00	62.7
tle 31024	2.19E-07	18 Jan 2023 09:59:34.991276782	3.37E+00	1.41E+00	3.03E+00	-4.66E-01	162.5
tle 29869	2.04E-07	18 Jan 2023 08:55:52.407944283	3.47E+00	-1.19E+00	3.25E+00	1.68E-01	174.2
tle 25160	1.78E-07	20 Jan 2023 21:36:25.261744731	4.16E+00	1.36E-01	-3.31E+00	2.51E+00	105.8
tle 21500	1.77E-07	19 Jan 2023 12:55:07.945424648	4.26E+00	3.30E+00	2.01E+00	1.77E+00	95.6
tle 43324	1.55E-07	20 Jan 2023 05:59:38.976435970	4.08E+00	3.27E+00	-2.36E+00	6.10E-01	151
tle 02142	1.43E-07	18 Jan 2023 04:43:07.819946303	4.53E+00	-4.43E+00	7.98E-01	4.87E-01	117.4
tle 05599	1.17E-07	21 Jan 2023 07:52:19.124066336	4.97E+00	-2.53E+00	3.70E+00	-2.15E+00	119.6
tle 25477	1.14E-07	18 Jan 2023 07:54:05.831116351	5.74E+00	-1.60E+00	2.08E+00	5.11E+00	44.5
tle 22828	1.10E-07	20 Jan 2023 06:33:28.192916173	5.90E+00	5.21E+00	8.02E-01	-2.66E+00	33.4
tle 35422	1.00E-07	18 Jan 2023 09:16:56.521187671	5.98E+00	5.92E+00	4.64E-01	7.73E-01	62.6

Table 10.　　　　Screening process of Space X STARLINK-3068 against full SP catalog

Conjunction Report for object\49154 against the full SP Catalog							
Conjunctions with probability higher than the defined threshold = 1.00e-05							
Object 2	Max Collision Probability	TCA	Min Range (Km)	Min Range - Radial (Km)	Min Range - CrossTrack (Km)	Min Range - InTrack (Km)	Approach Angle (deg)
Conjunctions with probability higher than the defined threshold = 1.00e-07							
Object 2	Max Collision Probability	TCA	Min Range (Km)	Min Range - Radial (Km)	Min Range - CrossTrack (Km)	Min Range - InTrack (Km)	Approach Angle (deg)
46873.eci	3.42E-06	20 Jan 2023 08:23:45.120793426	8.60E-01	5.61E-01	6.38E-01	1.33E-01	156.3
35573.eci	2.28E-06	20 Jan 2023 04:58:39.425877745	1.06E+00	-2.76E-01	-9.92E-01	2.60E-01	150.6
19046.eci	7.95E-07	20 Jan 2023 01:50:26.018609799	2.00E+00	-2.83E-01	-1.48E+00	-1.32E+00	96.5
44641.eci	7.76E-07	17 Jan 2023 18:41:29.461015802	1.82E+00	2.01E-01	1.75E+00	-4.40E-01	151.8
43888.eci	3.78E-07	21 Jan 2023 00:49:05.678236217	3.19E+00	-3.09E+00	2.11E-01	-7.47E-01	31
46887.eci	3.40E-07	17 Jan 2023 17:05:03.644307544	2.75E+00	-2.75E+00	-6.61E-02	1.78E-02	151.3
39914.eci	2.91E-07	21 Jan 2023 06:27:48.043839512	3.00E+00	-3.00E+00	-1.48E-01	2.17E-02	145.3
31640.eci	2.79E-07	20 Jan 2023 17:09:36.873466274	3.53E+00	-5.20E-01	-2.08E+00	-2.80E+00	72.7
43787.eci	2.57E-07	18 Jan 2023 19:34:00.570867500	3.13E+00	1.30E+00	2.80E+00	5.41E-01	158.1
43780.eci	2.33E-07	19 Jan 2023 22:50:49.151121480	3.27E+00	-7.06E-01	-3.16E+00	-4.98E-01	162
46873.eci	2.29E-07	20 Jan 2023 07:35:40.069166359	3.32E+00	3.29E+00	-4.70E-01	9.88E-02	156.2
44890.eci	1.90E-07	20 Jan 2023 14:21:41.361797548	3.61E+00	1.59E+00	-3.22E+00	3.60E-01	167.2
43786.eci	1.80E-07	18 Jan 2023 21:58:37.100156681	3.74E+00	-3.24E+00	1.85E+00	-3.46E-01	158.8
33315.eci	1.46E-07	19 Jan 2023 14:45:52.401086734	4.18E+00	-4.16E+00	3.98E-01	9.39E-02	154.3
01672.eci	1.40E-07	18 Jan 2023 08:33:14.245019695	4.75E+00	4.23E+00	1.64E+00	1.39E+00	99.8
43785.eci	1.23E-07	20 Jan 2023 21:19:30.710770237	4.50E+00	-9.09E-01	-4.37E+00	-5.86E-01	164.7
43806.eci	1.20E-07	21 Jan 2023 04:30:51.937805476	4.56E+00	-2.79E+00	-3.57E+00	5.09E-01	163.8
44890.eci	1.12E-07	20 Jan 2023 15:58:09.268882676	4.71E+00	1.72E+00	4.36E+00	-4.90E-01	167.2
35905.eci	1.09E-07	17 Jan 2023 11:16:00.587334433	5.27E+00	-6.95E-02	-4.30E+00	3.04E+00	109.7

62

Table 11.   Screening process of Space X STARLINK-3068 against full TLE catalog

Conjunction Report for object\49154 against the full TLE Catalog							
Conjunctions with probability higher than the defined threshold = 1.00e-05							
Object 2	Max Collision Probability	TCA	Min Range (Km)	Min Range - Radial (Km)	Min Range - CrossTrack (Km)	Min Range - InTrack (Km)	Approach Angle (deg)
tle 19046	2.92E-05	20 Jan 2023 01:50:25.818953501	3.30E-01	-2.69E-01	-1.43E-01	-1.27E-01	96.5
Conjunctions with probability higher than the defined threshold = 1.00e-07							
Object 2	Max Collision Probability	TCA	Min Range (Km)	Min Range - Radial (Km)	Min Range - CrossTrack (Km)	Min Range - InTrack (Km)	Approach Angle (deg)
tle 43780	1.34E-06	19 Jan 2023 22:50:48.259904249	1.37E+00	-9.54E-01	-9.65E-01	-1.52E-01	162
tle 43785	1.26E-06	20 Jan 2023 21:19:28.358806295	1.40E+00	-1.34E+00	4.07E-01	5.57E-02	164.7
tle 44890	5.09E-07	20 Jan 2023 12:45:20.173453651	2.20E+00	1.75E+00	1.33E+00	-1.47E-01	167.3
tle 46512	4.77E-07	21 Jan 2023 02:49:31.322675542	2.30E+00	-2.28E+00	-2.99E-01	6.13E-02	157
tle 46887	3.85E-07	17 Jan 2023 17:05:03.522085468	2.58E+00	-2.57E+00	-2.60E-01	6.73E-02	151.3
tle 44641	2.96E-07	17 Jan 2023 18:41:29.769723593	2.94E+00	4.12E-01	2.82E+00	-7.10E-01	151.8
tle 10314	2.42E-07	20 Jan 2023 16:00:20.017914963	3.89E+00	2.93E+00	1.07E+00	-2.32E+00	54.3
tle 43786	2.31E-07	18 Jan 2023 21:58:36.914812682	3.30E+00	-3.11E+00	1.08E+00	-2.01E-01	158.8
tle 43806	1.71E-07	21 Jan 2023 04:30:52.283215078	3.82E+00	-2.91E+00	-2.45E+00	3.49E-01	163.8
tle 01672	1.53E-07	18 Jan 2023 08:33:14.703804995	4.53E+00	4.04E+00	-1.56E+00	-1.31E+00	99.8
tle 43787	1.38E-07	18 Jan 2023 19:34:00.169285372	4.27E+00	1.12E+00	4.04E+00	7.80E-01	158.1
tle 46873	1.24E-07	20 Jan 2023 03:35:06.860056636	4.52E+00	-6.55E-01	4.37E+00	9.41E-01	155.7
tle 33315	1.20E-07	19 Jan 2023 14:45:52.405205053	4.60E+00	-4.60E+00	8.99E-02	2.38E-02	154.3

63

Table 12.   Screening process of OneWeb-51645 satellite against full SP catalog

Conjunction Report for object\51645 against the full SP Catalog							
Conjunctions with probability higher than the defined threshold = 1.00e-05							
Object 2	Max Collision Probability	TCA	Min Range (Km)	Min Range - Radial (Km)	Min Range - CrossTrack (Km)	Min Range - InTrack (Km)	Approach Angle (deg)
Conjunctions with probability higher than the defined threshold = 1.00e-07							
Object 2	Max Collision Probability	TCA	Min Range (Km)	Min Range - Radial (Km)	Min Range - CrossTrack (Km)	Min Range - InTrack (Km)	Approach Angle (deg)
41717.eci	5.08E-06	17 Jan 2023 19:29:10.485326210	7.18E-01	-3.23E-02	6.84E-01	2.15E-01	145.1
41877.eci	3.63E-06	19 Jan 2023 04:28:13.835794131	8.28E-01	-1.04E-01	-8.14E-01	1.09E-01	164.7
34944.eci	6.33E-07	20 Jan 2023 11:40:00.433367606	2.36E+00	2.32E+00	-2.95E-01	3.50E-01	68
41717.eci	5.82E-07	17 Jan 2023 17:47:53.262152515	2.12E+00	-1.09E-01	-2.02E+00	-6.33E-01	145.2
31661.eci	5.19E-07	17 Jan 2023 07:16:27.876160057	2.18E+00	-4.90E-01	-2.12E+00	1.27E-01	173.2
37920.eci	4.96E-07	18 Jan 2023 10:16:17.382499511	2.23E+00	2.19E+00	4.16E-01	-2.85E-02	173.3
36652.eci	3.04E-07	18 Jan 2023 17:50:01.844803640	2.84E+00	-2.80E+00	5.14E-01	2.07E-02	173.4
40581.eci	2.58E-07	19 Jan 2023 05:08:48.519927466	3.21E+00	2.87E+00	1.35E+00	-4.83E-01	141.2
13487.eci	2.57E-07	18 Jan 2023 18:09:41.434069876	3.23E+00	-3.21E+00	-3.82E-01	1.46E-01	138.6
41717.eci	2.06E-07	18 Jan 2023 01:23:47.737068922	3.57E+00	-3.53E+00	-4.90E-01	1.59E-01	144.8
41717.eci	1.82E-07	17 Jan 2023 21:10:27.637946624	3.79E+00	1.06E-01	3.62E+00	1.14E+00	145
20974.eci	1.73E-07	20 Jan 2023 19:59:27.709444922	4.06E+00	-2.86E+00	2.53E+00	-1.37E+00	123.1
54558.eci	1.71E-07	18 Jan 2023 13:57:37.621582430	4.07E+00	1.12E+00	3.47E+00	-1.81E+00	125
15774.eci	1.70E-07	19 Jan 2023 02:00:09.957203856	3.99E+00	8.79E-01	3.61E+00	-1.44E+00	136.5
37907.eci	1.69E-07	21 Jan 2023 07:55:51.748044979	3.86E+00	2.38E+00	2.98E+00	6.12E-01	156.6
54985.eci	1.69E-07	20 Jan 2023 08:10:07.478892916	4.06E+00	3.68E+00	-1.55E+00	7.43E-01	129.6
40396.eci	1.67E-07	17 Jan 2023 21:55:16.543893138	4.10E+00	2.39E+00	2.99E+00	1.47E+00	127.6
42347.eci	1.64E-07	17 Jan 2023 06:48:35.951779188	4.22E+00	-4.16E+00	-6.06E-01	3.80E-01	117.4
41667.eci	1.55E-07	21 Jan 2023 07:03:46.113899689	4.11E+00	3.78E+00	-1.55E+00	4.80E-01	145.3
41717.eci	1.48E-07	17 Jan 2023 23:42:30.628586561	4.21E+00	-3.47E+00	2.28E+00	-7.19E-01	144.9
42259.eci	1.44E-07	20 Jan 2023 09:51:05.477930852	4.31E+00	-4.31E+00	-4.35E-02	2.17E-02	139.1
30390.eci	1.43E-07	20 Jan 2023 16:02:46.283837181	4.15E+00	4.11E+00	-5.20E-01	5.13E-02	171.6
41413.eci	1.34E-07	18 Jan 2023 01:00:12.204675796	4.28E+00	-4.05E+00	-1.36E+00	-8.30E-02	173.4
54522.eci	1.34E-07	20 Jan 2023 19:59:18.466684257	4.59E+00	-2.23E+00	-3.56E-01	1.84E+00	125.8
41518.eci	1.21E-07	19 Jan 2023 12:50:43.865435042	4.72E+00	3.44E+00	-3.00E+00	1.19E+00	136.7
29293.eci	1.08E-07	18 Jan 2023 21:43:17.883696031	6.02E+00	4.66E+00	5.04E-01	3.77E+00	15
41717.eci	1.06E-07	18 Jan 2023 03:05:04.872443491	4.98E+00	-3.57E+00	-3.30E+00	1.05E+00	144.7
41717.eci	1.05E-07	17 Jan 2023 16:06:36.028974836	4.99E+00	-1.77E-01	-4.76E+00	-1.49E+00	145.3
30336.eci	1.05E-07	18 Jan 2023 14:46:55.006068246	4.95E+00	1.41E-02	4.80E+00	1.19E+00	152.2
02153.eci	1.03E-07	19 Jan 2023 01:14:51.291844174	4.89E+00	3.80E+00	-3.02E+00	-5.99E-01	163.9
35165.eci	1.02E-07	16 Jan 2023 20:15:04.689604817	4.90E+00	-3.78E+00	3.12E+00	1.80E-01	173.5

64

Table 13.   Screening process of OneWeb-51645 satellite against full TLE catalog

Conjunction Report for object\51645 against the full TLE Catalog							
Conjunctions with probability higher than the defined threshold = 1.00e-05							
Object 2	Max Collision Probability	TCA	Min Range (Km)	Min Range - Radial (Km)	Min Range - CrossTrack (Km)	Min Range - InTrack (Km)	Approach Angle (deg)
tle 41877	2.12E-05	19 Jan 2023 04:28:14.455675486	3.43E-01	-3.06E-01	1.53E-01	-2.06E-02	164.7
tle 46987	1.45E-05	20 Jan 2023 20:05:17.398140008	4.24E-01	-3.78E-01	-1.84E-01	-5.77E-02	145.5
Conjunctions with probability higher than the defined threshold = 1.00e-07							
Object 2	Max Collision Probability	TCA	Min Range (Km)	Min Range - Radial (Km)	Min Range - CrossTrack (Km)	Min Range - InTrack (Km)	Approach Angle (deg)
tle 41717	3.65E-06	17 Jan 2023 19:29:10.417939663	8.47E-01	2.86E-01	7.61E-01	2.39E-01	145.1
tle 41717	5.55E-07	17 Jan 2023 17:47:53.264547748	2.17E+00	2.39E-01	-2.06E+00	-6.45E-01	145.2
tle 37920	4.74E-07	18 Jan 2023 10:16:17.854662619	2.28E+00	2.22E+00	5.17E-01	-3.45E-02	173.3
tle 31661	4.66E-07	17 Jan 2023 07:16:28.017120386	2.30E+00	-2.73E-01	-2.28E+00	1.36E-01	173.2
tle 36652	3.56E-07	18 Jan 2023 17:50:02.109377553	2.63E+00	-2.63E+00	8.23E-02	-3.60E-03	173.4
tle 15774	2.93E-07	19 Jan 2023 02:00:09.976168595	3.04E+00	9.36E-01	2.68E+00	-1.07E+00	136.5
tle 54558	2.02E-07	18 Jan 2023 13:57:37.690899356	3.74E+00	1.17E+00	3.15E+00	-1.64E+00	125
tle 30390	1.99E-07	20 Jan 2023 16:02:45.810641380	3.52E+00	3.27E+00	-1.30E+00	1.06E-01	171.6
tle 20974	1.94E-07	20 Jan 2023 19:59:27.642395582	3.83E+00	-2.94E+00	2.16E+00	-1.16E+00	123.1
tle 41717	1.93E-07	18 Jan 2023 01:23:47.727356332	3.68E+00	-3.67E+00	-2.54E-01	8.38E-02	144.8
tle 40396	1.86E-07	17 Jan 2023 21:55:16.505952999	3.88E+00	2.37E+00	2.76E+00	1.36E+00	127.6
tle 41717	1.81E-07	17 Jan 2023 21:10:27.567677061	3.81E+00	3.32E-01	3.62E+00	1.14E+00	145
tle 55197	1.69E-07	19 Jan 2023 11:54:38.754880103	4.09E+00	3.73E+00	-1.50E+00	7.66E-01	125.7
tle 41413	1.62E-07	18 Jan 2023 01:00:12.318852144	3.89E+00	-3.62E+00	-1.42E+00	-8.64E-02	173.4
tle 42347	1.60E-07	17 Jan 2023 06:48:35.922160693	4.28E+00	-4.27E+00	-2.19E-01	1.45E-01	117.4
tle 30119	1.56E-07	18 Jan 2023 16:35:24.747278316	4.07E+00	-3.40E+00	-2.15E+00	6.22E-01	149
tle 41667	1.52E-07	21 Jan 2023 07:03:46.849911495	4.14E+00	3.52E+00	2.09E+00	-6.56E-01	145.3
tle 12427	1.43E-07	17 Jan 2023 11:03:08.806760002	4.25E+00	-2.93E+00	2.96E+00	8.35E-01	149.2
tle 54522	1.31E-07	20 Jan 2023 19:59:18.466163287	4.65E+00	-2.38E+00	-3.55E+00	1.83E+00	125.8
tle 38022	1.27E-07	18 Jan 2023 21:33:06.698412543	4.53E+00	3.73E+00	2.47E+00	-7.30E-01	147
tle 41717	1.25E-07	17 Jan 2023 23:42:30.581471893	4.59E+00	-3.62E+00	2.69E+00	-8.49E-01	144.9
tle 30336	1.18E-07	18 Jan 2023 14:46:54.976864698	4.65E+00	-8.44E-02	4.51E+00	1.12E+00	152.2
tle 41274	1.13E-07	17 Jan 2023 09:20:25.891374900	5.08E+00	-1.53E+00	4.13E+00	2.53E+00	116.9
tle 35165	1.13E-07	16 Jan 2023 20:15:04.703027193	4.67E+00	-3.68E+00	2.87E+00	1.66E-01	173.5
tle 41717	1.03E-07	18 Jan 2023 03:05:04.869452731	5.05E+00	-3.73E+00	-3.23E+00	1.03E+00	144.7
tle 41717	1.02E-07	17 Jan 2023 16:06:36.107500565	5.08E+00	1.92E-01	-4.84E+00	-1.51E+00	145.3

Table 14 presents a summary of the results in terms of the number of conjunctions classified as in the red zone, with a collision probability greater than 10^{-5}. As we can see for the cases of the ICEYE and IRIDIUM, when using the TLE catalog the process returned fewer conjunctions in the red zone. On the other hand, for the cases of Starlink and OneWeb we see more conjunctions in the red zone when applying the TLE catalog.

Table 14.   Number of conjunctions in the red zone when applying SP and TLE catalogs

Object of Interest	SP catalog	TLE catalog
ICEYE X13	1	0
IRIDIUM 153	2	1
STARLINK-3068	0	1
OneWeb-51645	0	2

As described in Section II, the results presented here cover steps 01 and 02 of the conjunction analysis process. Therefore, HIEs reported as in the red zone will be subject to a more accurate analysis involving updated orbital data, which may require extra radar or optical tracking campaigns. Conjunctions in the red zone that appear only when TLE is used, as in the cases of Starlink and OneWeb, are called false alarms. These false alarms increase the operational team workload because all these alarms must be evaluated. In the results for the OneWeb satellite, the conjunction with the second object 46987 reported as being in the red zone when using the TLE catalog was not even listed in the conjunctions in the yellow zone when the SP catalog was applied. On the other hand, when the screening process fails to report a possible conjunction in the red zone, it causes the exposure of the object of interest to a high risk of collision that could be avoided. We see this situation in the results obtained for the ICEYE and IRIDIUM satellites where at least one high-risk conjunction was not reported for each of the satellites.

To see how these differences impact the work of a team operating a small constellation or group of satellites, we assumed the ICEYE constellation is operated by a

66

single team, and then the screening process was executed using the TLE and SP catalogs. Both catalogs are from 17 January 2023, and the orbital data has been propagated for five days. Table 15 presents a summary of the events with a collision probability greater than 10^{-5}. As we can see, there is a complete discrepancy in the results; none of the events reported when using the SP catalog appear in the results for the TLE catalog. Following the criteria that SP is more accurate than TLE, all four events reported using TLE can be considered false alarms; furthermore, the two events reported using the SP catalog are considered missed events if TLE is the catalog used for conjunction analysis. This means that using the TLE catalog resulted in four false alarms and failed to report two true possible conjunctions.

Table 15. Screening process of the ICEYE constellation against full TLE and SP catalogs

timespan	17 Jan 2023 12:00:00.000 UTCG	22 Jan 2023 12:00:00.000 UTCG					
Conjunction Report for the ICEYE Constellation against the full TLE Catalog							
Conjunctions with probability higher than the defined threshold = 1.00e-05							
Primary Vehicle: ICEYE-X2_43800							
Object Name	Max Collision Probability	Time of Close Appr (TCA) (UTCG)	Min Range (km)	Min Range - Normal (km)	Min Range - Radial (km)	Min Range - InTrack (km)	Approach Angle (deg)
tle 29043	2.93E-05	21 Jan 2023 18:18:34.34	0.358788	-0.355705	-0.355723	-0.043572	41.422
Primary Vehicle: ICEYE-X8_47510							
Object Name	Max Collision Probability	Time of Close Appr (TCA) (UTCG)	Min Range (km)	Min Range - Normal (km)	Min Range - Radial (km)	Min Range - InTrack (km)	Approach Angle (deg)
tle 16719	1.63E-05	21 Jan 2023 5:12:09.9	0.465427	0.442976	0.442934	-0.118308	68.663
Primary Vehicle: ICEYE-X13_48916							
Object Name	Max Collision Probability	Time of Close Appr (TCA) (UTCG)	Min Range (km)	Min Range - Normal (km)	Min Range - Radial (km)	Min Range - InTrack (km)	Approach Angle (deg)
tle 44498	3.13E-04	19 Jan 2023 17:42:15.15	0.093275	0.09146	0.091465	-0.006934	134.868
Primary Vehicle: ICEYE-X20_52759							
Object Name	Max Collision Probability	Time of Close Appr (TCA) (UTCG)	Min Range (km)	Min Range - Normal (km)	Min Range - Radial (km)	Min Range - InTrack (km)	Approach Angle (deg)
tle 53807	8.32E-05	22 Jan 2023 1:51:13.13	0.187522	0.050215	0.050016	0.094188	117.228
Conjunction Report for the ICEYE Constellation against the full SP Catalog							
Conjunctions with probability higher than the defined threshold = 1.00e-05							
Primary Vehicle: 46497.eci							
Object Name	Max Collision Probability	Time of Close Appr (TCA) (UTCG)	Min Range (km)	Min Range - Radial (km)	Min Range - CrossTrack (km)	Min Range - InTrack (km)	Approach Angle (deg)
49228.eci	5.57E-05	18 Jan 2023 23:57:04.4	0.232826	-0.013412	0.19013	0.133712	109.777
Primary Vehicle: 48916.eci							
Object Name	Max Collision Probability	Time of Close Appr (TCA) (UTCG)	Min Range (km)	Min Range - Radial (km)	Min Range - CrossTrack (km)	Min Range - InTrack (km)	Approach Angle (deg)
27119.eci	1.08E-05	19 Jan 2023 06:20:55.55	0.566093	-0.048258	0.337331	0.452041	73.356

A last possible arrangement between the catalogs was also included in the tests, that is, using the SP catalog ephemeris for the primary objects and comparing it against the TLE catalog. Table 16 presents the result for all combinations, ICEYE satellites using TLE data against the full TLE catalog, ICEYE satellites using the SP catalog ephemeris against the full SP catalog, and ICEYE satellites using the SP catalog ephemeris against the full TLE catalog. This last combination may be intuitive from the point of view that even assuming the limitation of using the complete SP catalog in the STK, the ephemeris for a few satellites is easily included in the STK. Thus, one would have the best possible match, the ephemeris of the SP catalog for the objects of interest to be compared against the complete TLE catalog. The screening process was performed between 24 and 29 January. As we can see, the use of the SP catalog ephemeris for the primary objects does not solve the problem of getting false alarms or avoiding miss events. In fact, the two options that apply TLE data return only false alarms and missed the real high-risk event, which, in this case, is a conjunction with a collision probability of 10^{-4}.

Table 16.　　　Screening process of the ICEYE constellation using ephemeris of SP catalog against full TLE SP catalog

timespan	24 Jan 2023 12:00:00.000 UTCG	29 Jan 2023 12:00:00.000 UTCG					
	Conjunction Report for the ICEYE Constellation against the full SP Catalog						
	Conjunctions with probability higher than the defined threshold = 1.00e-05						
Primary Vehicle: 51008.eci							
Object Name	Max Collision Probability	Time of Close Appr (TCA) (UTCG)	Min Range (km)	Min Range - Normal (km)	Min Range - Radial (km)	Min Range - InTrack (km)	Approach Angle (deg)
27657.eci	1.33E-04	26 Jan 2023 15:31:50.50 UTC	0.171437	-0.116854	-0.11671	0.125576	4.747
	Conjunction Report for the ICEYE Constellation against the full TLE Catalog						
	Conjunctions with probability higher than the defined threshold = 1.00e-05						
Primary Vehicle: ICEYE-X7_46496							
Object Name	Max Collision Probability	Time of Close Appr (TCA) (UTCG)	Min Range (km)	Min Range - Normal (km)	Min Range - Radial (km)	Min Range - InTrack (km)	Approach Angle (deg)
tle 22161	1.11E-05	26 Jan 2023 20:32:13.13 UTC	0.496824	0.397158	0.397057	0.113842	133.278
Primary Vehicle: ICEYE-X6_46497							
Object Name	Max Collision Probability	Time of Close Appr (TCA) (UTCG)	Min Range (km)	Min Range - Normal (km)	Min Range - Radial (km)	Min Range - InTrack (km)	Approach Angle (deg)
tle 45820	1.37E-05	24 Jan 2023 16:11:25.25 UTC	0.4629	0.272545	0.272389	-0.203595	117.113
Primary Vehicle: ICEYE-X13_48916							
Object Name	Max Collision Probability	Time of Close Appr (TCA) (UTCG)	Min Range (km)	Min Range - Normal (km)	Min Range - Radial (km)	Min Range - InTrack (km)	Approach Angle (deg)
tle 34993	1.56E-05	24 Jan 2023 17:51:07.7 UTC	0.49405	-0.166756	-0.166641	0.443187	35.25
Primary Vehicle: ICEYE-X24_52755							
Object Name	Max Collision Probability	Time of Close Appr (TCA) (UTCG)	Min Range (km)	Min Range - Normal (km)	Min Range - Radial (km)	Min Range - InTrack (km)	Approach Angle (deg)
tle 48954	3.98E-04	26 Jan 2023 18:30:17.17 UTC	0.098879	0.067043	0.067022	-0.071925	17.113
Primary Vehicle: ICEYE-X19_52758							
Object Name	Max Collision Probability	Time of Close Appr (TCA) (UTCG)	Min Range (km)	Min Range - Normal (km)	Min Range - Radial (km)	Min Range - InTrack (km)	Approach Angle (deg)
tle 52027	1.21E-05	28 Jan 2023 02:22:42.42 UTC	0.497317	0.285708	0.285526	-0.226474	112.498
	Conjunction Report for the ICEYE Constellation(using ephemeris of SP catalog) against the full TLE Catalog						
	Conjunctions with probability higher than the defined threshold = 1.00e-05						
Primary Vehicle: 44389.eci							
Object Name	Max Collision Probability	Time of Close Appr (TCA) (UTCG)	Min Range (km)	Min Range - Normal (km)	Min Range - Radial (km)	Min Range - InTrack (km)	Approach Angle (deg)
tle 53088	2.57E-05	27 Jan 2023 04:50:22.22 UTC	0.318435	0.318435	0.318435	-0.00023	148.859
Primary Vehicle: 51070.eci							
Object Name	Max Collision Probability	Time of Close Appr (TCA) (UTCG)	Min Range (km)	Min Range - Normal (km)	Min Range - Radial (km)	Min Range - InTrack (km)	Approach Angle (deg)
tle 35272	1.17E-04	26 Jan 2023 04:42:47.47 UTC	0.181802	0.003249	0.003445	0.172547	36.529
tle 55243	1.32E-05	25 Jan 2023 11:33:28.28 UTC	0.520968	-0.000003	-0.000976	-0.434213	67.136
Primary Vehicle: 52755.eci							
Object Name	Max Collision Probability	Time of Close Appr (TCA) (UTCG)	Min Range (km)	Min Range - Normal (km)	Min Range - Radial (km)	Min Range - InTrack (km)	Approach Angle (deg)
tle 51658	1.20E-05	27 Jan 2023 04:50:29.29 UTC	0.510826	-0.009279	-0.009199	0.314929	103.874
Primary Vehicle: 52762.eci							
Object Name	Max Collision Probability	Time of Close Appr (TCA) (UTCG)	Min Range (km)	Min Range - Normal (km)	Min Range - Radial (km)	Min Range - InTrack (km)	Approach Angle (deg)
tle 46459	2.05E-05	27 Jan 2023 04:27:31.31 UTC	0.420961	0.416044	0.416035	-0.054145	64.344

70

In daily operations, the owner always has the last state vector from the orbit determination process for the objects under control. This state vector can be propagated with the next station-keeping maneuvers and include the covariance matrix. Therefore, the most accurate screening process must compare the owner's ephemeris against the full SP catalog.

B.   TANGENTIAL COLLISION AVOIDANCE MANEUVER FOR THE CASE OF THE ICEYE SATELLITE

Based on the conclusion of Hernando-Ayuso and Bombardelli [32], in which the tangential maneuver performs similarly to the optimal solution at the minimum collision probability points, only the tangential strategy for the case of the ICEYE satellite was tested. We are interested in testing the performance of the tangential maneuver in two aspects; first, we want to know whether a 30-minute maneuver is sufficient to bring the maximum collision probability below the level of acceptable risk, and second, how long before TCA should this maneuver be performed.

Currently, the only way to perform a maneuver in the STK is through the Astrogator module, which is a specialized analysis module for interactive orbit maneuvers and spacecraft trajectory design. Appendix E shows a MATLAB-STK integration script developed to test how a tangential maneuver performs for the cases of the ICEYE satellite in conjunction with a second object. The script executes a routine that maintains all the initial parameters defined by the user, changing only the starting point of the maneuver. That is, the same maneuver is performed at different times before the TCA. Table 17 details the data used in the simulations for the ICEYE satellite and Table 18 to Table 21 present the orbital parameters for the objects involved in the conjunction.

71

Table 17.   ICEYE parameters

Total mass	92	Kg
Drag area	0.28	m^2
SRP area	1.28	m^2
Total Thrust	1.40E-03	N
Isp	4200	sec
Thrust arc	30	minutes

The four events with a collision probability greater than 10^{-5} resulting from the screening process applying the SP catalog presented in the previous section were tested. Figure 32 to Figure 35 show the results in terms of maximum collision probability versus the maneuver lead time to TCA. For each conjunction a prograde and retrograde maneuver were tested with the same thrust magnitude and thrust arc described in Table 17. We assumed all secondary objects are not cooperative, that is, they will not perform any collision avoidance action.

1.   Conjunction between ICEYE-X13 (NORAD 48916) and OBJECT K (NORAD 47941)

As we can see in Figure 32, for that conjunction a retrograde maneuver performs better than a prograde maneuver. The retrograde maneuver can bring the collision probability to under 10^{-7} if executed at least six orbital periods before the TCA. To get the same result with a prograde maneuver it must be executed ten orbital periods before TCA. It is interesting to see that a prograde maneuver when executed with less than four orbital periods before TCA increases rather than decreases the collision probability, which is the objective for a CAM. Table 18 details the orbital parameters used in the simulations.

72

Table 18.   ICEYE-X13 and Object K orbital elements at TCA

Orbital elements	ICEYE-X13	OBJECT K
Semi-major Axis	6893.73 km	6905.37 km
Apogee Altitude	519.784 km	536.963 km
Perigee Altitude	511.403 km	517.503 km
Eccentricity	0.000607871	0.0014091
Inclination	97.6508 deg	97.3922 deg
RAAN	148.802 deg	277.282 deg
Argument of Perigee	200.795 deg	124.847 deg
True Anomaly	232.778 deg	339.071 deg
Period	94.9382 min	95.1788 min
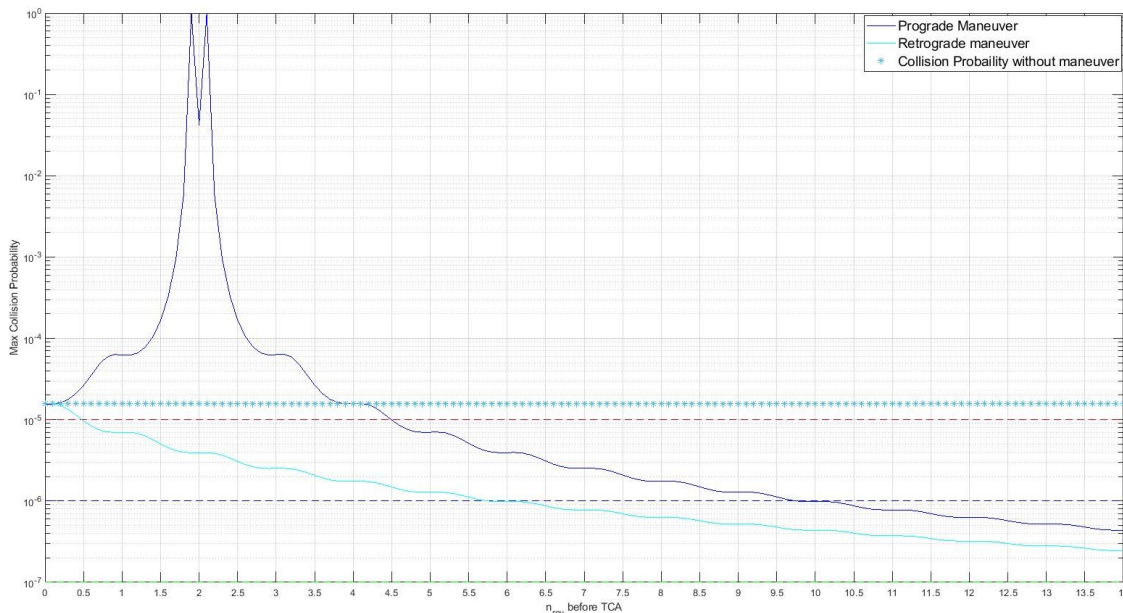
Figure 32.   Tangential CAM maneuvers to avoid collision between ICEYE-X13 (NORAD 48916) and OBJECT K (NORAD 47941)

2.   Conjunction between ICEYE-X6 (NORAD 46497) and RESURS O1 DEBRIS (NORAD 49228).

In this scenario, the prograde maneuver performs better than the retrograde one. The CAM reduces the collision probability to the level of 10^{-7} if executed at least five and a half orbital periods before TCA, as we can see in Figure 33. Table 19 details the orbital parameters used in the simulations.

73

Table 19.   ICEYE-X6 and RESURS O1 DEBRIS orbital elements at TCA

Orbital elements	ICEYE-X6	RESURS O1 DEBRIS
Semi-major Axis	6929.88 km	6934.99 km
Apogee Altitude	560.582 km	563.044 km
Perigee Altitude	542.902 km	550.671 km
Eccentricity	0.00127563	0.000892077
Inclination	97.7169 deg	98.0156 deg
RAAN	323.685 deg	75.0244 deg
Argument of Perigee	277.656 deg	339.766 deg
True Anomaly	164.43 deg	124.989 deg
Period	95.686 min	95.7919 min
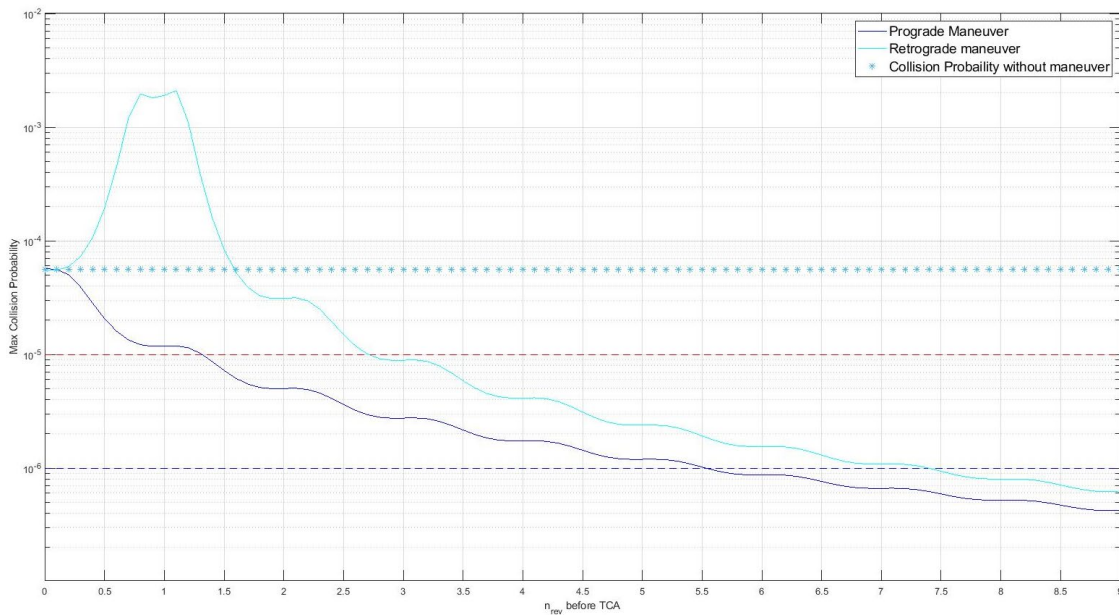
Figure 33.   Tangential CAM maneuvers to avoid collision between ICEYE-X6 (NORAD 46497) and RESURS O1 DEBRIS (NORAD 49228)

3.   Conjunction between ICEYE-X13 (NORAD 48916) and PSLV DEBRIS (NORAD 27119)

Figure 34 shows a prograde CAM can reduce the collision probability to under 10^{-7} when performed at least three and a half orbital periods before TCA. By contrast, the same result can only be achieved by the retrograde maneuver if performed six and a half

orbital periods before the TCA. Table 20 details the orbital parameters used in the simulations.

Table 20.   ICEYE-X13 and PSLV DEBRIS orbital elements at TCA

Orbital elements	ICEYE-X13	PSLV DEBRIS
Semi-major Axis	6892.26 km	6873.66 km
Apogee Altitude	535.043 km	534.913 km
Perigee Altitude	493.196 km	456.126 km
Eccentricity	0.00303581	0.00573111
Inclination	97.6459 deg	97.834 deg
RAAN	150.418 deg	76.2764 deg
Argument of Perigee	90.7054 deg	83.4368 deg
True Anomaly	181.791 deg	177.451 deg
Period	94.9078 min	94.5239 min
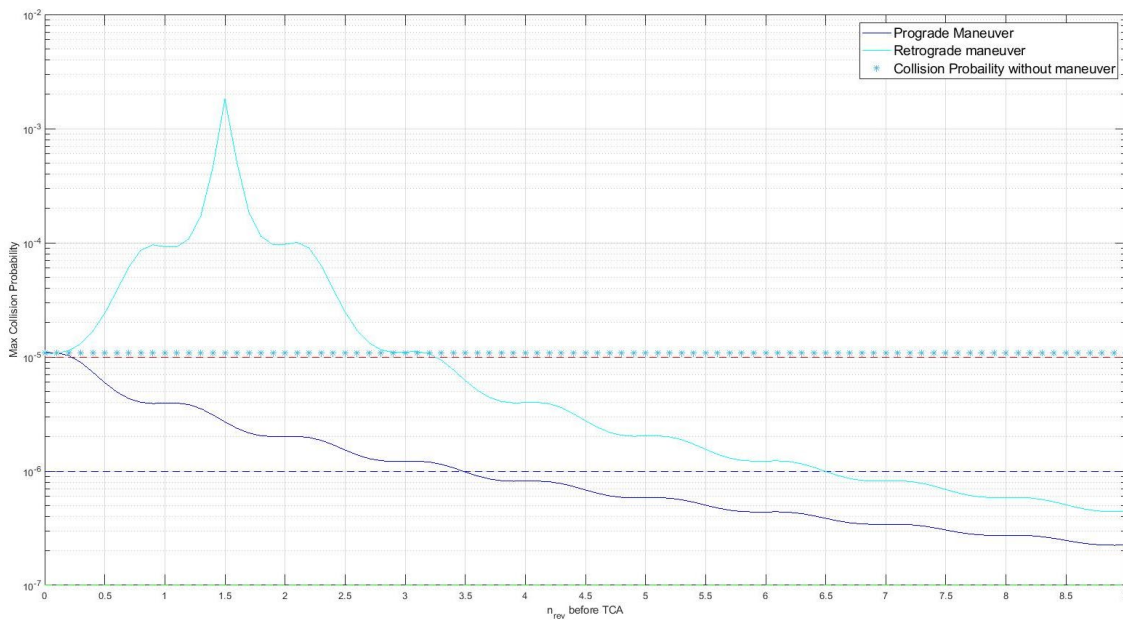
Figure 34.   Tangential CAM maneuvers to avoid collision between ICEYE-
X13 (NORAD 48916) and PSLV DEBRIS (NORAD 27119)

4. Conjunction between ICEYE-X16 (NORAD 51008) and PSLV DEBRIS (NORAD 27657)

Once again in this scenario the 30-minute low-thrust maneuver could reduce the collision probability to acceptable risk levels. As we can see in the Figure 35, the prograde maneuver performed better than the retrograde in reducing the collision probability to the acceptable level when performed at least four orbital periods before TCA. Table 21 details the orbital parameters used in the simulations.

Table 21.   ICEYE-X16 and PSLV DEBRIS orbital elements at TCA

Orbital elements	ICEYE-X16	PSLV DEBRIS
Semi-major Axis	6877.56 km	6888.78 km
Apogee Altitude	508.154 km	523.688 km
Perigee Altitude	490.687 km	497.602 km
Eccentricity	0.00126986	0.00189339
Inclination	97.5892 deg	97.9356 deg
RAAN	94.8933 deg	90.1175 deg
Argument of Perigee	342.371 deg	145.78 deg
True Anomaly	112.789 deg	308.736 deg
Period	94.6043 min	94.836 min
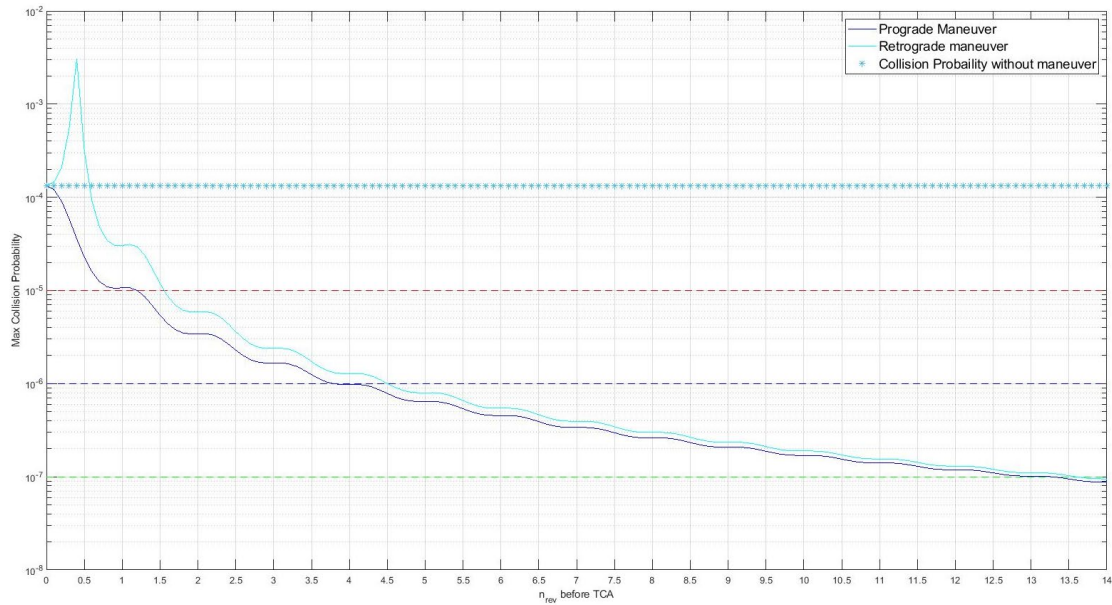
Figure 35. Tangential CAM maneuvers to avoid collision between ICEYE-X16 (NORAD 51008) and PSLV DEBRIS (NORAD 27657)

C. AERODYNAMIC COLLISION AVOIDANCE ACTION

We are also interested in testing the feasibility of the aerodynamic approach for the case of the ICEYE satellite. As mentioned previously, even if the satellite is equipped with a propulsion system, this strategy can be helpful in case of system failure or to save propellant.

In these tests, the solar pressure area was kept constant, and only the drag area was changed for a certain period before TCA, from the nominal condition of 0.28 m^2 (0.4 x 0.7 m) to the maximum of 1.28 m^2 (3.2 x 0.4 m), which is the area of the SAR antenna. A MATLAB-STK integrated program was developed to design the drag maneuvers and test how it performs for the ICEYE satellite (see Appendix F).

Figure 36 to Figure 39 present the results of the "drag maneuver" for the same conjunctions used in the tangential low-thrust CAM tests presented in the previous section. As we can observe, drag maneuvers have the same behavior as retrograde maneuvers, which is expected since the drag force also acts in the opposite direction to the velocity vector, but with a different magnitude. These results demonstrate that the drag maneuver

77

is feasible for the ICEYE case but requires a change in the satellite's attitude between 10.5 to 17.5 orbital periods, depending on the conjunction. It is important to observe that, in order to reach the maximum drag area, the satellite needs to point its antenna in the direction of movement. That is, its antenna can no longer point to the Earth's surface; therefore, the mission is interrupted for that time, which is not negligible, as 10.5 orbital periods equal approximately 16.7 hours and 17.5 orbital periods equal about 27.7 hours.
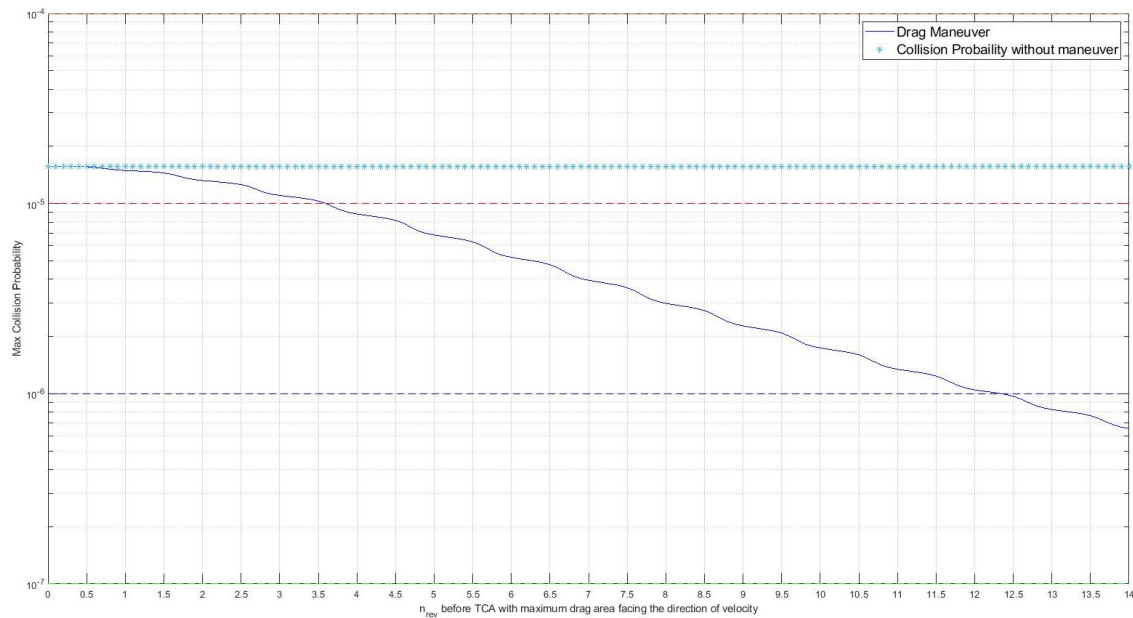
Figure 36.   Drag maneuver to avoid collision between ICEYE-X13 (NORAD 48916) and OBJECT K (NORAD 47941)
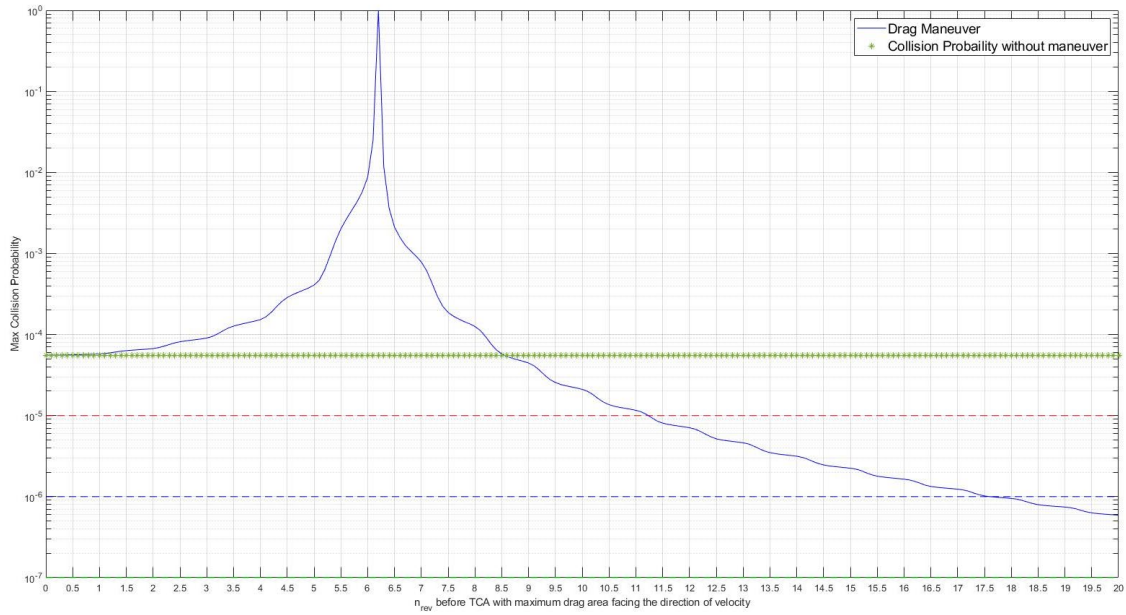
Figure 37.   Drag maneuver to avoid collision between ICEYE-X6 (NORAD 46497) and RESURS O1 DEBRIS (NORAD 49228)
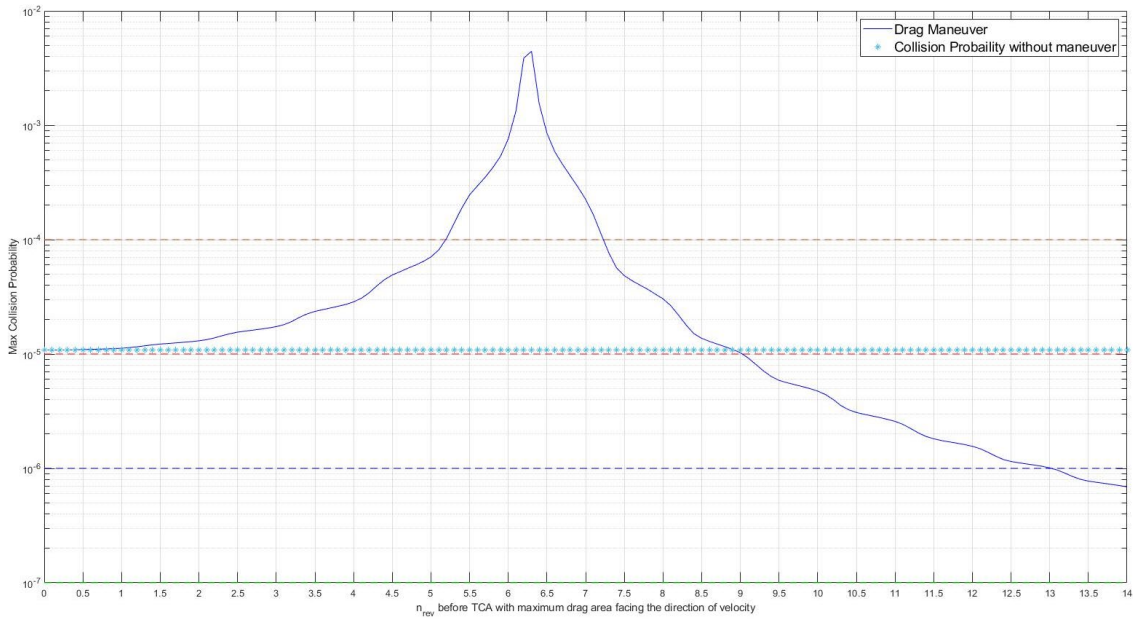
Figure 38.   Drag maneuver to avoid collision between ICEYE-X13 (NORAD 48916) and PSLV DEBRIS (NORAD 27119)
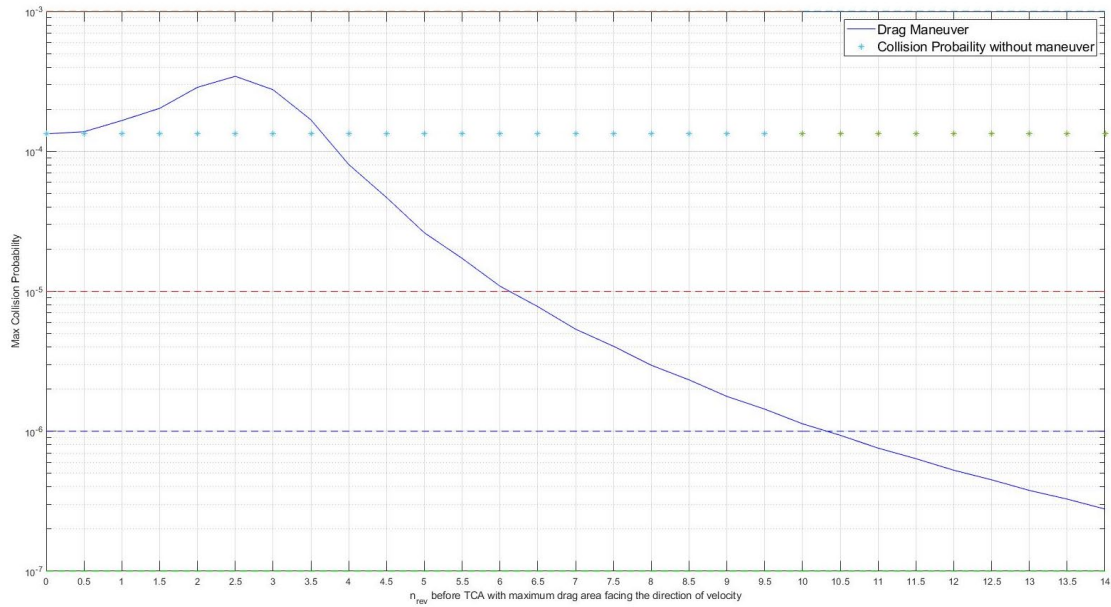
Figure 39. Drag maneuver to avoid collision between ICEYE-X16 (NORAD 51008) and PSLV DEBRIS (NORAD 27657)

Figure 40 shows the report criteria for 18 SPCS to send a CDM to an operator. As we can see for LEO satellites, referred to as near Earth in the table, a CDM is sent three days or less before TCA. This gives the operator enough—but not too much—time to run the conjunction analysis process and, if necessary, design and execute a tangential CAM (prograde/retrograde) or a drag maneuver to avoid a collision with a second object.

Table 5: Basic Reporting Criteria			
	Space-Track Criteria	**Emergency Criteria**	**Emergency Phone Call Criteria**
Notification Method	**Conjunction Data Message (CDM)**	**Conjunction Data Message (CDM) & Close Approach Notification (CAN) email**	**CDM, CAN email & phone call**
Deep Space HAC	TCA ≤ 10 days and Overall miss ≤ 5km	TCA ≤ 3 days and Overall miss ≤ 5km	TCA ≤ 3 days and Overall miss ≤ 500m
Deep Space O/O Ephemeris	TCA ≤ 10 days and Overall miss ≤ 5km	TCA ≤ 3 days and Overall miss ≤ 5km	N/A
Near Earth HAC	TCA ≤ 3 days and Overall miss ≤ 1km	TCA ≤ 3 days & Overall miss ≤ 1km & Probability of Collision ≥ e^-4	TCA ≤ 3 days and Overall miss ≤ 1km and Probability of Collision ≥ e^-2
Near Earth O/O Ephemeris	TCA ≤ 3 days and Overall miss ≤ 1km	TCA ≤ 3 days & Overall miss ≤ 1km & Probability of Collision ≥ e^-4	N/A

Figure 40.   Basic reporting criteria. Source: [13].

81

THIS PAGE INTENTIONALLY LEFT BLANK

VI.   ANALYSIS AND CONCLUSION

This thesis had three main objectives: to test the performance of a tangential low-thrust collision avoidance maneuver strategy for an ICEYE satellite, to develop a solution enabling the use of the full SP catalog in STK for the screening process, and to test the feasibility of aerodynamic maneuver as a collision avoidance action for the ICEYE satellite. The data used as parameters for the ICEYE satellite was based on the product documentation, and some assumptions were also made. The conjunctions used to test the tangential maneuvers and the aerodynamic solution result from the ICEYE constellation screening process against the full SP catalog.

A.   SCREENING PROCESS USING THE FULL SP CATALOG IN STK

A MATLAB-STK program is proposed to allow the use of the full SP catalog for the screening process in STK. Previously, the operator could only use the TLE catalog, which is not recommended by NASA operational security due to its low accuracy.

Comparing the outputs of the screening process using the SP and TLE catalogs, we noticed an increase in false alarms and a failure to report actual conjunctions when using the TLE catalog. These two situations are undesirable; in the first one, the operator has an increased workload analyzing unrealistic conjunctions. In the second situation, where actual conjunctions are not reported, the operator assumes an avoidable collision risk for the object of interest. In day-to-day operations, the owner usually has the most accurate state vector and covariance matrix for the objects under control. When using the STK as a conjunction analysis tool, the most accurate screening process must compare the ephemeris of the object of interest, obtained in the last orbit determination process performed by the operator, with the complete SP catalog by executing the proposed program.

B.   TANGENTIAL LOW-THRUST COLLISION AVOIDANCE MANEUVER STRATEGY FOR THE ICEYE SATELLITE

The collision avoidance maneuver strategies described in this work are divided into two large groups, tangential maneuvers, where the acceleration is applied in the direction of the velocity vector, or maneuvers with an optimized trajectory to reduce the collision

83

probability. Based on the conclusion of Hernando-Ayuso and Bombardelli [32], in which the tangential maneuver performs similarly to the optimal solution at the minimum collision probability points, only the tangential strategy was tested. A MATLAB-STK integrated program was developed to design the tangential maneuvers and test how it performs for the ICEYE satellite. Four scenarios involving an ICEYE satellite and a second object were tested by executing a (prograde/retrograde) tangential maneuver of $1.4 \cdot 10^{-3}$ N thrust magnitude for 30 minutes at different points before TCA.

Results showed that when performed with sufficient lead time to TCA, the tangential solution can reduce the collision probability by at least two orders of magnitude, from 10^{-5} to 10^{-7}, which brings the collision probability under the acceptable risk. For the tested cases, the advance time to TCA where the CAM must be executed to be effective varies between three and a half and six orbital periods. Another point to be observed is the fact that depending on the scenario, a retrograde or prograde maneuver can increase the probability of collision when executed close to the TCA. Therefore, it is essential to consider the direction of the maneuver (prograde/retrograde) together with the time of advance to the TCA when it will be executed.

C.   AERODYNAMIC COLLISION AVOIDANCE ACTION

The possibility of collision avoidance action using the aerodynamic effect of the spacecraft was also studied. This solution is more applicable for satellites that do not have a propulsion system; however, it is still an option for satellites equipped with a propulsion system that is degraded or that needs to save fuel. The feasibility of this solution is related to the ability of the satellite to change the drag or solar pressure area, which can be achieved by modulating its ballistic coefficient either by a retractable device or changing attitude. The ICEYE satellite is not equipped with any aerodynamic retractable device, so changing the attitude is the only option to apply this approach. For these tests, the solar pressure area was considered constant while the drag area was changed from the nominal to maximum value for a certain time before TCA.

The results demonstrate that changing the drag area as a collision prevention action is feasible for the ICEYE case since the change from the nominal to the maximum drag

84

area is done for 10.5 to 17.5 orbital periods, depending on the conjunction. It is important to observe that, in order to reach the maximum drag area, the satellite needs to point its antenna in the direction of movement, which means it can no longer point to the Earth's surface; therefore, the mission is stopped for that time, which is not negligible, as 10.5 orbital periods equal approximately 16.7 hours and 17.5 orbital periods equal about 27.7 hours.

18 SPCS sends a CDM to the operator of a LEO satellite three days or less before TCA. Therefore, the operator must have enough, but not too much, time to run the conjunction analysis process and, if necessary, design and execute a tangential CAM (prograde/retrograde) or a drag maneuver to avoid a collision with a second object.

D.   CONCLUSION

The program developed in this study demonstrated the feasibility of using the complete SP catalog in STK for conjunction analysis, which eliminates the need for the TLE catalog, the use of which is not recommended by NASA for this analysis. For the controlled object, we recommend using the ephemeris obtained by the controller in the last orbit determination process, including the covariance matrix and the orbit maintenance maneuvers predicted for the next few days.

The results of the four test cases for tangential or drag collision avoidance maneuvers demonstrated that both strategies are feasible for the ICEYE satellites, but maneuvers must be performed within a certain amount of time before the TCA, and for both strategies, the payload cannot be used during the maneuver. While a 30-minute tangential maneuver is enough for the tested cases, a 17 to 28 hour drag maneuver was required. Therefore, we recommend using a tangential CAM whenever possible to increase the efficiency of the payload usage. For tangential maneuvers, a point of attention is the direction of the maneuver, prograde or retrograde. The results show that depending on the conjunction, the prograde and retrograde maneuvers work differently; one even increases the probability of collision when performed close to the TCA.

THIS PAGE INTENTIONALLY LEFT BLANK

APPENDIX A. CONJUNCTION DATA MESSAGE (CDM)

```
CCSDS_CDM_VERS                      =1.0
COMMENT                             =CDM_ID :372311711
CREATION_DATE                       =2022-10-26T15:35:33.000000
ORIGINATOR                          =CspOC
MESSAGE_FOR                         =ICEYE-X17
MESSAGE_ID
=000052762_conj_000013068_2022301132344_29916102567270
TCA                                 =2022-10-28T13 :23 :44.206000
MISS_DISTANCE                       =88                          [m]
RELATIVE_SPEED                      =10744                       [m/s]
RELATIVE_POSITION_R                 =82.5                        [m]
RELATIVE_POSITION_T                 =21.6                        [m]
RELATIVE_POSITION_N                 =-25.2                       [m]
RELATIVE_VELOCITY_R                 =-8.4                        [m/s]
RELATIVE_VELOCITY_T                 =-7607                       [m/s]
RELATIVE_VELOCITY_N                 =-7588.6                     [m/s]
COLLISION_PROBABILITY               =0.0000050977
COLLISION_PROBABILITY_METHOD        =FOSTER-1992
COMMENT Screening Option = Covariance
OBJECT                              =OBJECT1
OBJECT_DESIGNATOR                   =52762
CATALOG_NAME                        =SATCAT
OBJECT_NAME                         =ICEYE-X17
INTERNATIONAL_DESIGNATOR            =2022-057AG
OBJECT_TYPE                         =PAYLOAD
OPERATOR_CONTACT_POSITION           =https://www.space-track.org/
expandedspacedata/query/class/organization/object/~~52762/orderby/
ORG_NAME,INFO_ID/format/html/emptyresult/show/
OPERATOR_ORGANIZATION               =ICEYE US,ICEYE
OPERATOR_PHONE                      =https://www.space-track.org/
expandedspacedata/query/class/organization/object/~~52762/orderby/
ORG_NAME,INFO_ID/format/html/emptyresult/show/
OPERATOR_EMAIL                      =https://www.space-track.org/
expandedspacedata/query/class/organization/object/~~52762/orderby/
ORG_NAME,INFO_ID/format/html/emptyresult/show/
EPHEMERIS_NAME                      =NONE
COVARIANCE_METHOD                   =CALCULATED
MANEUVERABLE                        =NO
REF_FRAME                           =ITRF
GRAVITY_MODEL                       =EGM-96: 36D 36O
ATMOSPHERIC_MODEL                   =JBH09
N_BODY_PERTURBATIONS                =MOON,SUN
SOLAR_RAD_PRESSURE                  =YES
EARTH_TIDES                         =YES
INTRACK_THRUST                      =NO
COMMENT Covariance Scale Factor = 1.000000
COMMENT Exclusion Volume Radius = 5.000000 [m]
TIME_LASTOB_START                   =2022-10-25T15:35:33.919000
TIME_LASTOB_END                     =2022-10-26T15:35:33.919000
```

```
RECOMMENDED_OD_SPAN                    =1.46                    [d]
ACTUAL_OD_SPAN                         =1.45                    [d]
OBS_AVAILABLE                          =196
OBS_USED                               =194
RESIDUALS_ACCEPTED                     =97.9                    [%]
WEIGHTED_RMS                           =1.304
COMMENT Apogee Altitude = 557    [km]
COMMENT Perigee Altitude = 503    [km]
COMMENT Inclination = 97.5  [deg]
COMMENT Operator Hard Body Radius = 0.00 [m]
AREA_PC                                =1.0309                  [m**2]
CD_AREA_OVER_MASS                      =0.037536118468          [m**2/
kg]
CR_AREA_OVER_MASS                      =0.021871854145          [m**2/
kg]
THRUST_ACCELERATION                    =0                       [m/
s**2]
SEDR                                   =0.00213353              [W/kg]
X                                      =-1113.186788            [km]
Y                                      =-835.053062             [km]
Z                                      =-6772.192084            [km]
X_DOT                                  =-7.527903208            [km/s]
Y_DOT                                  =0.653125236             [km/s]
Z_DOT                                  =1.162736538             [km/s]
COMMENT DCP Density Forecast Uncertainty = 1.903766130000000E-01
COMMENT DCP Sensitivity Vector RTN Pos = -1.128557275286270E+02
1.243062847347792E+04   1.341995793432415E+00   [m]
COMMENT DCP Sensitivity Vector RTN Vel = -1.367850252102217E+01
6.729677043428428E-02  -8.261823497645248E-03 [m/sec]
CR_R                                   =997.1738320780714       [m**2]
CT_R                                   =-53543.74368997059      [m**2]
CT_T                                   =6184616.559163199       [m**2]
CN_R                                   =-48.60781884183174      [m**2]
CN_T                                   =488.8061749750369       [m**2]
CN_N                                   =20.70350519720099       [m**2]
CRDOT_R                                =58.9994559989852        [m**2/
s]
CRDOT_T                                =-6804.872722018794      [m**2/
s]
CRDOT_N                                =-0.5416439726600534     [m**2/
s]
CRDOT_RDOT                             =7.487387322175244       [m**2/
s**2]
CTDOT_R                                =-0.8491519560402649     [m**2/
s]
CTDOT_T                                =31.04662708486413       [m**2/
s]
CTDOT_N                                =0.05086509399245132     [m**2/
s]
CTDOT_RDOT                             =-0.03425310361444973    [m**2/
s**2]
CTDOT_TDOT                             =0.0007874868901286095   [m**2/
s**2]
```

```
CNDOT_R                               =0.01745269228958502          [m**2/
s]
CNDOT_T                               =-4.164875527724961           [m**2/
s]
CNDOT_N                               =0.01068790413040317          [m**2/
s]
CNDOT_RDOT                            =0.004583545306761906         [m**2/
s**2]
CNDOT_TDOT                            =-0.000000569606390339  7228  [m**2/
s**2]
CNDOT_NDOT                            =0.00005174788141397241       [m**2/
s**2]
CDRG_R                                =0                            [m**3/
kg]
CDRG_T                                =0                            [m**3/
kg]
CDRG_N                                =0                            [m**3/
kg]
CDRG_RDOT                             =0
[m**3/(kg*s)]
CDRG_TDOT                             =0
[m**3/(kg*s)]
CDRG_NDOT                             =0
[m**3/(kg*s)]
CDRG_DRG                              =0                            [m**4/
kg**2]
CSRP_R                                =0                            [m**3/
kg]
CSRP_T                                =0                            [m**3/
kg]
CSRP_N                                =0                            [m**3/
kg]
CSRP_RDOT                             =0
[m**3/(kg*s)]
CSRP_TDOT                             =0
[m**3/(kg*s)]
CSRP_NDOT                             =0
[m**3/(kg*s)]
CSRP_DRG                              =0                            [m**4/
kg**2]
CSRP_SRP                              =0                            [m**4/
kg**2]
OBJECT                                =OBJECT2
OBJECT_DESIGNATOR                     =13068
CATALOG_NAME                          =SATCAT
OBJECT_NAME                           =SL-3 R/B
INTERNATIONAL_DESIGNATOR              =1982-013B
OBJECT_TYPE                           =ROCKET BODY
OPERATOR_CONTACT_POSITION             =https://www.space-track.org/
expandedspacedata/query/class/organization/object/~~13068/orderby/
ORG_NAME,INFO_ID/format/html/emptyresult/show/
OPERATOR_ORGANIZATION                 =NONE
```

89

```
OPERATOR_PHONE                      =https://www.space-track.org/
expandedspacedata/query/class/organization/object/~~13068/orderby/
ORG_NAME,INFO_ID/format/html/emptyresult/show/
OPERATOR_EMAIL                      =https://www.space-track.org/
expandedspacedata/query/class/organization/object/~~13068/orderby/
ORG_NAME,INFO_ID/format/html/emptyresult/show/
EPHEMERIS_NAME                      =NONE
COVARIANCE_METHOD                   =CALCULATED
MANEUVERABLE                        =N/A
REF_FRAME                           =ITRF
GRAVITY_MODEL                       =EGM-96: 36D 36O
ATMOSPHERIC_MODEL                   =JBH09
N_BODY_PERTURBATIONS                =MOON,SUN
SOLAR_RAD_PRESSURE                  =YES
EARTH_TIDES                         =YES
INTRACK_THRUST                      =NO
COMMENT Covariance Scale Factor = 1.000000
COMMENT Exclusion Volume Radius = 5.000000 [m]
TIME_LASTOB_START                   =2022-10-25T15:35:33.416000
TIME_LASTOB_END                     =2022-10-26T15:35:33.416000
RECOMMENDED_OD_SPAN                 =3.5                      [d]
ACTUAL_OD_SPAN                      =3.5                      [d]
OBS_AVAILABLE                       =753
OBS_USED                            =748
RESIDUALS_ACCEPTED                  =99.7                     [%]
WEIGHTED_RMS                        =1.032
COMMENT Apogee Altitude = 551    [km]
COMMENT Perigee Altitude = 521    [km]
COMMENT Inclination = 81.2  [deg]
AREA_PC                             =6.0699                   [m**2]
CD_AREA_OVER_MASS                   =0.012170671629           [m**2/
kg]
CR_AREA_OVER_MASS                   =0.001269785242           [m**2/
kg]
THRUST_ACCELERATION                 =0                        [m/
s**2]
SEDR                                =0.0004589                [W/kg]
X                                   =-1113.22278              [km]
Y                                   =-835.086318              [km]
Z                                   =-6772.266249             [km]
X_DOT                               =-0.451013356             [km/s]
Y_DOT                               =-7.430598325             [km/s]
Z_DOT                               =1.004779913              [km/s]
COMMENT DCP Density Forecast Uncertainty = 1.924108880000000E-01
COMMENT DCP Sensitivity Vector RTN Pos = -1.941926593906495E+01
2.138388640215040E+03   3.809492659589557E-01   [m]
COMMENT DCP Sensitivity Vector RTN Vel = -2.343937278178833E+00
8.883361836353828E-03   1.587470773511255E-03   [m/sec]
CR_R                                =56.77580027419289        [m**2]
CT_R                                =-1683.141861209677       [m**2]
CT_T                                =184619.3545189274        [m**2]
CN_R                                =-5.848362778938688       [m**2]
CN_T                                =38.90099522464033        [m**2]
```

90

```
CN_N                          =6.05237797927004              [m**2]
CRDOT_R                       =1.826287658568663             [m**2/
s]
CRDOT_T                       =-202.2880769570989            [m**2/
s]
CRDOT_N                       =-0.03928895482549575          [m**2/
s]
CRDOT_RDOT                    =0.2216719002659967            [m**2/
s**2]
CTDOT_R                       =-0.05290565867681885          [m**2/
s]
CTDOT_T                       =0.7989291534056178            [m**2/
s]
CTDOT_N                       =0.006237931042906348          [m**2/
s]
CTDOT_RDOT                    =-0.0008553378914286573        [m**2/
s**2]
CTDOT_TDOT                    =0.00005374379260052903        [m**2/
s**2]
CNDOT_R                       =-0.001105826137548899         [m**2/
s]
CNDOT_T                       =0.1401316156924459            [m**2/
s]
CNDOT_N                       =0.003650635599895444          [m**2/
s]
CNDOT_RDOT                    =-0.000151239962953566         [m**2/
s**2]
CNDOT_TDOT                    =0.0000004423564756567914      [m**2/
s**2]
CNDOT_NDOT                    =0.0000189526080388304         [m**2/
s**2]
CDRG_R                        =0                             [m**3/
kg]
CDRG_T                        =0                             [m**3/
kg]
CDRG_N                        =0                             [m**3/
kg]
CDRG_RDOT                     =0
[m**3/(kg*s)]
CDRG_TDOT                     =0
[m**3/(kg*s)]
CDRG_NDOT                     =0
[m**3/(kg*s)]
CDRG_DRG                      =0                             [m**4/
kg**2]
CSRP_R                        =0                             [m**3/
kg]
CSRP_T                        =0                             [m**3/
kg]
CSRP_N                        =0                             [m**3/
kg]
CSRP_RDOT                     =0
[m**3/(kg*s)]
```

91

```
CSRP_TDOT                          =0
[m**3/(kg*s)]
CSRP_NDOT                          =0
[m**3/(kg*s)]
CSRP_DRG                           =0                        [m**4/
kg**2]
CSRP_SRP                           =0                        [m**4/
kg**2]
```

92

APPENDIX B. AUTOMATED SCREENING PROCESS–MATLAB SCRIPT

This MATLAB script performs an automatic screening process of an object of interest against the complete SP catalog. To use this script, the user must download the SP catalog from the Space-Track website and unzip the folder. To use .eci files (SP format), the STK 12.6 and plugging are required (to get a plugging email AGI Support - support@agi.com).

```matlab
%
% Conjunction Analysis
% Screening process
% Copyright: Giuliano F. B. de Oliveira, 2022-10-31
%
%
% This program performs a screening of one object of interest against all SP
% catalog.
% Change only parameters in the Input section

clear
clc
close all
global Scenario_start_time
global Scenario_stop_time
t = datetime

%%
% Input data

NORAD = "48916";
% insert the NORAD of the object of interest, standard "NORAD" (Example
"42692")
ephemeris_path = "D:\Google Drive\009 - Mestrado NPS\NPS\Thesis\final_scripts\
Screening_process\Scenario_1_01162023\ECI_E";    % folder path with ephemeris
files, standard "path" (example path = "I:\My Drive\009 - Mestrado NPS\NPS\
Thesis\Matlab\CAM")
Conjunction_report_name = "\Conjunction_Report.csv";
% define the conjunction report name (example "\Conjunction_Report.csv")
report_path = "D:\Users\giuli\Desktop\Screening_update\SPcatalog\SPcatalog";
% desired folder to save the conjunction report (example path = "I:\My Drive\
009 - Mestrado NPS\NPS\Thesis\Matlab\CAM")

Threshold = 5;
% sphere of exclusion in Km
Cp_Limit1 = 1e-5;
% Collision threshold to trigger a maneuver
Cp_Limit2 = 1e-7;
% Collision threshold, more analysis is needed.

% Pre filter on / off and parameters
%on / off 1 for On and 0 for Off
```

```matlab
ApogeePerigee_use = 1;                    %
OrbitPath_use = 0;
Time_use = 1;
OutOfDate_use = 0;

% custom orbit class
custom_orbit_class = 1;

% values
ApogeePerigee = 30;                       %
OrbitPath = 0;
Time = 30;
OutOfDate = 86400;   % seconds, minimum 86400 sec (1 day)


%%
% Start a new STK scenário

if exist('uiapp', 'var') == 0
    [uiapp, root, scenario] = connect_to_stk();
end
% Reset the animation time
root.ExecuteCommand('Animate * Reset');

%%
%3. Add objects to the scenario (satellite, SatelliteCollection, and advcat)

satellite = scenario.Children.New('eSatellite','MySatellite');
advcat = scenario.Children.New('eAdvCAT','Advcat');
satellitecollection = scenario.Children.New('eSatelliteCollection',
'SP_Catalog');

% import ephemeris of satellite of interest from SP Catalog
sl = "\";
object_of_interest = sprintf('%s%s',sl,NORAD);
s = sprintf('SetState */Satellite/MySatellite FromFile
"%s%s.eci"',ephemeris_path,object_of_interest);
root.ExecuteCommand(s);

% scenario configuration

SatelliteDP =
satellite.DataProviders.Item('Interval').Group.Item('EphemerisTimeSpan').Exec(
scenario.StartTime, scenario.StopTime);
Scenario_start_time = SatelliteDP.DataSets.GetDataSetByName('Start
Time').GetValues;
Scenario_start_time = cell2mat(Scenario_start_time);
Scenario_stop_time = SatelliteDP.DataSets.GetDataSetByName('Stop
Time').GetValues;
Scenario_stop_time = cell2mat(Scenario_stop_time);
object_setup(root);

% create .csv file
name = "SP_catalog.csv";                          % csv file name
```

94

```matlab
filename = fullfile(ephemeris_path, name);
fp=fopen(filename,'w');                      % the .csv file will be
created in the same folder as the ephemeris files
fprintf(fp,'%s\n\n','VERSION 1.0');
fprintf(fp,'%s\n\n','ContentType EphemerisFile');

fprintf(fp,'%s\n','Begin CustomColumns');

fprintf(fp,'    %s, %s, %s\n','ColumnName', 'DataType', 'Required');
fprintf(fp,'    %s, %s, %s\n\n','FileName', 'String', 'Yes');

fprintf(fp,'%s\n\n','End CustomColumns');

fprintf(fp,'%s\n','Begin Columns');
fprintf(fp,'    %s, %s, %s\n','Name', 'FileName', 'Required');

filePattern = fullfile(ephemeris_path, '*.eci');
files = dir(filePattern);
for i=1:length(files)
    filename = files(i);
    filename.name;
    fprintf(fp,'    %s, %s, %s\n',filename.name, filename.name, 'Yes');
    %stlread(filename); %you can try this out by uncommenting
end
fprintf(fp,'%s\n','End Columns');


%%

% configure satelliteCollection with full SP Catalog
csv = '\SP_Catalog.csv';
s = sprintf('Collection */SatelliteCollection/SP_Catalog Define Custom File
"%s%s" EphemerisDirectory "%s"',ephemeris_path,csv,ephemeris_path);
% s = sprintf('Collection */SatelliteCollection/SP_Catalog Define Custom File
"%s%s"',dir,csv);
root.ExecuteCommand(s);


% Advcat configuration
root.ExecuteCommand('ACAT */AdvCAT/Advcat Primary Add "Satellite/MySatellite"
OrbitClass');
root.ExecuteCommand('ACat */AdvCAT/Advcat Secondary Add "SP_Catalog/
AllSatellites" OrbitClass');
s = sprintf('ACat */AdvCAT/Advcat Threshold %d', Threshold);
root.ExecuteCommand(s);
if custom_orbit_class == 1
    root.ExecuteCommand('ACAT */AdvCAT/AdvCat FixedOCDB "C:\ProgramData\AGI\
STK 12\Databases\Satellite\stkFxdOrbCls_GIULIANO.foc"');
end

% pre filtering
if ApogeePerigee_use == 1
    ApogeePerigee_use = 'On';
```

95

```matlab
    s = sprintf('ACat */AdvCAT/Advcat PreFilters "ApogeePerigee" %s',
ApogeePerigee_use);
    root.ExecuteCommand(s);
    s = sprintf('ACat */AdvCAT/Advcat PreFilters "ApogeePerigee" %d',
ApogeePerigee);
    root.ExecuteCommand(s);
else
    ApogeePerigee_use = 'Off';
    s = sprintf('ACat */AdvCAT/Advcat PreFilters "ApogeePerigee" %s',
ApogeePerigee_use);
    root.ExecuteCommand(s);
end
if OrbitPath_use == 1
    OrbitPath_use = 'On';
    s = sprintf('ACat */AdvCAT/Advcat PreFilters "OrbitPath" %s',
OrbitPath_use);
    root.ExecuteCommand(s);
    s = sprintf('ACat */AdvCAT/Advcat PreFilters "OrbitPath" %d', OrbitPath);
    root.ExecuteCommand(s);
else
    OrbitPath_use = 'Off';
    s = sprintf('ACat */AdvCAT/Advcat PreFilters "OrbitPath" %s',
OrbitPath_use);
    root.ExecuteCommand(s);
end

if Time_use == 1
    Time_use = 'On';
    s = sprintf('ACat */AdvCAT/Advcat PreFilters "Time" %s', Time_use);
    root.ExecuteCommand(s);
    s = sprintf('ACat */AdvCAT/Advcat PreFilters "Time" %d', Time);
    root.ExecuteCommand(s);
else
    Time_use = 'Off';
    s = sprintf('ACat */AdvCAT/Advcat PreFilters "Time" %s', Time_use);
    root.ExecuteCommand(s);
end
if OutOfDate_use == 1
    OutOfDate_use = 'On';
    s = sprintf('ACat */AdvCAT/Advcat PreFilters "OutOfDate" %s',
OutOfDate_use);
    root.ExecuteCommand(s);
    s = sprintf('ACat */AdvCAT/Advcat PreFilters "OutOfDate" %d', OutOfDate);
    root.ExecuteCommand(s);
else
    OutOfDate_use = 'Off';
    s = sprintf('ACat */AdvCAT/Advcat PreFilters "OutOfDate" %s',
OutOfDate_use);
    root.ExecuteCommand(s);
end


% time interval
```

```matlab
root.ExecuteCommand('ACat */AdvCAT/Advcat TimePeriod "Satellite/MySatellite
EphemerisTimeSpan Interval"');

% Specify whether an object with an ephemeris that does not span the entire
analysis interval will still be processed.
root.ExecuteCommand('ACat */AdvCAT/Advcat AllowPartialEphem On')

%% Advcat Run (conjunction analysis)

root.ExecuteCommand('ACat */AdvCAT/Advcat Compute "ShowProgress" On');

Collision_Probability_DP = advcat.DataProviders.Item('Events by Time
In').ExecElements(scenario.StartTime, scenario.StopTime, {'Approach Angle';
'Min Range';'Min Range - InTrack';'Min Range - CrossTrack';'Min Range -
Radial';'Object Name';'Time of Close Appr (TCA)';'Relative Velocity';
'Probability Linearity Speed (Fine)'; 'Collision Probability (Nonlinear -
Cylinders)'; 'Max Collision Probability'});
Max_CP = cell2mat(Collision_Probability_DP.DataSets.GetDataSetByName('Max
Collision Probability').GetValues);
Min_Range = cell2mat(Collision_Probability_DP.DataSets.GetDataSetByName('Min
Range').GetValues);
Min_Range_cross =
cell2mat(Collision_Probability_DP.DataSets.GetDataSetByName('Min Range -
CrossTrack').GetValues);
Min_Range_in =
cell2mat(Collision_Probability_DP.DataSets.GetDataSetByName('Min Range -
InTrack').GetValues);
Min_Range_Radial =
cell2mat(Collision_Probability_DP.DataSets.GetDataSetByName('Min Range -
Radial').GetValues);
Approach_Angle =
cell2mat(Collision_Probability_DP.DataSets.GetDataSetByName('Approach
Angle').GetValues);
TCA = Collision_Probability_DP.DataSets.GetDataSetByName('Time of Close Appr
(TCA)').GetValues;
Secondary_Name = Collision_Probability_DP.DataSets.GetDataSetByName('Object
Name').GetValues;

% Filter conjunctions by collision probability and write a report
filename = fullfile(report_path, Conjunction_report_name);
fp=fopen(filename,'w');
fprintf(fp,'%s%s %s\n\n','Conjunction Report for object', object_of_interest,
'against the full SP Catalog');
fprintf(fp,'%s = %1.2s\n\n','Conjunctions with probability higher than the
defined threshold', Cp_Limit1);

fprintf(fp,'     %s, %s, %s, %s, %s, %s, %s, %s\n', 'Object 2', 'Max Collision
Probability', 'TCA', 'Min Range (Km)', 'Min Range - Radial (Km)', 'Min Range -
CrossTrack (Km)', 'Min Range - InTrack (Km)', 'Approach Angle (deg)');

e = ".eci";
NORAD = sprintf('%s%s', NORAD,e);
for i=1:length(Max_CP)
    filter = Max_CP(i);
```

```matlab
    if filter > Cp_Limit1
        x = convertCharsToStrings(Secundary_Name(i));
        y = convertCharsToStrings(TCA(i));

        if contains(x, NORAD)
        else
            fprintf(fp,'      %s, %s, %s, %s, %s, %s, %s, %1.1f\n', x,
Max_CP(i), y,
Min_Range(i),Min_Range_Radial(i),Min_Range_cross(i),Min_Range_in(i),
Approach_Angle(i));
        end
    else
    end
end
fprintf(fp,'\n\n');

fprintf(fp,'%s = %1.2s\n\n','Conjunctions with probability higher than the
defined threshold', Cp_Limit2);

fprintf(fp,'      %s, %s, %s, %s, %s, %s, %s, %s\n', 'Object 2', 'Max Collision
Probability', 'TCA', 'Min Range (Km)', 'Min Range - Radial (Km)', 'Min Range -
CrossTrack (Km)', 'Min Range - InTrack (Km)', 'Approach Angle (deg)');
for i=1:length(Max_CP)
    filter = Max_CP(i);
    if filter > Cp_Limit2 && filter < Cp_Limit1
        x = convertCharsToStrings(Secundary_Name(i));
        y = convertCharsToStrings(TCA(i));
        if contains(x, NORAD)
        else
            fprintf(fp,'      %s, %s, %s, %s, %s, %s, %s, %1.1f\n', x,
Max_CP(i), y,
Min_Range(i),Min_Range_Radial(i),Min_Range_cross(i),Min_Range_in(i),
Approach_Angle(i));
        end
    else
    end
end
fclose(fp);
t = datetime

%%
function [uiapp, root, scenario] = connect_to_stk()
    % Initialize STK and establish the connection
    try
        % Grab an existing instance of STK
        uiapp = actxGetRunningServer('STK12.application');
        root = uiapp.Personality2;
        checkempty = root.Children.Count;
        if checkempty == 0
            %If a Scenario is not open, create a new scenario
            uiapp.visible = 1;
            root.NewScenario('Conjunctio_analysis');
            scenario = root.CurrentScenario;
        else
```

98

```matlab
            %If a Scenario is open, prompt the user to accept closing it or
not
            rtn = questdlg({'Close the current scenario?',' ','(WARNING: If
you have not saved your progress will be lost)'});
            if ~strcmp(rtn,'Yes')
                return
            else
                root.CurrentScenario.Unload
                uiapp.visible = 1;
                root.NewScenario('Conjunctio_analysis');
                scenario = root.CurrentScenario;
            end
        end
    catch
        % STK is not running, launch new instance
        % Launch a new instance of STK12 and grab it
        uiapp = actxserver('STK12.application');
        root = uiapp.Personality2;
        uiapp.visible = 1;
        root.NewScenario('Conjunctio_analysis');
        scenario = root.CurrentScenario;
    end
end
function object_setup(root)
    %set units to utcg before setting scenario time period and animation
period
    root.UnitPreferences.Item('DateFormat').SetCurrentUnit('UTCG');
    root.UnitPreferences.Item('Mass').SetCurrentUnit('kg');

    %set scenario time period and animation period
    global Scenario_start_time
    global Scenario_stop_time
    root.CurrentScenario.SetTimePeriod(Scenario_start_time,
Scenario_stop_time);
    root.CurrentScenario.Epoch = Scenario_start_time;
    root.CurrentScenario.Animation.EnableAnimCycleTime = true;
    root.CurrentScenario.Animation.AnimCycleType = 'eEndTime';
%     root.CurrentScenario.Animation.AnimCycleTime = '2 Jul 2017
12:00:00.000';
%     root.CurrentScenario.Animation.StartTime = '1 Jul 2017 12:00:00.000';
    root.CurrentScenario.Animation.EnableAnimCycleTime = false;
    root.Rewind();
    root.ExecuteCommand('SetUnits / km sec UTCG');
%     root.ExecuteCommand('New / */Satellite Chase');
%     root.ExecuteCommand('New / */Satellite Target');
End
```

THIS PAGE INTENTIONALLY LEFT BLANK

APPENDIX C. COMPUTATION OF COLLISION PROBABILITY BETWEEN TWO OBJECTS—MATLAB SCRIPT

```matlab
%
% Conjunction Analysis
% Collision Probability between two objects
% Copyright: Giuliano F. B. de Oliveira, 2023-01-12
%
%
% This program tests the validity of a rectilinear motion approximation
between two objects and computes the Collision probability accordingly.
% Computation considers the available ephemeris time span of the object
defined as primary
%
% Change only parameters in the Input section
%


%%
clc
clear
close all

%%
% Inputs
% Collision probability parameters
Threshold = 1;
EndSigma = 6;
FracProbLimit = 0.001;

% ephemeris_path is the folder path with ephemeris files,
ephemeris_path = "D:\Google Drive\009 – Mestrado NPS\NPS\Thesis\final_scripts\
Linear_vs_nonlinear_CP\STK_training_files";

% enter the name of .e file to be loaded as primary and secondary objecs, do
not including the extention
primary = "Primary";
secondary = "Secondary";

% enter the name of the reporter and the path where it should be saved
Conjunction_report_name = "\Conjunction_Report.csv";
report_path = "D:\Google Drive\009 – Mestrado NPS\NPS\Thesis\final_scripts\
Linear_vs_nonlinear_CP\STK_training_files"; % desired folder to save the
conjunction report (example path = "I:\My Drive\009 – Mestrado NPS\NPS\Thesis\
Matlab\CAM")

%%
% STK STK STK
% Start a new STK scenário
```

```
if exist('uiapp', 'var') == 0
    [uiapp, root, scenario] = connect_to_stk();
    object_setup(root);
end


%%
%3. Add objects to the scenario (satellite, debris, and advcat)
debri = scenario.Children.New('eSatellite','Debri');
satellite = scenario.Children.New('eSatellite','MySatellite');
advcat = scenario.Children.New('eAdvCAT','Advcat');

%%
% Object configurations

% Configure the Local_vertical-Local Horizontal reference frame (orbit system)
% for Satellite with debri at the cener of reference frame

root.ExecuteCommand('VO */Satellite/MySatellite OrbitSystem Add System
"InertialByWindow" Show off ');
root.ExecuteCommand('VO */Satellite/MySatellite OrbitSystem Add System
"Satellite/Debri VVLH"');

% Advcat configuration
root.ExecuteCommand('ACAT */AdvCAT/Advcat Primary Add "Satellite/MySatellite"
Cov');
root.ExecuteCommand('Acat */AdvCAT/Advcat Secondary Add "Satellite/Debri"
Cov');
s = sprintf('Acat */AdvCAT/Advcat Threshold %d', Threshold);
root.ExecuteCommand(s);
s = sprintf('ACAT */AdvCAT/Advcat Probability EndSigma %d FracProbLimit %d',
EndSigma, FracProbLimit);
root.ExecuteCommand(s);  % Set the parameters used to compute conjunction
probability for nonlinear relative motion.

%%
%4. Propagate the Satellite object's orbit.
Sl = "\";
object_of_interest = sprintf('%s%s',sl,primary);
s = sprintf('SetState */Satellite/MySatellite FromFile
"%s%s.e"',ephemeris_path,object_of_interest);
root.ExecuteCommand(s);
object_of_interest = sprintf('%s%s',sl,secondary);
s = sprintf('SetState */Satellite/Debri FromFile
"%s%s.e"',ephemeris_path,object_of_interest);
root.ExecuteCommand(s);
root.ExecuteCommand('SetAnalysisTimePeriod * "Satellite/MySatellite
EphemerisTimeSpan Interval"') % define the timespan for advcat computation
% Reset the animation time
root.ExecuteCommand('Animate * Reset');

%%
% STK STK STK
% Compute conjunctions and calculate probabilities
```

102

```matlab
% Search for TCAs during the analysis period
root.ExecuteCommand('Acat */AdvCAT/Advcat TimePeriod "Satellite/MySatellite
EphemerisTimeSpan Interval"');
root.ExecuteCommand('Acat */AdvCAT/Advcat Compute "ShowProgress" On')
advcatDP = advcat.DataProviders.Item('Time
Events').Group.Item('TCA').Exec(scenario.StartTime, scenario.StopTime);
TCA = advcatDP.DataSets.GetDataSetByName('EventTime').GetValues;
z=length(TCA);

% Create a report
filename = fullfile(report_path, Conjunction_report_name);
fp=fopen(filename,'w');
fprintf(fp,'%s %s %s %s %s\n\n','Conjunction assessment between', primary,
'and', secondary, 'objects');
fprintf(fp,'       %s, %s, %s, %s\n', 'TCA (UTCG)', 'Collision Probability',
'Comp. Method', 'Min Range (Km)');

% Test the valid of rectilinear motion approximation and collision
% probability computation and write the result in the report.
For i=1:z
    TCA = cell2mat(TCA(i));
    TCA = convertCharsToStrings(TCA);
    s = sprintf('ACATProbability_R */AdvCAT/Advcat Primary "MySatellite"
Secondary "Debri" TCA "%s" Method CoarseLinearitySpeed', TCA);
    returnValue = root.ExecuteCommand(s);
    s = sprintf('ACATProbability_R */AdvCAT/Advcat Primary "MySatellite"
Secondary "Debri" TCA "%s" Method Nonlinear-Cylinders', TCA);
    returnValue = root.ExecuteCommand(s);
    s = sprintf('ACATProbability_R */AdvCAT/Advcat Primary "MySatellite"
Secondary "Debri" TCA "%s" Method Numeric', TCA);
    returnValue = root.ExecuteCommand(s);
    Collision_Probability_DP = advcat.DataProviders.Item('Events by Time
In').ExecElements(scenario.StartTime, scenario.StopTime, {'Min
Range';'Relative Velocity'; 'Probability Linearity Speed (Fine)'; 'Collision
Probability (Nonlinear – Cylinders)'; 'Collision Probability (Numeric)'});
    Non_linear_Cylinders =
Collision_Probability_DP.DataSets.GetDataSetByName('Collision Probability
(Nonlinear – Cylinders)').GetValues;
    RelVel =
cell2mat(Collision_Probability_DP.DataSets.GetDataSetByName('Relative
Velocity').GetValues);
    MinRelVel =
cell2mat(Collision_Probability_DP.DataSets.GetDataSetByName('Probability
Linearity Speed (Fine)').GetValues);
    Linear_CP =
cell2mat(Collision_Probability_DP.DataSets.GetDataSetByName('Collision
Probability (Numeric)').GetValues);
    NonLinear_CP =
cell2mat(Collision_Probability_DP.DataSets.GetDataSetByName('Collision
Probability (Nonlinear – Cylinders)').GetValues);
    Min_Range =
cell2mat(Collision_Probability_DP.DataSets.GetDataSetByName('Min
Range').GetValues);
```

103

```matlab
    if RelVel >=MinRelVel
        fprintf(fp,'      %s, %s, %s, %s\n', TCA, Linear_CP(i),'Numeric',
Min_Range(i));

    else
        fprintf(fp,'      %s, %s, %s, %s\n', TCA, NonLinear_CP(i),'Nonlinear-
Cylinders', Min_Range(i));

    end
    fprintf(fp,'      %s\n', 'End of Report');
end
fclose( fp );


%%%% Functions %%%%


function [uiapp, root, scenario] = connect_to_stk()
    % Initialize STK and establish the connection

    try
        % Grab an existing instance of STK
        uiapp = actxGetRunningServer('STK12.application');
        root = uiapp.Personality2;
        checkempty = root.Children.Count;
        if checkempty == 0
            %If a Scenario is not open, create a new scenario
            uiapp.visible = 1;
            root.NewScenario('Collision_Probability');
            scenario = root.CurrentScenario;
        else
            %If a Scenario is open, prompt the user to accept closing it or
not
            rtn = questdlg({'Close the current scenario?',' ','(WARNING: If
you have not saved your progress will be lost)'});
            if ~strcmp(rtn,'Yes')
                return
            else
                root.CurrentScenario.Unload
                uiapp.visible = 1;
                root.NewScenario('Collision_Probability');
                scenario = root.CurrentScenario;
            end
        end
    catch
        % STK is not running, launch new instance
        % Launch a new instance of STK12 and grab it
        uiapp = actxserver('STK12.application');
        root = uiapp.Personality2;
        uiapp.visible = 1;
        root.NewScenario('Collision_Probability');
        scenario = root.CurrentScenario;
    end
end
```

104

```
function object_setup(root)
    %set units to utcg before setting scenario time period and animation
period
    root.UnitPreferences.Item('DateFormat').SetCurrentUnit('UTCG');
    root.UnitPreferences.Item('Mass').SetCurrentUnit('kg');

    %set scenario time period and animation period

    root.CurrentScenario.Animation.EnableAnimCycleTime = true;
    root.CurrentScenario.Animation.AnimCycleType = 'eEndTime';

    root.CurrentScenario.Animation.EnableAnimCycleTime = false;
    root.Rewind();
    root.ExecuteCommand('SetUnits / km sec UTCG');

end
```

THIS PAGE INTENTIONALLY LEFT BLANK

APPENDIX D. LOW-THRUST COLLISION AVOIDANCE IN CIRCULAR ORBITS—MATLAB SCRIPT

```
%
% Low-Thrust Collision Avoidance in Circular Orbits
% Copyright: Giuliano F. B. de Oliveira, 2022-10-31
%
% This program computes the collision probability between two objects in
circular ORBIT
% Reference:
% J. Hernando-Ayuso and C. Bombardelli, "Low-Thrust Collision Avoidance in
Circular Orbits," Journal of Guidance, Control, and Dynamics,
% vol. 44, no. 5, pp. 983–995, May 2021, doi: 10.2514/1.G005547.

%*****************************************************************************
% variables description
    % Sa → sphere radius
    % sigmax --> semi-principal axes σx of the 1-sigma covariance ellipse
    % sigmay --> semi-principal axes σy of the 1-sigma covariance ellipse
    % x --> B-plane position vector component along the x eigenaxes
    % y --> B-plane position vector component along the y eigenaxes
    % Zeta --> ζ 0
    % Csi --> ξ 200
    % η --> Eta
        % B-plane reference frame frame hξ; η; ζi is defined with ξ
        % pointing toward the cross product of the velocity vector of S2
        % with the velocity vector of S1, η along the velocity of S1
        % relatively to an S2-centered inertial frame, and ζ to complete a
right-handed coordinate systemas
    % Teta --> the angle θ between the combined position covariance and the B-
plane axis.
% Scale thrust for constant total impulse (10 mN when thrust arc is 60 deg)
%%
clc
clear
close all
%%
% initial conditions and constants

mu = 3.98600e14;
mass = 300;               % mass in g, is it right???????
thrust_nominal = 10e-3; %N = kg*m/s^2
tarc_nominal = 60*pi/180; %rad
total_impulse = thrust_nominal*tarc_nominal;
k =106*pi/180;            %angle between the two orbital planes (mutual
inclination);
Re = 6378e3;              % Earth radius
alt_debri = 550.2e3;      % Debris altitude
r_debri = (Re + alt_debri);     % Spacecraft radius
h_SC = 550e3;             % Spacecraft altitude
```

```matlab
r_SC = (Re + h_SC);      % Spacecraft radius
v_SC = sqrt(mu/r_SC);    % Spacecraft velocity
sigmax = 80;
sigmay = 1500;
S1 = 8;                  % spacecraft radius
S2 = 8;                  % non-cooperative object radias
Sa = S1 + S2;
Zeta = 0;
Csi = 200;

%% inputs

Teta = 5*pi/180;         % angle θ between the ζ axis and the x axis
Tarc_vector = [60,120,200]; % Tarc in degrees, enter three different Tarc
lengths for comparison between them.

%%
% initial Collision Probability computation
x = Csi*cos(Teta) + Zeta*sin(Teta);
y = Csi*sin(T—ta) - Zeta*cos(Teta);

% Collision probability (equation 5)
P = Sa^2/(2*sigmax*sigmay)*(1+1/8*((x^2/sigmax^2-1)/sigmax^2+(y^2/sigmay^2-
1)/sigmay^2))*exp(-0.5*(x^2/sigmax^2+y^2/sigmay^2));

fprintf("Initial Collision Probability = %1.4d\n", P);

%%

% Collision Avoidance Maneuver
% variables description

% Tarc --> thrust arc width Δθt
% N_rev --> the number of revolutions from the middle of the thrust arc until
the conjunction event.
% mass --> spacecraft mass
% r1 --> SC radius
% r2 --> debri radius
% v1 --> SC velocity
% mu --> Earthus gravitational parameter
% κ --> the angle between the two orbital planes (mutual inclination);

N_rev_vector = [0:0.01:7];
Csi_i = Csi;
Zeta_i = Zeta;
t=length(N_rev_vector);
z=length(Tarc_vector);
color = ['b','g','r'];

for i=1:z
    Tarc = Tarc_vector(i)*pi/180;
    thrust = total_impulse/Tarc; % N
    a0 = thrust/mass; %m/s^2 thrust accel magnitude
```

108

```matlab
    for n=1:t
        N_rev = N_rev_vector(n);
        Tarc_i = 2*pi*N_rev + Tarc/2;
        Tarc_f = 2*pi*N—rev - Tarc/2;
        Tarc_c = Tarc_f;

        delta_r_SC = 2*a0*r_as^3/mu*(Tarc+sin(Tarc_c)-sin(Tarc+Tarc_c));
        %delta_t = a0*(r_as^3.5/mu^1.5)*((3*Tarc*(Tarc/2+—arc_c)) -
8*sin(Tarc/2)*sin(Tarc/2+Tarc_c));


        Csi—= Csi_i - delta_r_SC;
        Zeta = Zeta_i + a0*r_SC^3/mu * cos(k/2) * (3*Tarc*(Tarc/2—Tarc_c) -
8*sin(Tarc/2)*sin(Tarc/2+Tarc_c));

        x = Csi*cos(Teta) + Zeta*sin(Teta);
        y = Csi*s—n(Teta) - Zeta*cos(Teta);

        as(n) = (Sa^2 / (2*sigmax*sigmay)) * (1 + 1/8 * (((x^2/sigmax^2-
1)/sigmax^2) + ((y^2/sigmay^2 -1)/sigmay^2))) * (exp(-0.5*((x^2/sigmax^2) +
(y^2/sigmay^2)))));
        c = color(i);
    end

    plot = semilogy(N_rev_vector, P1);
    grid on
    hold on
    plot.Color = c;

end
xlabel('Number of revolutions before TCA')
ylabel('Collision P—obability - log scale')
Initial_CP = ones(1,length(N_rev_vector))*P;
threshold = 1e-6;
threshold_vector = ones(1,length(N_rev_vector))*threshold;
semilogy(N_rev_vector, In—ial_CP, '--');
semilogy(N_rev_vector, threshold, '-.');
s1 = sprintf ('thrust arc = %d deg', Tarc_vector(1));
s2 = sprintf ('thrust arc = %d deg', Tarc_vector(2));
s3 = sprintf ('thrust arc = %d deg', Tarc_vector(3));
s4 = sprintf ('CP without maneuver');
s5 = sprintf ('CP threshold = %1.1d', threshold);
legend (s1,s2,s3,s4,s5)
```

THIS PAGE INTENTIONALLY LEFT BLANK

APPENDIX E. ICEYE COLLISION AVOIDANCE MANEUVER— MATLAB-STK SCRIPT

```matlab
% ICEYE Collision Avoidance Maneuver
% Copyright: Giuliano F. B. de Oliveira, 2022-10-31
%
% This program performs tangential CAM for ICEYE satellite.
%


%%
clc
clear
close all
global Scenario_start_time
global Scenario_stop_time



% ephemeris_path is the folder path with ephemeris files,
ephemeris_path = "D:\Google Drive\009 - Mestrado NPS\NPS\Thesis\final_scripts\
Low_thrust_CAM_Astrogator\Scenarios\Scenario_3_01242023";

% enter the name of the reporter and the path where it should be saved
% Conjunction_report_name = "\Conjunction_Report1.csv";
% report_path = "D:\Google Drive\009 - Mestrado NPS\NPS\Thesis\final_scripts\
Linear_vs_nonlinear_CP\STK_training_files"; % desired folder to save the
conjunction report (example path = "I:\My Drive\009 - Mestrado NPS\NPS\Thesis\
Matlab\CAM")

% enter the name of .e file to be loaded as primary and secondary objecs, do
not including the extention
primary = "ICEYE_51008";
secondary = "SecObj_27657";

TCA = '26 Jan 2023 15:31:50.50';

% Collision probability parameters
Threshold = 5;
EndSigma = 6;
FracProbLimit = 0.001;

% Maneuver parameters

Maneuver_duration = 1800; %seconds (30 minutes)
% to use Thurst arc in degreee uncomment line 214 and set the Tarc in next
line
% Tarc = 90;  %Thrus duration arc in degrees
Thrust = 1.4e-3;  %thrust force in Newtons
Isp = 4200;  % Specific Impulse in seconds
```

111

```matlab
%spacecraft parameters

dry_mass = 87;  % spacecraft mass (Kg)
drag_area = 0.7*0.4; %nominal drag area (m^2)
Cp = 2.2; %drag coeff (2.2 spherica, 4 bxox)
Cr = 1; %Solar radiation coeff
SRP_area = 0.4*3.2;  %solar radiation pressure area
RadPressureArea = 0.4*3.2; %radiation pressure area (albedo)
MaxFuelMass = 5;
FuelMass = 5;
TankVolume = 1;

% defaut values
TankPressure = 5000; %Pa
TankTemperature = 293.15; %Kelvin
FuelDensity = 1000.0; %kg/m^3


% Start a new scenário

if exist('uiapp', 'var') == 0
    [uiapp, root, scenario] = connect_to_stk();
%     object_setup(root);
end
% Reset the animation time
root.ExecuteCommand('Animate * Reset');


%%
% Add objects to the scenario (satellite, debris, and advcat)

debris = scenario.Children.New('eSatellite','Debris');
satellite = scenario.Children.New('eSatellite','MySatellite');
advcat = scenario.Children.New('eAdvCAT','Advcat');

% secondary object configuration

s = sprintf('SetState */Satellite/Debris FromFile
"%s%s%s.e"',ephemeris_path,'\',secondary);
root.ExecuteCommand(s);
root.ExecuteCommand('SetAnalysisTimePeriod * "Satellite/Debris
EphemerisTimeSpan Interval"'); % define the timespan for advcat computation

% scenario Interval conficuration
SatelliteDP =
debris.DataProviders.Item('Interval').Group.Item('EphemerisTimeSpan').Exec(sce
nario.StartTime, scenario.StopTime);
Scenario_start_time = SatelliteDP.DataSets.GetDataSetByName('Start
Time').GetValues;
Scenario_start_time = cell2mat(Scenario_start_time);
Scenario_stop_time = SatelliteDP.DataSets.GetDataSetByName('Stop
Time').GetValues;
Scenario_stop_time = cell2mat(Scenario_stop_time);
```

112

```matlab
Debris_ephemerisTimeSpan =
SatelliteDP.DataSets.GetDataSetByName('Duration').GetValues;
Debris_ephemerisTimeSpan = cell2mat(Debris_ephemerisTimeSpan);
object_setup(root);

% Reset the animation time
root.ExecuteCommand('Animate * Reset');

%%
% Object configurations
% Coordinate System Local Vertical Local Horizontal
% Configure the Local_vertical-Local Horizontal reference frame (orbit system)
for Satellite with debri at the cener of reference frame

root.ExecuteCommand('VO */Satellite/MySatellite OrbitSystem Add System
"InertialByWindow" Show off ');
root.ExecuteCommand('VO */Satellite/MySatellite OrbitSystem Add System
"Satellite/Debris VVLH"');


% Advcat configuration
root.ExecuteCommand('ACAT */AdvCAT/Advcat Primary Add "Satellite/MySatellite"
OrbitClass');
root.ExecuteCommand('ACat */AdvCAT/Advcat Secondary Add "Satellite/Debris"
OrbitClass');
s = sprintf('ACat */AdvCAT/Advcat Threshold %d', Threshold);
root.ExecuteCommand(s);
s = sprintf('ACAT */AdvCAT/Advcat Probability EndSigma %d FracProbLimit %d',
EndSigma, FracProbLimit);
root.ExecuteCommand(s);  % Set the parameters used to compute conjunction
probability for nonlinear relative motion.


% Primary
% Change Satellite propagator to Astrogator
root.ExecuteCommand('Astrogator */Satellite/MySatellite SetProp');
% Determine what segments are in the MCS currently
ASTGSegments = root.ExecuteCommand('Astrogator_RM */Satellite/MySatellite
GetValue MainSequence.SegmentList');

% Delete all the segments.
for j = 0:ASTGSegments.Count - 2
    Segment = strread(ASTGSegments.Item(j), '%s');
    root.ExecuteCommand(['Astrogator */Satellite/MySatellite DeleteSegment '
Segment{1}]);
end

% Insert an Initial State Segment into the MCS and configure

root.ExecuteCommand('Astrogator */Satellite/MySatellite InsertSegment -
Initial_State');
root.ExecuteCommand('Astrogator */Satellite/MySatellite SetValue
MainSequence.SegmentList.Initial_State.ComponentName Initial_Orbit'); %change
name of the segment
```

113

```
root.ExecuteCommand('Astrogator */Satellite/MySatellite SetValue
MainSequence.SegmentList.Initial_Orbit.InitialState.Epoch 0 EpSec'); %set
epoch
root.ExecuteCommand('Astrogator */Satellite/MySatellite SetValue
MainSequence.SegmentList.Initial_Orbit.CoordinateSystem "CentralBody/Earth
ICRF" ');

% Load state vector from STK ephemeris file
s = sprintf('InitialState */Satellite/MySatellite Import STKFile "%s%s%s.e"
GatorPath
"MainSEQUENCE.SegmentList.Initial_Orbit"',ephemeris_path,'\',primary);
root.ExecuteCommand(s);

% satellite parameters configuration
s = sprintf('Astrogator */Satellite/MySatellite SetValue
MainSequence.SegmentList.Initial_Orbit.MaxFuelMass %d kg',MaxFuelMass);
root.ExecuteCommand(s);
s = sprintf ('Astrogator */Satellite/MySatellite SetValue
MainSequence.SegmentList.Initial_Orbit.FuelMass %d kg', FuelMass);
root.ExecuteCommand(s);
s = sprintf('Astrogator */Satellite/MySatellite SetValue
MainSequence.SegmentList.Initial_Orbit.InitialState.DryMass %d Kg', dry_mass);
root.ExecuteCommand(s);
s = sprintf('Astrogator */Satellite/MySatellite SetValue
MainSequence.SegmentList.Initial_Orbit.InitialState.DragArea %d m^2',
drag_area);
root.ExecuteCommand(s);
s = sprintf('Astrogator */Satellite/MySatellite SetValue
MainSequence.SegmentList.Initial_Orbit.InitialState.Cd %d', Cp);
root.ExecuteCommand(s);
s = sprintf('Astrogator */Satellite/MySatellite SetValue
MainSequence.SegmentList.Initial_Orbit.InitialState.SRPArea %d m^2',
SRP_area);
root.ExecuteCommand(s);
s = sprintf('Astrogator */Satellite/MySatellite SetValue
MainSequence.SegmentList.Initial_Orbit.InitialState.Cr %d', Cr);
root.ExecuteCommand(s);
s = sprintf('Astrogator */Satellite/MySatellite SetValue
MainSequence.SegmentList.Initial_Orbit.InitialState.RadPressureArea %d m^2',
RadPressureArea);
root.ExecuteCommand(s);

% s = sprintf('Astrogator */Satellite/MySatellite SetValue
MainSequence.SegmentList.Initial_Orbit.InitialState.TankPressure %d Pa',
TankPressure);
% root.ExecuteCommand(s);
% s = sprintf('Astrogator */Satellite/MySatellite SetValue
MainSequence.SegmentList.Initial_Orbit.InitialState.TankTemperature %d K',
TankTemperature);
% root.ExecuteCommand(s);
% s = sprintf('Astrogator */Satellite/MySatellite SetValue
MainSequence.SegmentList.Initial_Orbit.InitialState.TankVolume %d m^3',
TankVolume);
% root.ExecuteCommand(s);
```

114

```matlab
% s = sprintf('Astrogator */Satellite/MySatellite SetValue
MainSequence.SegmentList.Initial_Orbit.InitialState.FuelDensity %d Kg/m^3',
FuelDensity);
% root.ExecuteCommand(s);

% Insert and rename propagator before maneuver

root.ExecuteCommand('Astrogator */Satellite/MySatellite InsertSegment -
Propagate');
root.ExecuteCommand('Astrogator */Satellite/MySatellite SetValue
MainSequence.SegmentList.Propagate.ComponentName Initial_Prop');

%% Initial Collision Probability computation
% Set the propagation duration to Debris ephemeris timespan
s= sprintf('Astrogator */Satellite/MySatellite SetValue
MainSequence.SegmentList.Initial_Prop.StoppingConditions.Duration.TripValue
%d', Debris_ephemerisTimeSpan);
root.ExecuteCommand(s)

% runs the Mission Control Sequence (MCS).
root.ExecuteCommand('Astrogator */Satellite/MySatellite RunMCS');

% collision probability computation

root.ExecuteCommand('ACat */AdvCAT/Advcat TimePeriod "Satellite/MySatellite
EphemerisTimeSpan Interval"');
root.ExecuteCommand('ACat */AdvCAT/Advcat Compute "ShowProgress" On');

Collision_Probability_DP = advcat.DataProviders.Item('Events by Time
In').ExecElements(scenario.StartTime, scenario.StopTime, {'Max Collision
Probability'});
Max_CP_before_maneuver =
cell2mat(Collision_Probability_DP.DataSets.GetDataSetByName('Max Collision
Probability').GetValues);
Max_CP_before_maneuver = Max_CP_before_maneuver(3);
% Maneuver parameters configuration

% insert a maneuver, rename the segment, and set as Finite maneuver
root.ExecuteCommand('Astrogator */Satellite/MySatellite InsertSegment -
Maneuver'); % insert a maneuver after the initial propagation
root.ExecuteCommand('Astrogator */Satellite/MySatellite SetValue
MainSequence.SegmentList.Maneuver.ComponentName FiniteManeuver'); %change name
of the segment
root.ExecuteCommand('Astrogator */Satellite/MySatellite SetValue
MainSequence.SegmentList.FiniteManeuver.MnvrType Finite'); %change Maneuver
type from Impulsive to Finite

% engine configuration
root.ExecuteCommand('ComponentBrowser */ Duplicate "Engine Models" "Constant
Thrust and Isp" "My Engine" ');
s = sprintf('ComponentBrowser */ SetValue "Engine Models" "My Engine" Thrust
%d', Thrust);
root.ExecuteCommand(s);
```

115

```matlab
s = sprintf('ComponentBrowser */ SetValue "Engine Models" "My Engine" Isp %d',
Isp);
root.ExecuteCommand(s);
% root.ExecuteCommand('ComponentBrowser */ SetValue "Engine Models" "My
Engine" g 0.00980665')  %%%%%calculate the g based on satellite altitude
root.ExecuteCommand('Astrogator */Satellite/MySatellite SetValue
MainSequence.SegmentList.FiniteManeuver.FiniteMnvr.EngineModel "My Engine"');

% Insert and rename propagator after maneuver

root.ExecuteCommand('Astrogator */Satellite/MySatellite InsertSegment -
Propagate');
root.ExecuteCommand('Astrogator */Satellite/MySatellite SetValue
MainSequence.SegmentList.Propagate.ComponentName Final_Prop');

%read satellite period

SatelliteDP = satellite.DataProviders.Item('Classical
Elements').Group.Item('ICRF').ExecSingle(scenario.StartTime);
Period = SatelliteDP.DataSets.GetDataSetByName('Period').GetValues;
Period = cell2mat(Period);

% Set maneuver duration

% Maneuver_duration = Period*(Tarc/360);  % (Thrust arc in seconds)
s1 = sprintf('Astrogator */Satellite/MySatellite SetValue
MainSequence.SegmentList.FiniteManeuver.StoppingConditions.Duration.TripValue
%d', Maneuver_duration);
root.ExecuteCommand(s1);

advcatDP = advcat.DataProviders.Item('Time
Events').Group.Item('TCA').Exec(scenario.StartTime, scenario.StopTime);
TCA = advcatDP.DataSets.GetDataSetByName('EventTime').GetValues;
TCA_epoch = cell2mat(advcatDP.DataSets.GetDataSetByName('Primary: Time Since
Epoch').GetValues);
TCA_epoch = TCA_epoch(3);

Scenario_start_time_JD =
juliandate(datetime(Scenario_start_time,'InputFormat','dd MMM yyyy
HH:mm:ss.S'));
Scenario_stop_time_JD =
juliandate(datetime(Scenario_stop_time,'InputFormat','dd MMM yyyy
HH:mm:ss.S'));
Scenario_epoch = (Scenario_stop_time_JD - Scenario_start_time_JD) * 86400;


%%
N_rev = 0:0.1:14;
i = length(N_rev);
root.ExecuteCommand('ACat */AdvCAT/Advcat AllowPartialEphem On')

for z = 1:i

    % Propagation Before maneuver
```

116

```matlab
    t1 = TCA_epoch - N_rev(z)*Period - Maneuver_duration/2;

    s2= sprintf('Astrogator */Satellite/MySatellite SetValue
MainSequence.SegmentList.Initial_Prop.StoppingConditions.Duration.TripValue
%d', t1); % propagation time span
    root.ExecuteCommand(s2) % change propagator duration
    % Finite Maneuver

    % Propagation after maneuver
    t2 = Scenario_epoch - (t1 + Maneuver_duration/2); % one day after TCA

    s3= sprintf('Astrogator */Satellite/MySatellite SetValue
MainSequence.SegmentList.Final_Prop.StoppingConditions.Duration.TripValue %d',
t2); % propagation time span
    root.ExecuteCommand(s3); % propagation time span
    % runs the Mission Control Sequence (MCS).
    root.ExecuteCommand('Astrogator */Satellite/MySatellite RunMCS');

    % Collision Probability calculation
    root.ExecuteCommand('ACat */AdvCAT/Advcat TimePeriod "Satellite/Debris
EphemerisTimeSpan Interval"');
    root.ExecuteCommand('ACat */AdvCAT/Advcat Compute "ShowProgress" On');

    Collision_Probability_DP = advcat.DataProviders.Item('Events by Time
In').ExecElements(scenario.StartTime, scenario.StopTime, {'Max Collision
Probability'});
    Max_CP = cell2mat(Collision_Probability_DP.DataSets.GetDataSetByName('Max
Collision Probability').GetValues);

    Max_Collision_Probability (z) = Max_CP(3);


end


%%
% retrograde maneuver
root.ExecuteCommand('Astrogator */Satellite/MySatellite SetValue
MainSequence.SegmentList.FiniteManeuver.FiniteMnvr.AttitudeControl
AntiVelocity Vector');
for z = 1:i

    % Propagation Before maneuver
    t1 = TCA_epoch - N_rev(z)*Period - Maneuver_duration/2;

    s2= sprintf('Astrogator */Satellite/MySatellite SetValue
MainSequence.SegmentList.Initial_Prop.StoppingConditions.Duration.TripValue
%d', t1); % propagation time span
    root.ExecuteCommand(s2) % change propagator duration
    % Finite Maneuver

    % Propagation after maneuver
    t2 = Scenario_epoch - (t1 + Maneuver_duration/2); % one day after TCA
```

```matlab
    s3= sprintf('Astrogator */Satellite/MySatellite SetValue
MainSequence.SegmentList.Final_Prop.StoppingConditions.Duration.TripValue %d',
t2); % propagation time span
    root.ExecuteCommand(s3); % propagation time span
    % runs the Mission Control Sequence (MCS).
    root.ExecuteCommand('Astrogator */Satellite/MySatellite RunMCS');

    % Collision Probability calculation
    root.ExecuteCommand('ACat */AdvCAT/Advcat TimePeriod "Satellite/Debris
EphemerisTimeSpan Interval"');
    root.ExecuteCommand('ACat */AdvCAT/Advcat Compute "ShowProgress" On');

    Collision_Probability_DP = advcat.DataProviders.Item('Events by Time
In').ExecElements(scenario.StartTime, scenario.StopTime, {'Max Collision
Probability'});
    Max_CP = cell2mat(Collision_Probability_DP.DataSets.GetDataSetByName('Max
Collision Probability').GetValues);

    Max_Collision_Probability_retrograde (z) = Max_CP(3);


end
% Plots

Threshold1 = ones(length(N_rev),1)*1e-5;
Threshold2 = ones(length(N_rev),1)*1e-7;
Threshold3 = ones(length(N_rev),1)*1e-6;

Max_CP_without_Manev = ones(length(N_rev),1)*Max_CP_before_maneuver;
figure()
semilogy(N_rev,Threshold1,'-- r')
hold on
semilogy(N_rev,Threshold2,'-- g')
hold on
semilogy(N_rev,Threshold3,'-- b')
hold on
semilogy(N_rev,Max_Collision_Probability,'b')
hold on
semilogy(N_rev,Max_Collision_Probability_retrograde,'c')
hold on
semilogy(N_rev,Max_CP_without_Manev,'*')
grid on
xlabel('n_{rev} before TCA'); ylabel('Max Collision Probability');
xticks(0:0.5:N_rev(end))
legend('','','','Prograde Maneuver', 'Retrograde maneuver', 'Collision
Probaility without maneuver')


%%


%%%% Functions %%%%
```

118

```matlab
function [uiapp, root, scenario] = connect_to_stk()
    % Initialize STK and establish the connection
    try
        % Grab an existing instance of STK
        uiapp = actxGetRunningServer('STK12.application');
        root = uiapp.Personality2;
        checkempty = root.Children.Count;
        if checkempty == 0
            %If a Scenario is not open, create a new scenario
            uiapp.visible = 1;
            root.NewScenario('CAM');
            scenario = root.CurrentScenario;
        else
            %If a Scenario is open, prompt the user to accept closing it or
not
            rtn = questdlg({'Close the current scenario?',' ','(WARNING: If
you have not saved your progress will be lost)'});
            if ~strcmp(rtn,'Yes')
                return
            else
                root.CurrentScenario.Unload
                uiapp.visible = 1;
                root.NewScenario('CAM');
                scenario = root.CurrentScenario;
            end
        end
    catch
        % STK is not running, launch new instance
        % Launch a new instance of STK12 and grab it
        uiapp = actxserver('STK12.application');
        root = uiapp.Personality2;
        uiapp.visible = 1;
        root.NewScenario('CAM');
        scenario = root.CurrentScenario;
    end
end

function object_setup(root)
    %set units to utcg before setting scenario time period and animation
period
    root.UnitPreferences.Item('DateFormat').SetCurrentUnit('UTCG');
    root.UnitPreferences.Item('Mass').SetCurrentUnit('kg');

    %set scenario time period and animation period
    global Scenario_start_time
    global Scenario_stop_time
    root.CurrentScenario.SetTimePeriod(Scenario_start_time,
Scenario_stop_time);
    root.CurrentScenario.Epoch = Scenario_start_time;
    root.CurrentScenario.Animation.EnableAnimCycleTime = true;
    root.CurrentScenario.Animation.AnimCycleType = 'eEndTime';
%    root.CurrentScenario.Animation.AnimCycleTime = '2 Jul 2017
12:00:00.000';
%    root.CurrentScenario.Animation.StartTime = '1 Jul 2017 12:00:00.000';
```

119

```matlab
    root.CurrentScenario.Animation.EnableAnimCycleTime = false;
    root.Rewind();
    root.ExecuteCommand('SetUnits / km sec UTCG');
%       root.ExecuteCommand('New / */Satellite Chase');
%       root.ExecuteCommand('New / */Satellite Target');
end
```

APPENDIX F. ICEYE DRAG MANEUVER—MATLAB-STK SCRIPT

```matlab
% ICEYE Drag Maneuver
% Copyright: Giuliano F. B. de Oliveira, 2022-10-31
%
% This program perform an aerodynamic maneuver changing the drag area from
% nominal to max for a certain time before TCA.

%%
clc
clear
close all
global Scenario_start_time
global Scenario_stop_time


%% Input
% ephemeris_path is the folder path with ephemeris files,
ephemeris_path = "I:\My Drive\009 - Mestrado NPS\NPS\Thesis\final_scripts\
Aerodynamic_test\Scenario_1";

% enter the name of .e file to be loaded as primary and secondary objecs, do
not including the extention
primary = "ICEYE_48916";
secondary = "SecObj_47941";

TCA = ' 17 Jan 2023 15:22:20.854';

Max_CP_before_maneuver = 1.5689e-05; % enter the max collision probability

% Collision probability parameters
Threshold = 5;
EndSigma = 6;
FracProbLimit = 0.001;

%spacecraft parameters

dry_mass = 87;  % spacecraft mass (Kg)
drag_area = 3.2*0.4; % Maximum drag area (m^2)
drag_area_nominal = 0.7*0.4;%nominal drag area (m^2)
Cp = 2.2; %drag coeff (2.2 spherica, 4 bxox)
Cr = 1; %Solar radiation coeff
SRP_area = 0.4*3.2;  %solar radiation pressure area
RadPressureArea = 0.4*3.2; %radiation pressure area (albedo)
MaxFuelMass = 5;
FuelMass = 5;
TankVolume = 1;

% defaut values
TankPressure = 5000; %Pa
```

121

```matlab
TankTemperature = 293.15; %Kelvin
FuelDensity = 1000.0; %kg/m^3


% Start a new scenário

if exist('uiapp', 'var') == 0
    [uiapp, root, scenario] = connect_to_stk();
%     object_setup(root);
end
% Reset the animation time
root.ExecuteCommand('Animate * Reset');


%%
% Add objects to the scenario (satellite, debris, and advcat)

debris = scenario.Children.New('eSatellite','Debris');
satellite = scenario.Children.New('eSatellite','MySatellite');
satellite1 = scenario.Children.New('eSatellite','MySatellite_nominal');

advcat = scenario.Children.New('eAdvCAT','Advcat');

% secondary object configuration

s = sprintf('SetState */Satellite/Debris FromFile
"%s%s%s.e"',ephemeris_path,'\',secondary);
root.ExecuteCommand(s);
% Primary object ephemeris using nominal configuration

s = sprintf('SetState */Satellite/MySatellite_nominal FromFile
"%s%s%s.e"',ephemeris_path,'\',primary);
root.ExecuteCommand(s);

% scenario Interval conficuration
root.ExecuteCommand('SetAnalysisTimePeriod * "Satellite/MySatellite_nominal
EphemerisTimeSpan Interval"');
SatelliteDP =
satellite1.DataProviders.Item('Interval').Group.Item('EphemerisTimeSpan').Exec
(scenario.StartTime, scenario.StopTime);
Scenario_start_time = SatelliteDP.DataSets.GetDataSetByName('Start
Time').GetValues;
Scenario_start_time = cell2mat(Scenario_start_time);
Scenario_stop_time = SatelliteDP.DataSets.GetDataSetByName('Stop
Time').GetValues;
Scenario_stop_time = cell2mat(Scenario_stop_time);
object_setup(root);

% Reset the animation time
root.ExecuteCommand('Animate * Reset');


SatelliteDP = satellite1.DataProviders.Item('Classical
Elements').Group.Item('ICRF').ExecSingle(scenario.StartTime);
```

```matlab
Period = SatelliteDP.DataSets.GetDataSetByName('Period').GetValues;
Period = cell2mat(Period);

%%
% Object configurations

% Advcat configuration
root.ExecuteCommand('ACAT */AdvCAT/Advcat Primary Add "Satellite/MySatellite"
OrbitClass');
root.ExecuteCommand('ACat */AdvCAT/Advcat Secondary Add "Satellite/Debris"
OrbitClass');
s = sprintf('ACat */AdvCAT/Advcat Threshold %d', Threshold);
root.ExecuteCommand(s);


% Primary
% Change Satellite propagator to Astrogator
root.ExecuteCommand('Astrogator */Satellite/MySatellite SetProp');

% Determine what segments are in the MCS currently
ASTGSegments = root.ExecuteCommand('Astrogator_RM */Satellite/MySatellite
GetValue MainSequence.SegmentList');

% Delete all the segments.
for j = 0:ASTGSegments.Count - 2
    Segment = strread(ASTGSegments.Item(j), '%s');
    root.ExecuteCommand(['Astrogator */Satellite/MySatellite DeleteSegment '
Segment{1}]);
end

% Insert an Initial State Segment into the MCS and configure

root.ExecuteCommand('Astrogator */Satellite/MySatellite InsertSegment -
Initial_State');
root.ExecuteCommand('Astrogator */Satellite/MySatellite SetValue
MainSequence.SegmentList.Initial_State.ComponentName Initial_Orbit'); %change
name of the segment
root.ExecuteCommand('Astrogator */Satellite/MySatellite SetValue
MainSequence.SegmentList.Initial_Orbit.InitialState.Epoch 0 EpSec'); %set
epoch
%%
% satellite parameters configuration
s = sprintf('Astrogator */Satellite/MySatellite SetValue
MainSequence.SegmentList.Initial_Orbit.MaxFuelMass %d kg',MaxFuelMass);
root.ExecuteCommand(s);
s = sprintf ('Astrogator */Satellite/MySatellite SetValue
MainSequence.SegmentList.Initial_Orbit.FuelMass %d kg', FuelMass);
root.ExecuteCommand(s);
s = sprintf('Astrogator */Satellite/MySatellite SetValue
MainSequence.SegmentList.Initial_Orbit.InitialState.DryMass %d Kg', dry_mass);
root.ExecuteCommand(s);
s = sprintf('Astrogator */Satellite/MySatellite SetValue
MainSequence.SegmentList.Initial_Orbit.InitialState.DragArea %d m^2',
drag_area);
```

123

```matlab
root.ExecuteCommand(s);
s = sprintf('Astrogator */Satellite/MySatellite SetValue
MainSequence.SegmentList.Initial_Orbit.InitialState.Cd %d', Cp);
root.ExecuteCommand(s);
s = sprintf('Astrogator */Satellite/MySatellite SetValue
MainSequence.SegmentList.Initial_Orbit.InitialState.SRPArea %d m^2',
SRP_area);
root.ExecuteCommand(s);
s = sprintf('Astrogator */Satellite/MySatellite SetValue
MainSequence.SegmentList.Initial_Orbit.InitialState.Cr %d', Cr);
root.ExecuteCommand(s);
s = sprintf('Astrogator */Satellite/MySatellite SetValue
MainSequence.SegmentList.Initial_Orbit.InitialState.RadPressureArea %d m^2',
RadPressureArea);
root.ExecuteCommand(s);

% s = sprintf('Astrogator */Satellite/MySatellite SetValue
MainSequence.SegmentList.Backward_Sequence.SegmentList.Initial_Orbit.InitialSt
ate.TankPressure %d Pa', TankPressure);
% root.ExecuteCommand(s);
% s = sprintf('Astrogator */Satellite/MySatellite SetValue
MainSequence.SegmentList.Backward_Sequence.SegmentList.Initial_Orbit.InitialSt
ate.TankTemperature %d K', TankTemperature);
% root.ExecuteCommand(s);
% s = sprintf('Astrogator */Satellite/MySatellite SetValue
MainSequence.SegmentList.Backward_Sequence.SegmentList.Initial_Orbit.InitialSt
ate.TankVolume %d m^3', TankVolume);
% root.ExecuteCommand(s);
% s = sprintf('Astrogator */Satellite/MySatellite SetValue
MainSequence.SegmentList.Backward_Sequence.SegmentList.Initial_Orbit.InitialSt
ate.FuelDensity %d Kg/m^3', FuelDensity);
% root.ExecuteCommand(s);

% Insert and rename propagator
root.ExecuteCommand('Astrogator */Satellite/MySatellite InsertSegment -
Propagate');

% Define the desired timespan for TCA
TCA = datetime(TCA,'InputFormat','dd MMM yyyy HH:mm:ss.S');
TCA1 = TCA - seconds(60);
TCA1 = datestr(TCA1);
TCA2 = TCA + seconds(60);
TCA2 = datestr(TCA2);

%%
% Collision probability computation
N_rev = 0:0.5:14;
i = length(N_rev);
root.ExecuteCommand('ACat */AdvCAT/Advcat AllowPartialEphem On')

for z = 1:i

    % Initial state setup
    t1 = TCA - seconds(N_rev(z)*Period);
```
124

```matlab
    s = sprintf('InitialState */Satellite/MySatellite Import STKFile
"%s%s%s.e" GatorPath "MainSequence.SegmentList.Initial_Orbit" Epoch "%s"
EpochSelect ClosestPrevious',ephemeris_path,'\',primary, t1);
    root.ExecuteCommand(s);
    root.ExecuteCommand('Astrogator */Satellite/MySatellite SetValue
MainSequence.SegmentList.Initial_Orbit.CoordinateSystem "CentralBody/Earth
ICRF" ');


    % Propagation after maneuver
    t2 = N_rev(z)*Period + 43200; % half day after TCA

    s3= sprintf('Astrogator */Satellite/MySatellite SetValue
MainSequence.SegmentList.Propagate.StoppingConditions.Duration.TripValue %d',
t2); % propagation time span
    root.ExecuteCommand(s3); % propagation time span
    % runs the Mission Control Sequence (MCS).
    root.ExecuteCommand('Astrogator */Satellite/MySatellite RunMCS');

    % Collision Probability calculation
    root.ExecuteCommand('ACat */AdvCAT/Advcat TimePeriod "Satellite/
MySatellite EphemerisTimeSpan Interval"');
    root.ExecuteCommand('ACat */AdvCAT/Advcat Compute "ShowProgress" On');

    Collision_Probability_DP = advcat.DataProviders.Item('Events by Time
In').ExecElements(TCA1, TCA2, {'Max Collision Probability'});

%     Collision_Probability_DP = advcat.DataProviders.Item('Events by Time
In').ExecElements(scenario.StartTime, scenario.StopTime, {'Max Collision
Probability'});
    Max_CP = cell2mat(Collision_Probability_DP.DataSets.GetDataSetByName('Max
Collision Probability').GetValues);

    Max_Collision_Probability (z) = Max_CP


end

%%
% Plot

Threshold1 = ones(length(N_rev),1)*1e-5;
Threshold2 = ones(length(N_rev),1)*1e-7;
Threshold3 = ones(length(N_rev),1)*1e-6;
Threshold4 = ones(length(N_rev),1)*1e-4;

Max_CP_without_Manev = ones(length(N_rev),1)*Max_CP_before_maneuver;
figure()
semilogy(N_rev,Threshold1,'-- r')
hold on
semilogy(N_rev,Threshold4,'--')
hold on
semilogy(N_rev,Threshold2,'-- g')
```

125

```matlab
hold on
semilogy(N_rev,Threshold3,'-- b')
hold on
semilogy(N_rev,Max_Collision_Probability,'b')
hold on
semilogy(N_rev,Max_CP_without_Manev,'*')
grid on
xlabel('n_{rev} before TCA with maximum drag area facing the direction of
velocity'); ylabel('Max Collision Probability');
xticks(0:0.5:N_rev(end))
legend('','','','','Drag Maneuver', 'Collision Probaility without maneuver')


%%%% Functions %%%%


function [uiapp, root, scenario] = connect_to_stk()
    % Initialize STK and establish the connection
    try
        % Grab an existing instance of STK
        uiapp = actxGetRunningServer('STK12.application');
        root = uiapp.Personality2;
        checkempty = root.Children.Count;
        if checkempty == 0
            %If a Scenario is not open, create a new scenario
            uiapp.visible = 1;
            root.NewScenario('Drag_Maneuver');
            scenario = root.CurrentScenario;
        else
            %If a Scenario is open, prompt the user to accept closing it or
not
            rtn = questdlg({'Close the current scenario?',' ','(WARNING: If
you have not saved your progress will be lost)'});
            if ~strcmp(rtn,'Yes')
                return
            else
                root.CurrentScenario.Unload
                uiapp.visible = 1;
                root.NewScenario('Drag_Maneuver');
                scenario = root.CurrentScenario;
            end
        end
    catch
        % STK is not running, launch new instance
        % Launch a new instance of STK12 and grab it
        uiapp = actxserver('STK12.application');
        root = uiapp.Personality2;
        uiapp.visible = 1;
        root.NewScenario('Drag_Maneuver');
        scenario = root.CurrentScenario;
    end
end

function object_setup(root)
```

126

```matlab
    %set units to utcg before setting scenario time period and animation
period
    root.UnitPreferences.Item('DateFormat').SetCurrentUnit('UTCG');
    root.UnitPreferences.Item('Mass').SetCurrentUnit('kg');

    %set scenario time period and animation period
    global Scenario_start_time
    global Scenario_stop_time
    root.CurrentScenario.SetTimePeriod(Scenario_start_time,
Scenario_stop_time);
    root.CurrentScenario.Epoch = Scenario_start_time;
    root.CurrentScenario.Animation.EnableAnimCycleTime = true;
    root.CurrentScenario.Animation.AnimCycleType = 'eEndTime';
%    root.CurrentScenario.Animation.AnimCycleTime = '2 Jul 2017
12:00:00.000';
%    root.CurrentScenario.Animation.StartTime = '1 Jul 2017 12:00:00.000';
    root.CurrentScenario.Animation.EnableAnimCycleTime = false;
    root.Rewind();
    root.ExecuteCommand('SetUnits / km sec UTCG');
%    root.ExecuteCommand('New / */Satellite Chase');
%    root.ExecuteCommand('New / */Satellite Target');
end
```

THIS PAGE INTENTIONALLY LEFT BLANK

LIST OF REFERENCES

[1]   C. Henry, "SpaceX submits paperwork for 30,000 more Starlink satellites," *SpaceNews*, Oct. 15, 2019. https://spacenews.com/spacex-submits-paperwork-for-30000-more-starlink-satellites/ (accessed Oct. 23, 2022).

[2]   "Spaec Objects/Public catalog database." USSPACECOM, Aug. 31, 2022. Accessed: Aug. 31, 2022. [Online]. Available: https://www.space-track.org/#publicCatalogGrowth

[3]   "IADC-02-01 Space Debris Guidelines Rev 3," IADC, Guideline IADC-02-01 Rev. 3, Jun. 2021. Accessed: Feb. 02, 2023. [Online]. Available: https://www.iadc-home.org/documents_public/view/id/172#u

[4]   T. S. Kelso, "Analysis of the 2007 Chinese ASAT Test and the Impact of its Debris on the Space Environment," in *8th Advanced Maui Optical and Space Surveillance Technologies Conference, Maui, HI*, 2007, vol. 7.

[5]   S. Valencia and B. Eng, "Analyses of the Russian antisatellite ASAT missile test on Kosmos-1408 and its impact on space sustainability." 2021.

[6]   V. V. Svotina and M. V. Cherkasova, "Space debris removal – Review of technologies and techniques. Flexible or virtual connection between space debris and service spacecraft," *Acta Astronautica*, Sep. 2022, doi: 10.1016/j.actaastro.2022.09.027.

[7]   E. Kerr and N. S. Ortiz, "State of the Art and Future Needs in Conjunction Analysis Methods, Processes and Software'," in *Proceedings of 8th European Conference on Space Debris (virtual edition, SDC8)*, pp. 20–23.

[8]   F. J. Krage, "NASA Spacecraft Conjunction Assessment and Collision Avoidance Best Practices Handbook," NASA, handbook NASA/SP-20205011318, 2020.

[9]   H. C. P. D. P. University, *Orbital Mechanics for Engineering Students: Revised Reprint*, 4th edition. Oxford England ; Cambridge, MA: Butterworth-Heinemann, 2020.

[10]   S. Aida and M. Kirschner, "Operational Results of Conjunction Assessment and Mitigation at GSOC," *The ISTS special issue of Transactions of JSASS, Aerospace Technology Japan*, 2011.

[11]   F. R. Hoots, L. L. Crawford, and R. L. Roehrich, "An analytic method to determine future close approaches between satellites," *Celestial Mechanics*, vol. 33, no. 2, pp. 143–158, Jun. 1984, doi: 10.1007/BF01234152.

[12]   S. Alfano and D. Finkleman, "Operating characteristic approach to effective satellite conjunction filtering," *Advances in the Astronautical Sciences*, vol. 148, pp. 3647–3662, 2013.

[13]   18th Space Control Squadron, "Spaceflight Safety Handbook for Satellite Operators," handbook, Aug. 2020. [Online]. Available: https://www.space-track.org/

[14]   "Conjunction Data Message Recommended Standard CCSDS 508.0-B-1 BLUE BOOK." CCSDS Secretariat Space Communications and Navigation Office, 7L70 Space Operations Mission Directorate NASA Headquarters Washington, DC 20546-0001, USA, Jun. 2013. [Online]. Available: https://public.ccsds.org/Pubs/508x0b1e2c2.pdf

[15]   J. V. Cabrera, S. Nag, and D. D. Murakami, "An Initial Analysis of Automating Conjunction Assessment and Collision Avoidance Planning in Space Traffic Management," presented at the AAS/AIAA Space Flight Mechanics Meeting, Ka''anapali, HI, Jan. 2019. Accessed: Jan. 06, 2023. [Online]. Available: https://ntrs.nasa.gov/citations/20190001614

[16]   "Systems Tool Kit (STK 12)." AGI. Accessed: Nov. 01, 2022. [Online]. Available: https://help.agi.com/stk/

[17]   S. Alfano, "Relating position uncertainty to maximum conjunction probability," *The Journal of the Astronautical Sciences*, vol. 53, no. 2, pp. 193–205, 2005.

[18]   U. E. Núñez Garzón and E. G. Lightsey, "Relating Collision Probability and Separation Indicators in Spacecraft Formation Collision Risk Analysis," *Journal of Guidance, Control, and Dynamics*, vol. 45, no. 3, pp. 517–532, 2022, doi: 10.2514/1.G005744.

[19]   M. S. Balch, "A Corrector for Probability Dilution in Satellite Conjunction Analysis," in *18th AIAA Non-Deterministic Approaches Conference*, American Institute of Aeronautics and Astronautics, 2016. doi: 10.2514/6.2016-1445.

[20]   M. D. Hejduk, D. Snow, and L. K. Newman, "Satellite Conjunction Assessment Risk Analysis for 'Dilution Region' Events: Issues and Operational Approaches," presented at the Space Traffic Management 2019, Austin, TX, Feb. 2019. Accessed: Nov. 09, 2022. [Online]. Available: https://ntrs.nasa.gov/citations/20220004118

[21]   R. C. Frigm and L. K. Newman, "A Single Conjunction Risk Assessment Metric: the F-Value," presented at the 2009 AAS/AIAA Astrodynamics Specialist Conference, Pittsburgh, PA, Aug. 2009. Accessed: Nov. 10, 2022. [Online]. Available: https://ntrs.nasa.gov/citations/20090032016

[22]   Z. Sun, Y. Luo, and Z. Niu, "Spacecraft rendezvous trajectory safety quantitative performance index eliminating probability dilution," *Sci. China Technol. Sci.*, vol. 57, no. 6, pp. 1219–1228, Jun. 2014, doi: 10.1007/s11431-014-5523-3.

[23]   F. K. Chan, *Spacecraft Collision Probability*. Washington, DC: American Institute of Aeronautics and Astronautics, Inc., 2008. doi: 10.2514/4.989186.

[24]   "Advanced CAT - Nonlinear Probability Tool." AGI. Accessed: Jan. 11, 2023. [Online]. Available: https://help.agi.com/stk/index.htm#cat/Cat03-08.htm#lineartest

[25]   A. K. Maini and V. Agrawal, *Satellite Technology: Principles and Applications*, 3rd Edition. Wiley, 2014.

[26]   M. Villano, J. Márquez-Martínez, D. Moller, and M. Younis, "Overview of Newspace Synthetic Aperture Radar Instrument Activities," in *IGARSS 2022 - 2022 IEEE International Geoscience and Remote Sensing Symposium*, Jul. 2022, pp. 4130–4132. doi: 10.1109/IGARSS46834.2022.9883128.

[27]   "A revolution in synthetic aperture radar (SAR) data Earth observation," ICEYE, Finland, System Documentation ICEYE-BDS-BRO-339, 2022. Accessed: Jan. 23, 2023. [Online]. Available: https://www.iceye.com/downloads

[28]   "The ICEYE Fleet," Finland, System Documentation ICEYE Product Documentation 5.0. Accessed: Nov. 22, 2022. [Online]. Available: https://iceye-ltd.github.io/product-documentation/5.0/productguide/fleet/

[29]   D. Muff *et al.*, "The ICEYE Constellation - Some New Achievements," in *2022 IEEE Radar Conference (RadarConf22)*, Mar. 2022, pp. 1–4. doi: 10.1109/RadarConf2248738.2022.9764281.

[30]   "ICEYE imaging modes," ICEYE, Finland, System Documentation ICEYE Product Documentation 5.0. Accessed: Nov. 21, 2022. [Online]. Available: https://iceye-ltd.github.io/product-documentation/5.0/productguide/products/

[31]   S. W. Paek, S. Balasubramanian, S. Kim, and O. de Weck, "Small-Satellite Synthetic Aperture Radar for Continuous Global Biospheric Monitoring: A Review," *Remote Sensing*, vol. 12, no. 16, Art. no. 16, Jan. 2020, doi: 10.3390/rs12162546.

[32]   D. Krejci, A. Reissner, T. Schönherr, B. Seifert, Z. Saleem, and R. Alejos, "Recent flight data from IFM Nano Thrusters in a low earth orbit," in *Proceedings of the 36th International Electric Propulsion Conference, Vienna, Austria*, 2019, pp. 15–20.

[33] T. Schönherr, B. Little, D. Krejci, A. Reissner, and B. Seifert, "Development, production, and testing of the IFM nano FEEP thruster," in *36th International Electric Propulsion Conference*, 2019, pp. 1–11.

[34] M. Laaninen, M. Neerot, J. Homssi, K. Szczygielska, and J. Niemczyk, "ICEYE Radar Constellation Development and Evolution," in *EUSAR 2022; 14th European Conference on Synthetic Aperture Radar*, Jul. 2022, pp. 1–3.

[35] J. Hernando-Ayuso and C. Bombardelli, "Low-Thrust Collision Avoidance in Circular Orbits," *Journal of Guidance, Control, and Dynamics*, vol. 44, no. 5, pp. 983–995, May 2021, doi: 10.2514/1.G005547.

[36] J. L. Gonzalo Gomez, C. Colombo, and P. Di Lizia, "A semi-analytical approach to low-thrust collision avoidance manoeuvre design," in *70th International Astronautical Congress (IAC 2019)*, 2019, pp. 1–9.

[37] D. Mishne and E. Edlerman, "Collision-Avoidance Maneuver of Satellites Using Drag and Solar Radiation Pressure," *Journal of Guidance, Control, and Dynamics*, vol. 40, no. 5, pp. 1191–1205, 2017, doi: 10.2514/1.G002376.

[38] A. Viquerat, M. Schenk, B. Sanders, and V. Lappas, "Inflatable rigidisable mast for end-of-life deorbiting system," in *European Conference on Spacecraft Structures, Materials and Environmental Testing (SSMET)*, 2014, vol. 2014, pp. 1–10.

[39] S. R. Omar and R. Bevilacqua, "Spacecraft Collision Avoidance Using Aerodynamic Drag," *Journal of Guidance, Control, and Dynamics*, vol. 43, no. 3, pp. 567–573, 2020, doi: 10.2514/1.G004518.

INITIAL DISTRIBUTION LIST

1.   Defense Technical Information Center
        Ft. Belvoir, Virginia

2.   Dudley Knox Library
        Naval Postgraduate School
        Monterey, California